1. Report No.	2. Government Accession No.	3. Recipient's Catalog No.
FHWA/TX-01/2134-1		

4. Title and Subtitle	5. Report Date
PERFORMANCE PREDICTION WITH THE MMLS3 AT WESTRACK	May 2001
	6. Performing Organization Code

7. Author(s)	8. Performing Organization Report No.
Amy L. Epps, Tazeen Ahmed, Dallas C. Little, and Fred Hugo	Report 2134-1

9. Performing Organization Name and Address	10. Work Unit No. (TRAIS)
Texas Transportation Institute The Texas A&M University System College Station, Texas 77843-3135	11. Contract or Grant No. Project No. 0-2134

12. Sponsoring Agency Name and Address	13. Type of Report and Period Covered
Texas Department of Transportation Construction Division Research and Technology Transfer Section P. O. Box 5080 Austin Texas 78763-5080	Research: July 1999-August 2000
	14. Sponsoring Agency Code

15. Supplementary Notes

Research performed in cooperation with the Texas Department of Transportation and the U.S. Department of Transportation, Federal Highway Administration.

Research Project Title: Evaluation of Model Mobile Load Simulator Using WesTrack Sections

16. Abstract

The one-third scale Model Mobile Load Simulator (MMLS3) was used to traffic four pavement sections at WesTrack to establish and validate its ability to reliably predict rutting performance under full-scale trafficking. Researchers utilized two different analysis methods in determining rut depth (RD) from transverse profiles under both scaled (MMLS3) and full-scale (WesTrack trucks) loading. Researchers also completed a limited laboratory testing program to complement results contained in the WesTrack database.

Researchers ranked performance and conducted statistical analyses using both field and laboratory results to compare the rutting performance of three coarse-graded replacement sections that showed poor performance and one fine-graded section with good performance. They also compared results from both RD analysis methods and both loading conditions. Rankings based on field results using either RD analysis method were in close agreement, and the majority of the rankings based on laboratory results matched those from the field.

Two methodologies to predict rutting performance using the MMLS3 were also demonstrated. For both, researchers recommend the critical temperature for permanent deformation over a hot week during the summer of a 30-year period for MMLS3 testing. A minimum of 100,000 load repetitions, three RD measurements along the length of an MMLS3 section, and a standard RD analysis method were suggested to determine a mean RD for (1) comparison with acceptable performance criteria for the first prediction method and (2) use with a theoretical rutting ratio based on stress analyses for the second method.

The second prediction methodology involves a quantitative comparative analysis based on the hypothesis that the extent of rutting is dependent on the nature of the vertical contact stress under the tire, the material characteristics and pavement structural composition, and the prevailing environmental conditions prior to and during trafficking. Results from the initial analysis using this second methodology exhibited some apparent inconsistencies that led to a second, more detailed analysis that included additional important factors necessary for successful implementation of this performance prediction methodology. These factors included lateral wander effects, transverse profile measurement errors, misalignment of the MMLS3, and tire contact stresses at elevated temperatures. This more comprehensive analysis involved improving material property estimates, revising RDs, considering deformation throughout the pavement structure, and accounting for differences in lateral wander between the two loading conditions. Results from this second analysis indicated that the hypothesis required in the performance prediction methodology appears to hold for the four independent pavement sections at WesTrack, provided steps are taken to factor in differences in loading and environmental conditions between MMLS3 and full-scale truck trafficking.

17. Key Words	18. Distribution Statement
Accelerated Pavement Testing, MMLS, Rutting, Performance Prediction, Quantitative Rutting Comparison	No restrictions. This document is available to the public through NTIS: National Technical Information Service 5285 Port Royal Road Springfield, Virginia 22161

19. Security Classif.(of this report)	20. Security Classif.(of this page)	21. No. of Pages	22. Price
Unclassified	Unclassified	132	

PERFORMANCE PREDICTION WITH THE MMLS3 AT WESTRACK

by

Amy L. Epps
Assistant Research Scientist
Texas Transportation Institute

Tazeen Ahmed
Graduate Assistant Researcher
Texas Transportation Institute

Dallas C. Little
Graduate Assistant Researcher
Texas Transportation Institute

and

Frederick Hugo
Research Fellow
Center for Transportation Research

Report 2134-1
Project Number 0-2134
Research Project Title: Evaluation of Model Mobile Load Simulator Using WesTrack Sections

Sponsored by the
Texas Department of Transportation
In Cooperation with the
U.S. Department of Transportation
Federal Highway Administration

May 2001

TEXAS TRANSPORTATION INSTITUTE
The Texas A&M University System
College Station, Texas 77843-3135

and the

CENTER FOR TRANSPORTATION RESEARCH
The University of Texas at Austin

DISCLAIMER

The contents of this report reflect the views of the authors, who are responsible for the facts and the accuracy of the data presented herein. The contents do not necessarily reflect the official view or policies of the Federal Highway Administration and the Texas Department of Transportation. This report does not constitute a standard, specification, or regulation, nor it is intended for construction, bidding, or permit purposes. Trade names were used solely for information and not for product endorsement. The engineer in charge was Frederick Hugo, P.E. (Texas No. 67246).

ACKNOWLEDGMENTS

The authors wish to thank Maghsoud Tahmoressi, formerly of TxDOT, and Magdy Mikhail of TxDOT for their efforts in providing technical guidance, support, and direction to this project. Thanks also to Jon Bilyeu of TxDOT for taking SASW measurements at the test site and other TxDOT personnel in Austin for conducting the laboratory testing program. Thanks to Colin Ashmore and Ron Show from the Nevada Automotive Testing Center (NATC) for their tremendous help in collecting samples, trafficking with the MMLS3, and making this project a reality. Thanks to Pieter Poolman of the Center for Transportation Research (CTR) and the Institute for Transport Technology (ITT) at the University of Stellenbosch for his help and support in training the NATC personnel in the operation of the MMLS3, taking SASW measurements, transporting the equipment to Nevada, and further analyzing the data as reported in the appendices. Finally, thanks to Paul Nehring, formerly from the Texas Transportation Institute (TTI), for retrieval of the equipment from Nevada.

TABLE OF CONTENTS

TABLE OF CONTENTS (continued)

LIST OF FIGURES

Figure **Page**

LIST OF TABLES

Table **Page**

LIST OF TABLES (Continued)

Table **Page**

CHAPTER 1. INTRODUCTION

Primary forms of distress in asphalt concrete pavements include permanent deformation, traffic load-induced fatigue cracking, and environmentally induced thermal cracking. Excessive permanent deformation creates a safety problem because vehicle steering becomes impaired and the possibility for hydroplaning due to water accumulation is enhanced.

Several millions of dollars are allocated annually to repair damage caused by permanent deformation. Transportation agencies and roadway users alike may realize significant savings if this type of distress could be minimized through predictive measures. To obtain these benefits, accurate data must be collected at relatively low cost. Accelerated pavement testing (APT) devices, such as the one-third scale Model Mobile Load Simulator (MMLS3), can be used to predict pavement performance while minimizing time and expenditures. To validate MMLS3 results, full-scale trafficking must be used in some capacity to correlate the amount of deformation expected from full-scale vehicles to that induced by the MMLS3.

The objectives of this project, funded by the Texas Department of Transportation (TxDOT), were to establish the predictive capability of the MMLS3 and validate its use in reliably predicting rutting performance near the surface. By conducting five MMLS3 tests (including one replicate) on four pavement sections at WesTrack, a tie was made with existing field performance and materials characterization data gathered as part of the $15 million WesTrack project sponsored by the Federal Highway Administration (FHWA) and the National Cooperative Highway Research Program (NCHRP) (*1*). Researchers compared measured performance under full-scale loading and performance predicted from laboratory tests with performance predicted using the MMLS3. From this comparison, an additional performance prediction tool between relatively inexpensive laboratory testing and expensive but more realistic full-scale accelerated load testing was validated and linked to actual field performance. With this tool, sections or mixtures that exhibit poor or unacceptable rutting performance near the surface when evaluated through laboratory testing or MMLS3 testing can be eliminated prior to expensive full-scale tests or use in service.

Relevant background information on the WesTrack project and the MMLS3 is provided, followed by a description of the experimental design for this project and rutting performance results from the field and the laboratory. Performance rankings are provided, and two

methodologies for using the MMLS3 as a performance prediction tool are demonstrated. After completion of the project and prior to submission of the final report, one of the researchers, Dr. Hugo, performed further analysis of the project data in collaboration with Mr. Pieter Poolman at the University of Stellenbosch in South Africa. The purpose of this second analysis was to explore possible reasons for the apparent inconsistency of results required for the hypothesis used in the quantitative performance prediction methodology. Results from this second, more detailed analysis highlighted important factors that must be considered for the methodology described to produce accurate prediction of rutting performance under full-scale trafficking. These results are incorporated in two appendices, related performance prediction discussion, and the summary, conclusions, and recommendations that conclude the report.

CHAPTER 2. WESTRACK

The WesTrack project, sponsored by FHWA and NCHRP, was a $15 million, 3 km* (1.9 mile) full-scale test track near Reno, Nevada, that included 26 pavement test section locations (*2*). Each section was 70 m (230 ft) in length with 25 m (82 ft) for transitioning between sections, 40 m (131 ft) for performance monitoring, and 5 m (16 ft) for destructive sampling. The facility was originally constructed between October 1994 and October 1995 and was subjected to traffic from March 1996 through March 1999. During this three-year period, 5.0 million 80 kN (18,000 lbs) equivalent single axle loads (ESALs) were applied. The pavement was loaded by means of four driverless tractor/triple-trailer combinations. Each truck pass applied 10.48 ESALs. Tire pressures were 700 kPa (101 psi), and the speed of the vehicles was 64 km/hr (40 mph) or 17.9 m/sec (58.7 ft/sec) (*1*).

The objectives of the project were two-fold, but both focused on the 150 mm (6 in) hot mix asphalt (HMA) surface layer of each pavement section that rested on 300 mm (12 in) of dense-graded crushed aggregate base course, 300 mm (12 in) of engineered fill obtained from natural subgrade materials, and 150 mm (6 in) of scarified and mixed subgrade soil. The first objective was to continue the development of performance-related specifications for HMA pavements by evaluating the impact on performance of deviations in materials and construction properties including asphalt content (AC), aggregate gradation in terms of percent passing the 0.075 mm (No. 200) sieve (p0.075), and in-place air void (AV) content. The second objective was to provide early field verification of the Superpave mix design and analysis system. To accomplish these objectives, WesTrack researchers monitored performance under full-scale loading and predicted performance using mix design and test methods developed during the Strategic Highway Research Program (SHRP) (*1*).

Performance monitoring of the pavement sections at WesTrack was extensive and frequent. Monitoring data gathered for each section relevant to this project include transverse profiles at the surface and resulting permanent deformation under full-scale loading. In addition, environmental monitoring was conducted through a Long-Term Pavement Performance (LTPP) weather station and two LTPP seasonal monitoring devices for measuring temperature variations

*Given that researchers in APT use metric units and that TRB Task Force A2B52, now Committee A2B09, has set guidelines that include the exclusive use of metric units, metric units are used as the primary system in this report.

of the pavement layers. Furthermore, WesTrack researchers used thermocouples to monitor temperature in the asphalt concrete surface layer of one section at five different depths (*1*). These environmental data were used in determining an approximate MMLS3 testing temperature and appropriate temperatures for characterizing materials in the quantitative performance prediction methodology.

As originally constructed, the 26 sections included both fine-graded and coarse-graded asphalt concrete mixtures designed using the Superpave volumetric process. These mixtures incorporated partially crushed gravel aggregate, primarily andesite, and an unmodified PG64-22 binder (*1*, *3*, *4*). Aggregate gradation in terms of p0.075, AC, and in-place AV were systematically varied among the test sections to simulate typical construction variability. The experimental design is shown in Table 1.

Table 1. Experimental Design for WesTrack* and MMLS3 Testing (*1*).**

Design Air Void Content (%)	Aggregate Gradation								
	Fine			Fine Plus			Coarse		
	Design Asphalt Content (%)								
	Low	Optimum	High	Low	Optimum	High	Low	Optimum	High
Low		04	18		12	09 / 21		23 (39)	25 (55)
Medium	02	01 / 15 [01A]	14	22	11 / 19	13	08 (38) [38A] [38B]	05 / 24 (35 / 54) [35A]	07 (37) [37A]
High	03 / 16	17		10	20		26 (56)	06 (36)	

* Numbers indicate WesTrack original construction sections with replacement sections shown in parentheses.

** Hatched cells indicate sections tested with the MMLS3 with the corresponding section number shown in brackets.

Three aggregate gradations meeting the Superpave 19 mm nominal maximum size specification were utilized (*1*, *4*). The experimental design included one S-shaped coarse gradation that plots below the restricted zone and one fine gradation that plots above the

restricted zone. These gradations were designated “coarse” and “fine,” respectively, with the fine gradation containing approximately 25 percent decomposed granite natural sand in addition to the primary partially crushed gravel aggregate. The third gradation, designated “fine plus,” was obtained by adding approximately 1.5 percent bag house fines to the fine gradation. All three aggregate gradations are shown in Figure 1.

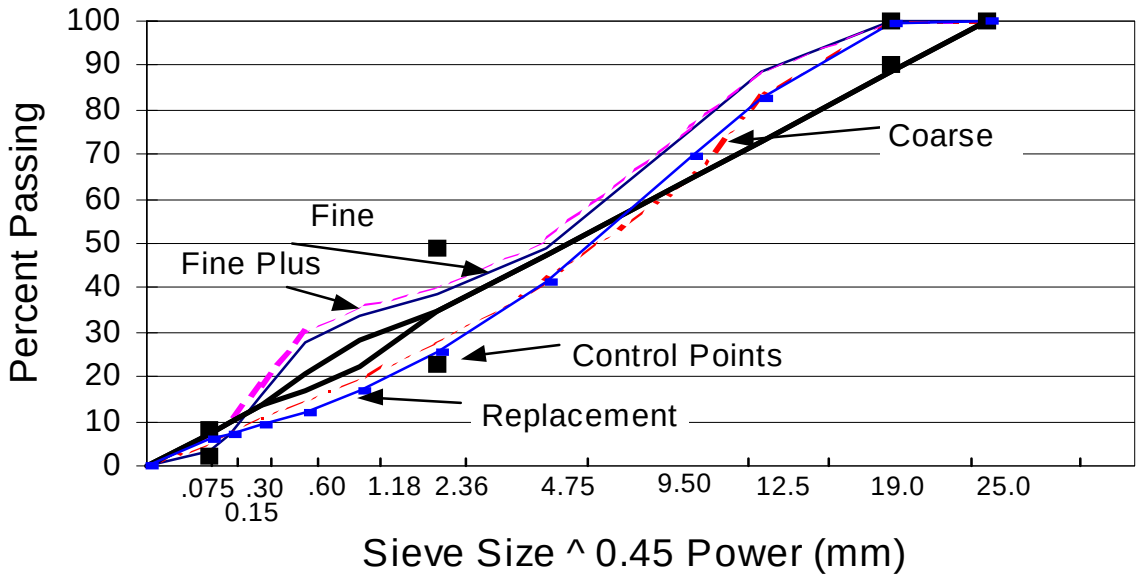

Figure 1. WesTrack HMA Aggregate Gradations.

Three levels of AC were also considered in the experiment. WesTrack researchers determined optimum AC using the Superpave volumetric mix design process for the coarse and fine aggregate gradations, and they set the optimum for the fine plus gradation equal to the optimum for the fine gradation. The remaining two levels of AC included in the experimental design varied plus and minus 0.7 percent from the respective optimums. These values of AC were designated as high and low, respectively. The third variable considered in the experimental design was in-place AV, and three values were also used for this variable. Eight percent AV was considered typical of HMA construction in the United States, and this level of AV was designated as medium. Low and high values of in-place AV were selected as 4 and 12 percent, respectively. Five replicate sections were used, and a few combinations of the three mixture variables (i.e. high AC with high AV) were not considered in the experiment, as these combinations are not likely to occur during actual HMA construction.

Ten sections were replaced in June 1997 after 2.8 million ESALs due to excessive rutting and fatigue cracking. All eight of the original coarse-graded sections were replaced with similar coarse-graded sections using a 100 percent crushed andesite aggregate from a second aggregate source and a second unmodified PG64-22 binder. This mixture, termed the "replacement mixture," contained no natural sand, and again WesTrack researchers used the Superpave volumetric mix design process to determine optimum AC. The replacement sections are also indicated in the experimental design (Table 1). Many of these replacement sections rutted even more rapidly than the original sections, failing after the application of less than 50,000 ESALs.

In addition to monitoring performance of the pavement sections, the WesTrack project included an extensive materials sampling and testing program to control quality during construction and facilitate the development of performance prediction models (*1*, *5*). Laboratory test data relevant to this project include the Repeated Simple Shear Test at Constant Height (RSST-CH) results before and after WesTrack truck trafficking. Analysis of these data for field mixed-field compacted specimens from the replacement sections indicated a good correlation with permanent deformation at WesTrack (*6*). Performance of samples removed from these sections was also measured in a separate study using empirical laboratory-scale accelerated load testing devices, including the Asphalt Pavement Analyzer (APA), the French Pavement Rutting Tester (FPRT), and the Hamburg Wheel-Tracking Device (HWTD) (*7*, *8*). Results from these APT tools satisfactorily correlated with permanent deformation measured at WesTrack when an appropriate testing temperature was selected to reflect in-service temperature (*8*). For use with laboratory compacted specimens, this study emphasized that laboratory compaction methods must simulate field compaction.

CHAPTER 3. MODEL MOBILE LOAD SIMILATOR (MMLS3)

The MMLS3 shown in Figure 2 is a unidirectional, vehicle-load simulator for accelerated trafficking of model or full-scale, dry and wet pavements. The temperature during trafficking can be controlled by placing the MMLS3 in an environmental chamber (Figure 3). This APT device is low-cost and applies a scaled load on 300 mm (12 in) diameter, pneumatic tires that are 3/10 or approximately one-third the diameter of standard truck tires (9). The MMLS3 has four wheels with a distance between centerlines of 1.05 m (3.4 ft). A wheel load of up to 2.7 kN (607 lbs or approximately one-ninth of the load on one wheel of a dual tire standard single axle) is utilized for trafficking the pavement. The pneumatic tires are normally inflated to 690 kPa (100 psi), but maximum pressures up to 800 kPa (116 psi) can be used. A maximum of 7200 single-wheel load repetitions can be applied per hour at a speed of up to 2.6 m/sec (8.5 ft/sec) that corresponds approximately to a 4 Hz frequency of loading for a measured tread length of 0.11 m (0.36 ft) (9). For a standard truck tire with a measured tread length of approximately 0.25 m (0.8 ft), the simulated speed of the MMLS3 is calculated as 21 km/hr (13 mph) or 5.9 m/sec (19.4 ft/sec). The MMLS3 device is 2.4 m (7.9 ft) long by 0.6 m (2 ft) wide by 1.2 m (3.9 ft) high.

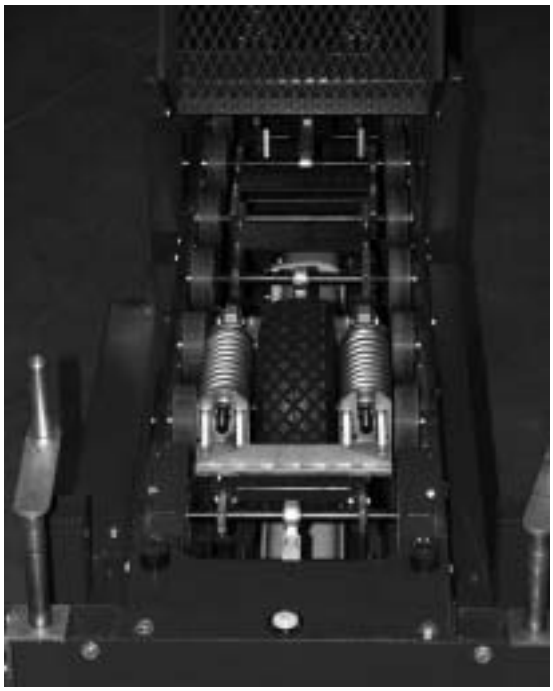

Figure 2. MMLS3.

Figure 3. MMLS3 at WesTrack Inside Environmental Chamber.

There are currently seven operational MMLS3 machines. Apart from tests discussed in this report, a total of more than 40 tests have been successfully completed by applying in excess of 11.5 million load repetitions. These tests have been conducted in laboratories, on specially prepared experimental pavements at fixed sites, and on existing pavements in South Africa, Switzerland, and the United States. The majority has thus far been on operational highways (23 tests). Tables 2 and 3 provide a list of applications.

Table 2. Laboratory and Fixed Site Applications of the MMLS3.

Number of Tests	Type of Test
2	Evaluating Durability of Block Pavers
1	Evaluating Performance of Pavement Joint Materials
2	Evaluating Rutting Resistance of Steel Reinforced Asphalt Concrete at Elevated Temperature
11	Evaluating Seal Coat Performance
3	Proofing a Composite Roof Deck for Use as a Parking Lot
1	Evaluating Fatigue Performance of a Scaled Asphalt Concrete Pavement in Terms of Layer Thicknesses (in progress)

.

Table 3. MMLS3 Applications on Existing Pavements in the Field.

Number of Tests	Type of Test
3	Evaluating Durability of Block Pavers
3	Quantifying Distress of Lightweight Aggregate HMA Rehabilitation Strategies Due to Wet Trafficking
5	Evaluating the Impact of High Temperatures on Rutting Performance of Lightweight Aggregate HMA Rehabilitation Strategies
6	Comparing Foam and Emulsion-Treated Base Materials
3	Proofing Performance of a Large Aggregate Mix Base on Trial Sections of an International Airport Runway
4	Comparing Performance of Polymer-Modified Asphalt Concrete and Conventional Asphalt Concrete in Base and Surfacing Mixes for Design Decisions

MMLS3 field tests have been conducted for TxDOT on eight full-scale pavement sections on US 281 near Jacksboro, Texas, adjacent to sections trafficked with the full-scale Texas Mobile Load Simulator (TxMLS) (*9*, *10*, *11*). In these tests, the relative performance of two rehabilitation processes was compared. Five hot tests and three wet tests were conducted on the surface and on milled pads on both the north and southbound lanes of the test site, with application of more than 3.6 million load repetitions. Researchers on the Jacksboro project conducted four of the five hot tests (50 °C (122 °F)) under controlled conditions in an environmental chamber. MMLS3 field testing combined with additional laboratory testing indicated that one of the rehabilitation processes was more susceptible to moisture damage and less resistant to fatigue cracking. During these tests, limestone HMA was found to be superior to both rehabilitation processes under wet trafficking. The untreated lightweight aggregate HMA was found to be very vulnerable to moisture damage and likely to limit the performance of both processes.

A quantitative comparison of pavement response and rutting performance at Jacksboro under full-scale (TxMLS) and scaled (MMLS3) accelerated loading showed good correlation when actual loading and environmental conditions were considered. Ratios between theoretically predicted rutting ratios (MMLS3 to TxMLS) and measured field rutting ratios were 1.2 and 1.0 for northbound and southbound sections, respectively. Theoretical rutting ratios were based on areas under the maximum vertical compressive stress distribution with depth corrected for temperature and frequency (*10*). Given the limited nature of this study and

considering all of the influencing factors and assumptions needed to account for these factors, these results were significant and promising for the limited number of pavement sections evaluated. These results first demonstrated the performance prediction capability of the MMLS3 through a methodology that requires ratios close to one. This methodology is described subsequently and was utilized in this project.

Previous MMLS3 research has led to the conclusion that a standard of practice is needed to enable accurate assessment of rutting performance based on MMLS3 testing. This standard would include a method for selecting testing temperature, number of load repetitions, and a method for determining rut depth (RD) based on transverse profile data. This report provides recommendations for these parameters.

CHAPTER 4. EXPERIMENTAL DESIGN

The experimental design for this project included selection of WesTrack sections for MMLS3 trafficking, a performance monitoring schedule and measurement locations, the MMLS3 testing temperature, and additional laboratory tests. This chapter describes each of the selected parameters and tests.

MMLS3 TRAFFICKING

Starting five months after completion of full-scale trafficking at WesTrack, five MMLS3 tests (including one replicate) were conducted on four pavement sections at WesTrack. Three of these sections were replacement sections, including one section (Section 35) with a coarse-graded mixture at optimum AC and medium AV and two sections with coarse-graded mixtures at medium AV and low (Section 38) and high (Section 37) AC. The fourth section (Section 01) selected was a fine-graded mixture at optimum AC and medium AV (*2*). The replicate MMLS3 test was conducted on Section 38, and the selected sections are shown on the WesTrack experimental design (Table 1). MMLS3 sections numbered 01A, 35A, 37A, 38A, and 38B as shown in Table 1 were marked on each corresponding WesTrack section between the full-scale truck wheelpaths. Each MMLS3 section was 1.2 m (3.9 ft) in length with transverse profiles measured with a laser profilometer at five locations at a 0.2 m (0.7 ft) spacing along the length of the section. The instrumentation layout in Figure 4 shows these measurement locations and the depths and locations of thermocouples used to measure temperature. Locations for collection of Spectral Analysis of Surface Waves (SASW) data are also indicated in Figure 4. In this project, the MMLS3 applied approximately 6900 single-wheel load repetitions per hour by means of four tires (each 300 mm (11.8 in) in diameter and 80 mm (3.1 in) wide) inflated to 690 kPa (100 psi) with a load of 2.1 kN (472.5 lbs). Five performance monitoring sessions (PMS) occurred during the test period from July 1999 to January 2000. Figure 5 shows the cumulative number of load repetitions for each MMLS3 PMS where transverse profiles were measured. SASW data were collected prior to MMLS3 trafficking and at MMLS3 PMS 1 and PMS 5. Temperature was controlled at approximately 60 °C (140 °F) at a depth of 12.5 mm (0.5 in) for all MMLS3 tests.

Researchers selected this temperature based on the critical temperature for permanent deformation during the four-day period when many of the replacement sections failed (*12*).

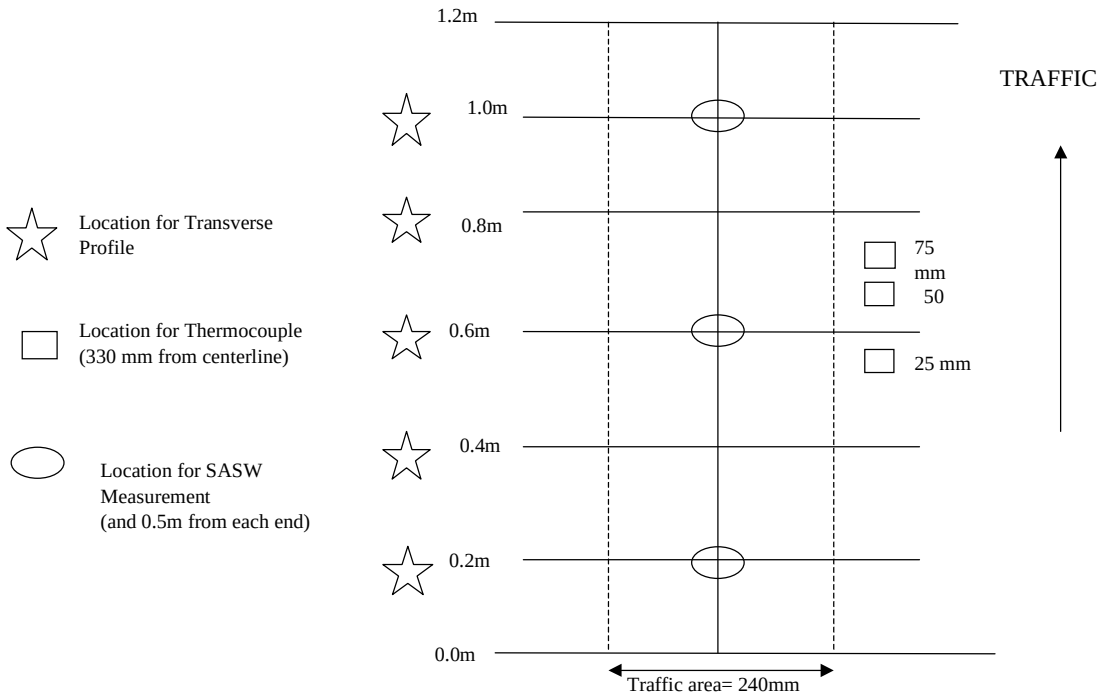

Figure 4. Instrumentation Layout (not to scale).

LABORATORY TESTS

In addition to performance monitoring during MMLS3 trafficking, researchers completed a limited laboratory testing program. During the summer of 1999, 15 cores were taken between the wheelpaths from each selected WesTrack section (Sections 01, 35, 37, and 38). Subsequent coring was conducted in March 2000 after MMLS3 trafficking was completed. At this time, two cores were obtained from each section in the MMLS3 wheelpath. Each core was cut into two specimens (150 mm (6 in) in diameter by 75 mm (3 in) in height), one from the top 75 mm (3 in) lift of the HMA layer and one from the bottom 75 mm (3 in) lift of this layer. For each core and/or specimen, bulk specific gravity, rice specific gravity, and calculated AV values were determined. Selected laboratory tests included two laboratory wheel-tracking devices (the HWTD and the APA), the TxDOT Static Creep test, and the indirect tensile (IDT) strength test. This section provides brief descriptions of each test.

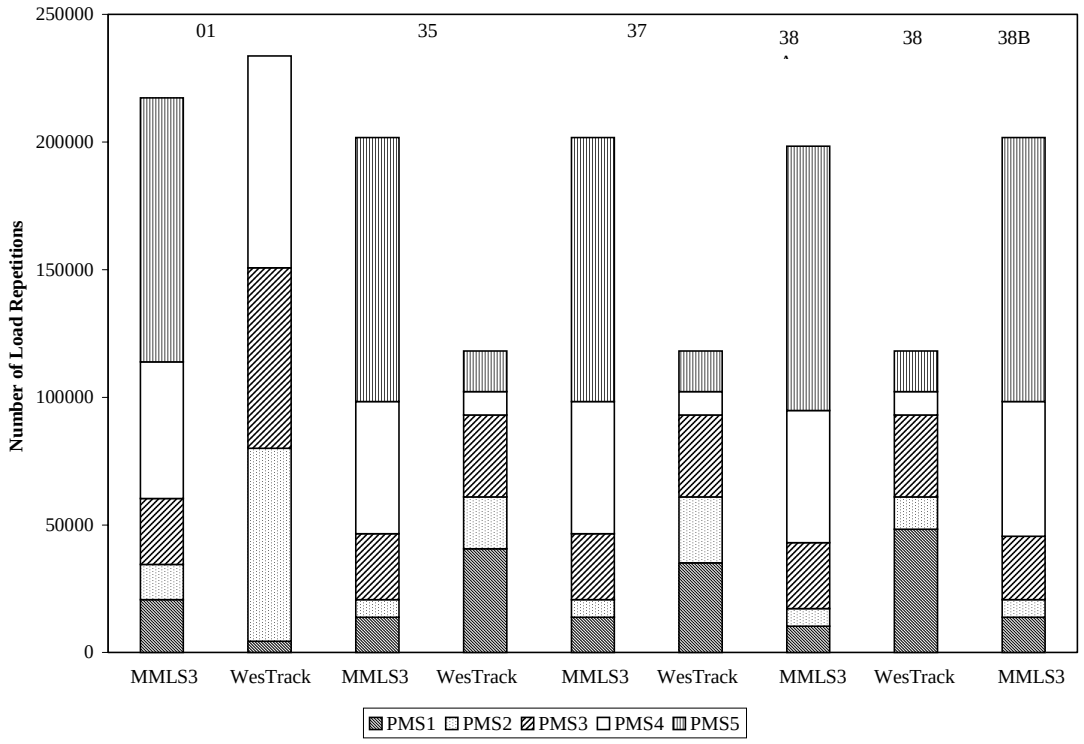

Figure 5. Performance Monitoring Session (PMS) Schedule.

Hamburg Wheel-Tracking Device (HWTD)

The HWTD was developed in Hamburg, Germany, during the 1980s and measures the combined effects of rutting and moisture susceptibility (*8*). TxDOT Test Method Tex-242-F gives a detailed description of the testing device, conditions, and procedure (*13*). TxDOT utilizes testing temperatures of 40 °C (104 °F) or 50 °C (122 °F) depending on the binder grade. Two steel wheels (204 mm (8 in) in diameter by 47 mm (1.9 in) in height) that each provide a 703 N (158 lbs) load move back and forth concurrently on two HWTD test specimens submerged in water. Each HWTD specimen is composed of two cylindrical specimens (150 mm (6 in) in diameter by 50 mm (2 in) in height) side by side with a flat surface cut off of each to fit them together. The wheels reciprocate over the specimen, and the maximum speed of the wheel is approximately 0.305 m/sec (1 ft/sec) at the midpoint of the specimen, where RD is measured. In addition to RD, a creep slope, stripping inflection point, and stripping slope are determined

(Figure 6). The creep slope relates to rutting primarily from plastic flow, and the stripping slope is a measure of the accumulation of rutting primarily from moisture damage. The stripping inflection point is the number of passes at the intersection of the creep slope and stripping slope lines, where stripping starts to dominate performance. This device is relatively new in the United States, and test or specification standards have not been developed. In Germany a maximum 4 mm (0.2 in) RD at 20,000 wheel passes is the failure criterion. The Colorado Department of Transportation recommends an allowable RD of 10 mm (0.4 in) at 20,000 wheel passes. TxDOT utilizes a 12.5 mm (0.5 in) failure limit for heavy duty stone matrix asphalt (SMA) and heavy duty stone filled asphalt concrete pavements. For research purposes, a 10 mm (0.4 in) failure at 20,000 wheel passes is used.

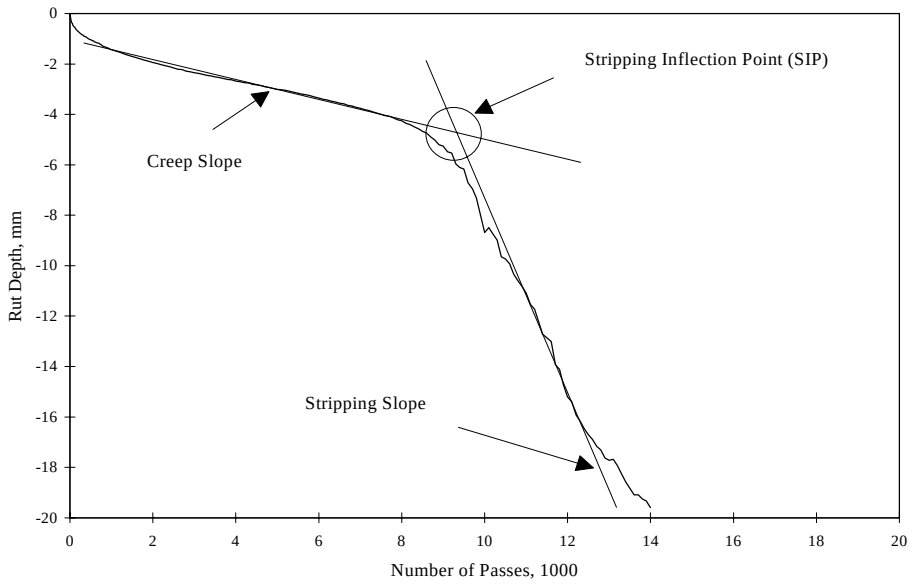

Figure 6. Hamburg Results Example.

Asphalt Pavement Analyzer (APA)

During the 1980s, the Georgia loaded wheel device was continuously under development by Lai under contract with the Georgia Department of Transportation (GDOT) (*8*). The APA was

developed in 1996 and is an updated version of the Georgia loaded wheel testing machine. This device is a multifunctional loaded wheel tester that has been used to evaluate permanent deformation, fatigue cracking, and moisture susceptibility (*14*, *15*, *16*, *17*).

Permanent deformation tests are conducted in a controlled temperature environment (30 °C to 70 °C (86 °F to 158 °F)) with either dry or submerged APA specimens. Each APA specimen is composed of two cylindrical specimens (150 mm (6 in) in diameter by 75 mm (3 in) in height) side by side with a flat surface cut off of each to fit them together. Each APA specimen is loaded independently up to 113 kg (250 lbs), and tire pressures up to 1380 kPa (200 psi) can be simulated. Two loaded wheels move concurrently back and forth on the top of inflated rubber hoses that each sit on a test specimen. The test runs for 8000 cycles, where a cycle is defined as two passes of the wheel, and an automated RD measuring system plots cycle or time versus average RD measured at four locations along the APA specimen. GDOT uses this test, and their performance criterion states that a mixture with an average RD of 7.6 mm (0.3 in) or greater is susceptible to rutting (*18*). For mixtures designed with the Superpave method, the criterion is lower at 5 mm (0.2 in) maximum average RD (*19*).

Static Creep Test

The TxDOT Static Creep test (Tex-231-F) is used to determine the resistance of bituminous mixtures to permanent deformation at temperatures similar to those experienced by materials in the field. Creep stiffness, permanent strain, and creep slope are determined in this test (*13*). A constant axial compressive stress (69 kPa (10 psi)) is applied to cylindrical specimens (101 mm (4 in) in diameter by 51 mm (2 in) in height) for one hour after three one-minute cycles of preloading with one-minute rest periods. After loading, the specimen is allowed to rebound for 10 minutes. The test is conducted at a constant temperature of 40 °C (104 °F). TxDOT has standard criteria for all three results obtained from this test, but they recently adopted a special provision that considers only a minimum creep stiffness criterion of 41 MPa (5950 psi) for use in ranking mixtures based on their relative performance.

Indirect Tensile (IDT) Strength Test

The TxDOT IDT strength test (Tex-226-F) is used to determine the indirect tensile strength of compacted bituminous material (*13*). A compressive load is applied (at a rate of 50 mm (2 in) per minute) across the diameter of a cylindrical specimen (150 mm (6 in) in diameter by 50 mm (2 in) in height) to induce tensile stress. When failure occurs, the maximum tensile stress is recorded as the IDT strength. This test can be used to rank relative performance of HMA mixtures or monitor damage due to trafficking.

CHAPTER 5. ANALYSIS METHODS

Researchers analyzed transverse profiles measured during both MMLS3 and full-scale truck trafficking by two different RD analysis methods. These methods are presented in this section, followed by a description of two methodologies for using the MMLS3 as a performance prediction tool. One methodology allows for the development of RD criteria, and the second methodology quantitatively predicts performance based on MMLS3 testing and theoretical analysis using measured laboratory data and maximum vertical compressive stress distributions under both loading conditions. This chapter concludes with a description of the use of SASW testing to track damage due to MMLS3 trafficking.

RUT DEPTH (RD)

Researchers used two methods of RD analysis to analyze and compare data from MMLS3 and full-scale truck trafficking at WesTrack. Descriptions of the Reference and Single Profile methods are presented in this section. For both the MMLS3 and full-scale trucks, the cumulative number of load repetitions for each PMS are provided in Figure 5.

Reference Method

The Reference method of analysis served as the primary means of calculating RD. This method requires measurement of two transverse profiles for each longitudinal location within a test section. An initial profile before trafficking and a second profile after a specific amount of trafficking for each PMS (Figure 5) are needed. In this report, average results at 0.4 m (1.3 ft), 0.6 m (2 ft), and 0.8 m (2.6 ft) are provided for the MMLS3. For the full-scale trucks, two replicate results at the beginning and end of the 40 m (131 ft) performance monitoring section were averaged. For the MMLS3 tests, all transverse profiles were measured using a laser profilometer. For the replacement sections (Sections 35, 37, and 38) during full-scale trafficking, the laser profilometer was also utilized. The more labor-intensive Dipstick, an Arizona DOT device, was used to gather data for Section 01 during full-scale truck trafficking, resulting in the collection of substantially fewer data points across the section. In addition, an initial profile for

this section before trafficking was not determined, so the initial profile was defined as that after approximately 4500 ESALs.

Since the two transverse profiles at each longitudinal location were taken on the same pavement section, the cross slope of each profile was assumed to be the same, and profiles of untrafficked regions were expected to be equivalent. Untrafficked regions for the MMLS3 included all areas across the pavement section except between the truck wheelpaths where MMLS3 trafficking occurred. For the full-scale trucks, untrafficked regions encompassed all areas except the two wheelpaths.

The first step in the analysis was to shift the trafficked profile vertically and rotate it about one end such that the sum of absolute differences between the two profiles in the untrafficked regions was minimized (Figure 7). This step was difficult to accomplish for Section 01 under full-scale trafficking due to a lack of detailed elevation data across the section, although estimates were obtained. This difficulty associated with differences in measuring equipment led to results for Section 01 RDs under full-scale traffficking by the Reference method that were not valid for comparative purposes and not included in most of the statistical analyses presented subsequently.

The second and final step was to determine RD at a given longitudinal location as the maximum difference between the two profiles in the trafficked region (between the wheelpaths for the MMLS3 and in the right wheelpath for the full-scale trucks) (Figure 7). Averages of the RDs at two (full-scale trucks) or three (MMLS3) replicate longitudinal locations were utilized in the subsequent analysis.

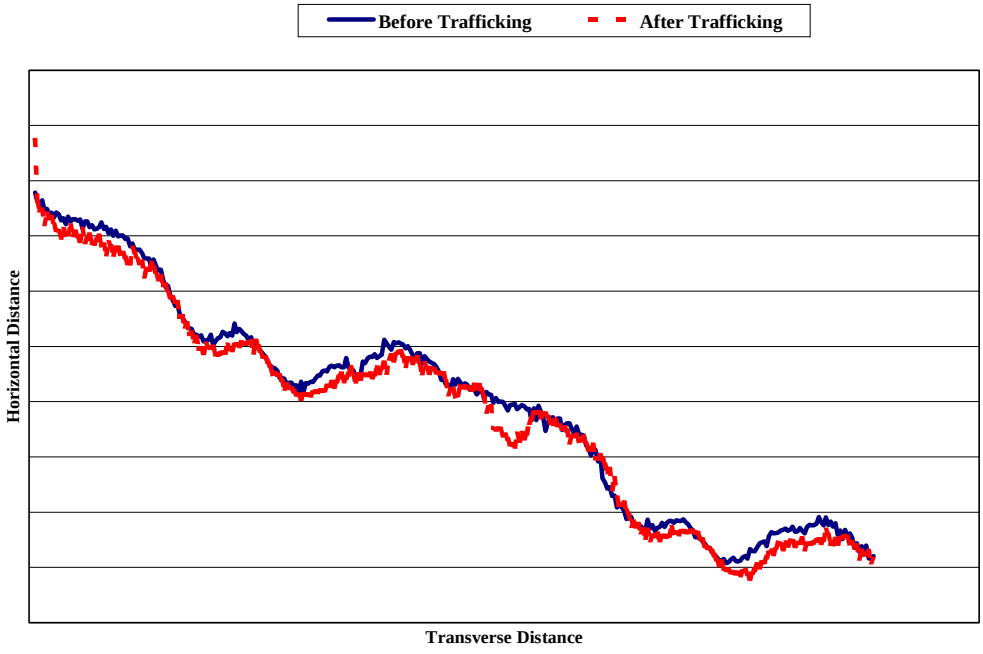

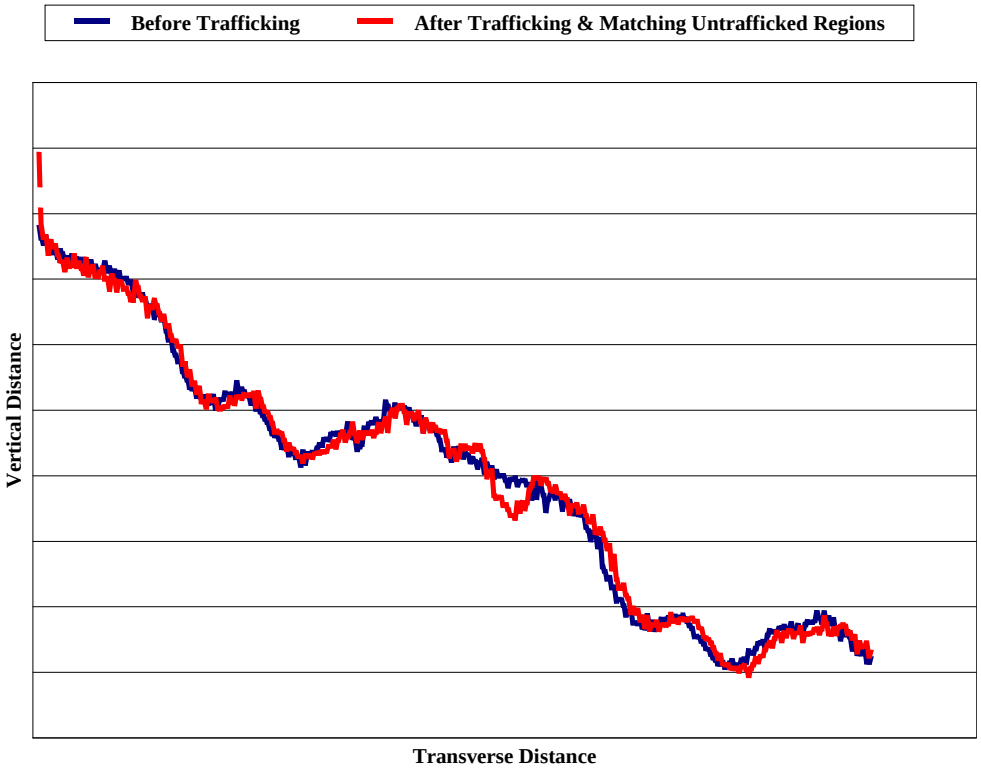

Figure 7. Reference Method

Single Profile Method

In determining RD at a specific PMS, the Single Profile method utilized only one transverse profile for each longitudinal location within a test section. Again, average RDs based on two (full-scale trucks) or three (MMLS3) profiles at replicate longitudinal locations are provided in this report. The first step in the analysis was to correct the profile for the cross-slope so that all RDs were determined from a single horizontal datum, defined as zero vertical elevation at one side of the section (Figure 8). The second step for laser profilometer data was to determine the moving average of vertical elevation for every five measurements (5 cm (2 in)). RD was then determined as the maximum difference between the horizontal datum and the corrected profile in the trafficked region (between the wheelpaths for the MMLS3 and in the right wheelpath of the full-scale trucks) (Figure 8). This method is somewhat subjective and does not account for variations in elevation that exist prior to trafficking. These variations can lead to appreciable errors, especially when measuring small RDs under scaled (MMLS3) loads.

RUT DEPTH CRITERIA

A methodology analogous to the one previously utilized by Williams and Prowell for other APT devices was used in this project to develop criteria for using the MMLS3 as a tool to assess rutting performance (*8*). First, corresponding average RDs by the Reference method after approximately 100,000 load repetitions under both the MMLS3 and full-scale trucks were plotted for all sections. For this analysis, RDs for Section 01 under full-scale trucks were interpolated using a linear trendline. Only RDs by the Reference method were utilized because this method is less subjective and accounts for variations in elevation that exist prior to trafficking. Using this plot, a maximum average RD under the MMLS3 corresponding to a user-defined unacceptable level of distress under full-scale loading (10mm (0.4 in)) was determined. This maximum average RD under the MMLS3 was then input to the following relationship to determine an average RD under the MMLS3 that was adjusted for variability associated with MMLS3 testing, a user-defined reliability level, and the number of replicates used to determine average RD:

$$\text{Maximum average sample RD} = y + t_{\alpha}(S/\sqrt{n})$$

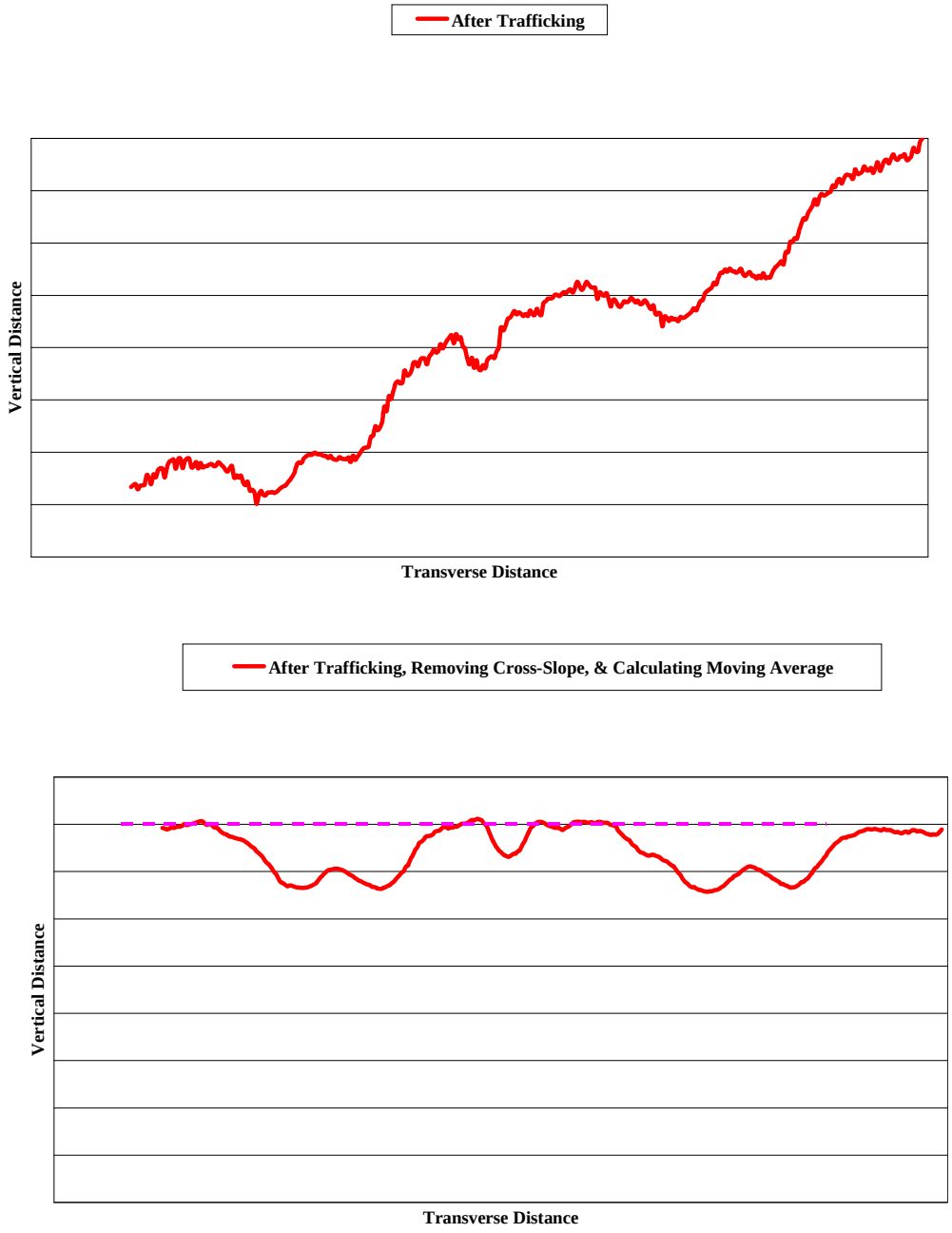

Figure 8. Single Profile Method.

where:

y= average RD

t_α= value of the *t* distribution with an area under the curve to the left of the value equal to (1-α)

S= standard deviation

n= sample size

The t_α value was based on the selected reliability level (1-α) and the *t* distribution. For this equation, the standard deviation (S) was determined based on a second plot of MMLS3 average RD versus standard deviation of RD at approximately 100,000 load repetitions for all sections. The selected standard deviation (S) value correlated with the maximum average RD under the MMLS3.

PERFORMANCE COMPARISON AND PREDICTION

For each of the four WesTrack sections investigated in this project, researchers conducted ELSYM5 analyses to compare theoretical and actual rutting performance under the MMLS3 and full-scale trucks. These comparisons were then used to demonstrate a methodology to predict performance based on MMLS3 testing and theoretical analysis using measured laboratory data and maximum vertical compressive stress distributions under both loading conditions.

ELSYM5 software was used to determine maximum vertical compressive stress with depth for each WesTrack section (Sections 01, 35, 37, and 38). Inputs to this analysis program included pavement structure (layer thicknesses), loading conditions (magnitude, location, and contact stress), and material properties (stiffness and Poisson's ratio for each layer or sublayer). All four sections consisted of 150 mm (6 in) of HMA on top of 300 mm (12 in) dense-graded crushed aggregate base course and 450 mm (18 in) of subgrade soil (including 300 mm (12 in) of engineered fill). In addition, the HMA layer was further divided into two sublayers, an upper 50 mm (2 in) layer and a lower 100 mm (4 in) layer to allow for more detailed temperature and material property characterization.

The loading conditions were also equivalent across sections. Researchers considered two different loading conditions for each section, one for the MMLS3 and one for the full-scale trucks. For the MMLS3 loading condition, a single tire inflated to 690 kPa (100 psi) at 25 °C (77 °F) with a wheel load of 2.1 kN (472.5 lbs) (approximately one-ninth of the load on one wheel of

a dual tire standard single axle) was used. For the full-scale truck condition, two dual tires inflated to 700 kPa (102 psi) at 25 °C (77 °F) each with a wheel load of 20 kN (4500 lbs) (the load on one wheel of a dual tire standard single axle) were utilized. For both cases, the maximum vertical compressive stress was beneath the center of a single tire.

Appropriate tire contact stresses for the MMLS3 tire were determined from a tire contact stress experiment and measurement of the increase in tire pressure with temperature. In the tire contact stress experiment, the MMLS3 was operated on top of a Kistler MODULAS Quartz Sensor Array at the Nevada Automotive Test Center (NATC) (*20*). This equipment was embedded in the pavement at WesTrack and measured vertical stresses under the moving MMLS3 tire at 17 mm (0.7 in) intervals. The maximum vertical contact stress for the MMLS3 tire was determined for inflation pressures of 552 kPa (80 psi), 690 kPa (100 psi), and 862 kPa (125 psi). These results are shown in Figure 9. Because the MMLS3 was used to traffick the WesTrack sections in an environmental chamber where the air temperature was held constant at 55 °C $\pm$ 3 °C (131 °F $\pm$ 5 °F), researchers conducted a second tire experiment to determine the tire pressure at this elevated temperature when the initial tire pressure was set to 690 kPa (100 psi) at ambient (25 °C (77 °F)) conditions. Using the results shown in Figure 9 for a tire pressure of 738 kPa (107 psi) at 55 °C (131 °F), a contact stress of 766 kPa (111 psi) was indicated and utilized with the MMLS3 load for the most representative results. The measured tire pressure at the elevated temperature was approximately three percent less than a value of 759 kPa (110 psi) determined using the ideal gas law at constant volume. The difference is probably due to a slight increase in the tire volume at the higher pressure.

These results were used to estimate an appropriate contact stress for the full-scale trucks. As described subsequently, the characteristic temperature of the HMA layer during truck trafficking of Section 01 varied substantially from that during trafficking of the replacement sections (Sections 35, 37, and 38). Using estimated air temperatures of 40 °C (104 °F) and 55 °C (131 °F) for Section 01 and the replacement sections, truck tire pressures were determined using the ideal gas law to be 735 kPa (107 psi) and 770 kPa (112 psi), respectively. These values were then adjusted according to the ratio of measured contact stress and theoretically calculated tire pressure for the MMLS3 tire to yield values for the truck stress analysis of 742 kPa (108 psi) and 777 kPa (113 psi) for Section 01 and the replacement sections, respectively.

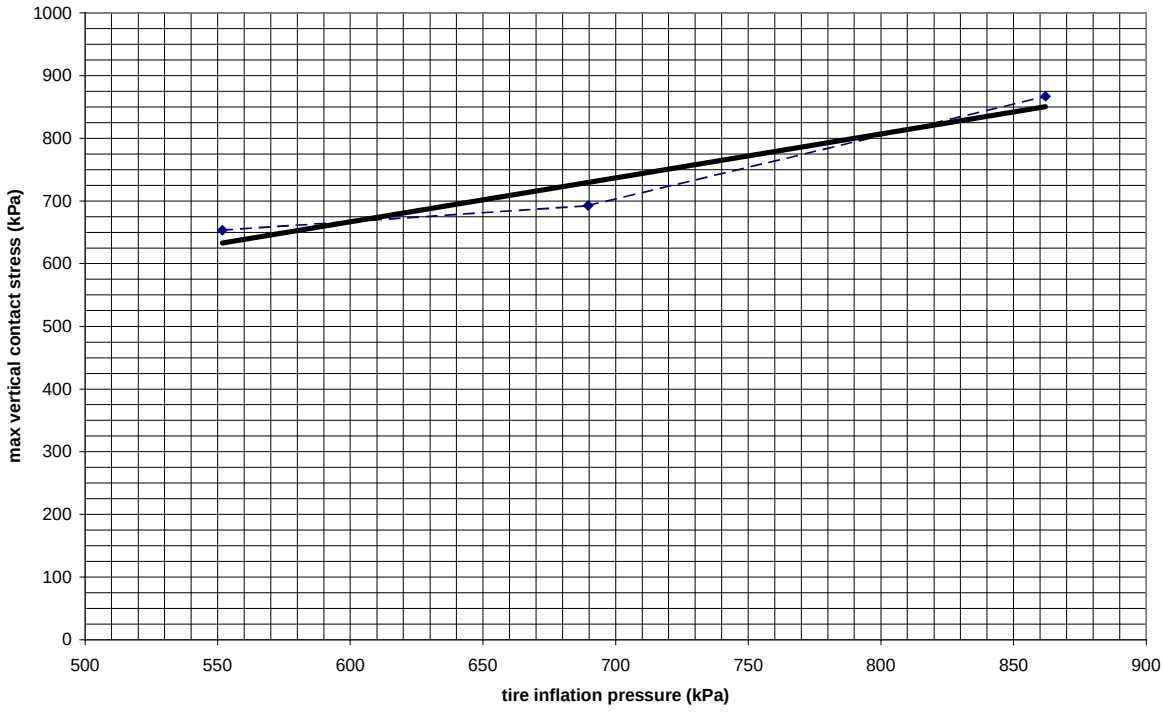

Figure 9. Tire Contact Stress Results.

Table 4 summarizes the material properties of each section under each loading condition and corresponding characteristic layer or sublayer temperatures. Poisson's ratio was assumed to be 0.35 for all layers of each section. Base and subgrade layers were characterized based on an extensive analysis by U.C. Berkeley to determine inputs for performance models (*21*).

Table 4. Material Properties of WesTrack Sections (@ Mid-Depth Temperature).

Loading	Section	Stiffness (MPa / psi) by Layer or Sublayer			
		50 mm (2 in) HMA	100 mm (4 in) HMA	300 mm (12 in) Base	450 mm (18 in) SG
MMLS3	01	308 / 44,660	596 / 86,420	138 / 20,010	117 / 16,965
Trucks		892 / 129,340	1359 / 197,055	138 / 20,010	110 / 15,950
MMLS3	35	197 / 28,565	359 / 52,055	138 / 20,010	117 / 16,965
Trucks		245 / 35,525	421 / 61,045	138 / 20,010	115 / 16,675
MMLS3	37	200 / 29,000	365 / 52,925	138 / 20,010	117 / 16,965
Trucks		249 / 36,105	428 / 62,060	138 / 20,010	109 / 15,805
MMLS3	38	248 / 35,960	453 / 65,685	138 / 20,010	117 / 16,965
Trucks		309 / 44,805	531 / 76,995	138 / 20,010	109 / 15,805

Researchers estimated the stiffness of each HMA sublayer from laboratory data adjusted for a dependency on loading frequency and temperature and the effect of aging (*22*). Complex shear moduli (G*) at 50 °C (122 °F) and 100 repetitions of the RSST-CH (1.4 Hz) for post-construction HMA specimens (sampled from Section 01 in October 1995 and from the replacement sections in July 1997) were used as an initial indicator of HMA stiffness. These values were then increased 75 percent and 30 percent for Section 01 and the replacement sections, respectively, based on the literature (*23*, *24*, *25*, *26*). These aged and untrafficked G* values were approximately equivalent to those measured for post-mortem HMA specimens sawn from cores sampled at the end of full-scale trafficking (March 1999). The aged and untrafficked G* values (based on measurements at 50 °C (122 °F) and 1.4 Hz) were then adjusted to loading frequencies of the MMLS3 (3.8 Hz) and the full-scale trucks (11.4 Hz) using a constant value of 0.493 at 50 °C (122 °F) for *A* in the following ratio (*27*):

$$A = \frac{\log \frac{E_1}{E_2}}{\log \frac{f_1}{f_2}}$$

Both of these frequencies were calculated based on measured tread lengths of 0.11 m (0.36 ft) and 0.25 m (0.82 ft) for an MMLS3 tire and a full-scale truck tire, respectively. After adjusting for frequency, these stiffnesses were further adjusted to characteristic mid-depth temperatures for the two HMA sublayers using semilog relationships between temperature and measured resilient

moduli of unaged HMA specimens for Sections 01 and 35 at –11.5 °C (11.3 °F), 2 °C (35.6 °F), 25 °C (77 °F), and 40 °C (104 °F) (*22*). An average slope (m) of 0.06 for the following relationship with *logk* a constant was utilized in this adjustment:

log (G* @ 50 °C, corrected for aging and frequency) = logk – m(Temperature)

The characteristic mid-depth temperatures for each section are provided in Table 5 and were based on time periods for full-scale truck trafficking to 100,000 ESALs or MMLS3 testing to 100,000 load repetitions. During MMLS3 trafficking, these temperatures were approximately constant due to the environmental chamber and determined from averages of temperature data measured with thermocouples near the surface (12.5 mm (0.5 in) depth) and at depths of 50 mm (2 in) and 75 mm (3 in). During full-scale truck trafficking, temperature was not controlled and varied daily and seasonally. For this case, measured peak pavement temperatures near the surface (12.5 mm (0.5 in)) were utilized with representative climate data and a similar pavement structure to determine the critical temperature for permanent deformation over the selected time period (*12*). For the replacement sections (Sections 35, 37, and 38) trafficked during July 1997, the characteristic critical temperatures for permanent deformation at 25 mm (1 in) and 100 mm (4 in) were approximately equal to those measured during the MMLS3 tests conducted at a controlled temperature from August through December 1999. For Section 01, however, there were much larger differences between corresponding characteristic temperatures (Table 5) due to the fact that full-scale truck trafficking occurred during the early spring (March through April 1996) when air and pavement temperatures were much cooler.

Table 5. Characteristic Mid-Depth Temperatures (°C / °F).

Section	Depth mm (in)	Loading	
		MMLS3	Trucks
01	25 (1)	55 / 131	37 / 99
	100 (4)	44 / 111	30 / 86
Replacement (35, 37, 38)	25 (1)	50 / 122	51 / 124
	100 (4)	40 / 104	42 / 108

Finally, researchers converted the *G** values adjusted for aging, frequency, and characteristic temperature to elastic stiffness (E) values by assuming elastic behavior and a Poisson's ratio of 0.35. This assumption is not correct, especially at high temperatures, but a more detailed viscoelastic characterization of the HMA material was not conducted in light of

the fact that ELSYM5 also assumes elastic behavior. It should be noted that these adjustments were necessary to characterize the materials tested in the field at WesTrack. If current laboratory testing results are available for materials to be tested with the MMLS3, the adjustment for aging becomes unnecessary. Temperature and frequency corrections, however, should still be considered and applied.

With these inputs, the distribution of maximum vertical compressive stress with depth was output from the ELSYM5 analysis for each section and loading condition. Post-mortem trenching investigations indicated that all permanent deformation under full-scale trucks occurred in the top 75 mm (3 in) of the HMA layer (*28*). A brief analysis of the relative deformation under the MMLS3 with a load significantly smaller in magnitude also showed that all deformation probably occurred in the top 75 mm (3 in) lift. Based on this information, the comparison of theoretical and actual rutting performance under the MMLS3 and full-scale trucks focused on the top 75 mm (3 in) of the HMA layer. A theoretical rutting ratio (TRR) was defined as the ratio of rutting determined using stress analysis under the MMLS3 to that under full-scale trucks:

$$TRR = \text{Theoretical } RD_{MMLS3} / \text{Theoretical } RD_{Trucks}$$

With examination of only the top 75 mm (3 in) of the HMA layer, the TRR could not be assumed equal to a one-third scaling factor and instead had to be based on pavement response and consideration of environmental and loading conditions. The first step in determining the TRR was to calculate a stress potential (SP) for each loading condition as the area under each respective maximum vertical compressive stress distribution curve to a depth of 75 mm (3 in). This methodology was first used in TxDOT Project No.0-1814 to analyze the Jacksboro results (*10*). Researchers calculated these areas with respect to depth using the trapezoidal rule as follows:

$$Area = (b-a)/n * [(f(a) + 2* [f(x_1) + f(x_2) \ldots f(x_{n-1})] + f(b)]$$

where a and b are the limits (0 mm (0 in) and 75 mm (3 in) depths), n is the increment of depth for which the function is determined (25 mm (1 in)), and $f(x)$ is the function (stress values). Next a correction factor to account for differences in temperature and frequency between the two loading conditions was calculated. This temperature-frequency correction (TFC) factor was determined as follows based on (1) the ratio of G* values adjusted for both temperature (T) and

frequency in the top 50 mm (2 in) HMA sublayer and (2) the assumption that the accumulation of permanent deformation is inversely proportional to shear stiffness (G*):

$$TFC = G^*_{\text{Truck T and 11.4 Hz}} / G^*_{\text{MMLS3 T and 3.8 Hz}}$$

Then the rutting potential ratio (RPR) under the MMLS3 to that under full-scale trucks was calculated as follows and used as the best estimate of the TRR:

$$RPR = TFC*SP_{MMLS3} / SP_{Trucks} = TRR$$

Next a field rutting ratio (FRR) was determined for each section as the ratio of RD under the MMLS3 to that measured under full-scale trucks:

$$FRR = RD_{MMLS3} / RD_{Trucks}$$

FRRs were calculated for RDs determined by the Reference RD analysis method because it was more systematic, less subject to error, and accounts for elevation variation prior to trafficking. Now a comparison was easily made between the TRR and the FRR through the use of yet another ratio, the rutting prediction ratio $(PR)_{rutting}$. The $PR_{rutting}$ was calculated simply by dividing the TRR by the FRR:

$$PR_{rutting} = TRR / FRR$$

With a desired $PR_{rutting}$ value of one, performance can be predicted for any pavement section following a theoretical analysis to determine the TRR, MMLS3 testing to determine the RD under this APT device, and final calculation of the predicted RD under full-scale trafficking through the use of the following relationships:

$$TRR = FRR = RD_{MMLS3} / RD_{Trucks}$$

$$RD_{Trucks} = RD_{MMLS3} / TRR$$

SPECTRAL ANALYSIS OF SURFACE WAVES (SASW)

SASW testing provided another means of tracking damage due to MMLS3 trafficking by evaluating changes in estimated moduli. Moduli within the trafficked section were expected to decrease when compared to moduli of a control section if fatigue or moisture damage occurred. Before MMLS3 trafficking began and at MMLS3 PMS 1 and PMS 5 (Figure 5), SASW data were collected at three locations within each test section (0.2 m (0.7 ft), 0.6 m (2 ft), and 1.0 m (3.3 ft)) and at two control points approximately 0.5 m (1.6 ft) from each end of a section (Figure 4). At each location, data were collected in both the longitudinal and transverse directions.

Resulting moduli within the trafficked sections were then compared to those at the control points to determine if damage was indicated. In addition, moduli measured at the control points at all three monitoring sessions were used to develop a temperature correction factor (CF) utilized in adjusting all moduli to a common temperature of 25 °C (77 °F).

SASW data were analyzed using the WinSASW computer program for a 150 mm (6 in) receiver spacing and a 150 mm (6 in) HMA layer thickness for each section. Inputs other than this spacing and layer thickness included waveforms from two receivers in the frequency domain that had been converted by a dynamic signal analyzer from the time domain (*29*). A plot of the relative phase of the cross-power spectrum (phase difference between two receivers) over the range of frequencies generated by a ball-bearing source was generated. Some of the poor quality data was then masked out of the analysis due to poor coherence (<0.9) or sharp changes in slope on the sawtooth plot (Figure 10) (*29*). Next, a dispersion curve of surface wave velocity (V_R) versus wavelength was generated based on the known distance and travel time (calculated from the phase difference) between sensors over all frequencies (Figure 11) (*29*). An average value of surface wave velocity (V_R) was calculated for wavelengths between 50 mm (2 in) and 150 mm (6 in) (the depth of the HMA layer), and this velocity was used with an assumed value of Poisson's ratio ($\nu = 0.35$) and a measured value of bulk specific gravity (γ / γ_{water}) to estimate Young's modulus (E) assuming elastic behavior from the following relationships (*30*):

$$V_S = C*V_R$$

$$G = (\gamma / g) * V_S^2$$

$$E = 2*G*(1 + \nu)$$

where V_S is the shear wave velocity, G is the shear modulus, γ is the measured unit weight, g is the acceleration due to gravity, and C is given by the following relationship:

$$C = 1.135 – 0.182 * \nu \text{ (for } \nu \geq 0.1)$$

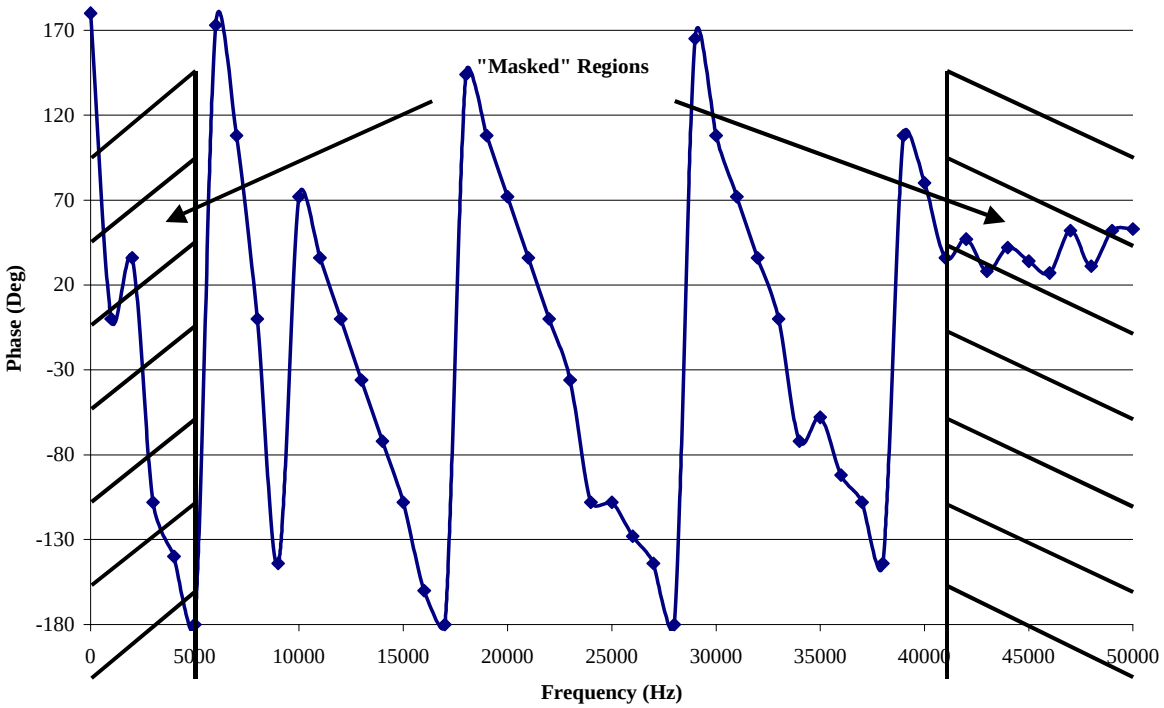

Figure 10. SASW Surface Wave Velocity versus Wavelength.

The next step in the SASW analysis was to correct the estimated SASW moduli to a standard temperature of 25 °C (77 °F) to allow for comparison and to account for differences in near surface pavement temperatures at each SASW monitoring session. Table 6 provides these pavement temperatures at the time the SASW measurements were collected. Moduli could not be corrected to the MMLS3 testing temperature (60 °C) (140 °F) because this high temperature was out of the range possible for collecting SASW data, and therefore, a correction factor (CF) could not be established. For each section, average moduli for the four control point measurements at each monitoring session were plotted against the temperature data to determine the slope of this relationship and the corresponding modulus at 25 °C (77 °F). CFs were then calculated for each section as the average ratio of this modulus and the modulus at the measured temperature. Finally, each modulus estimated from data collected within a trafficked section was multiplied by the corresponding CF to obtain a corrected modulus at 25 °C (77 °F).

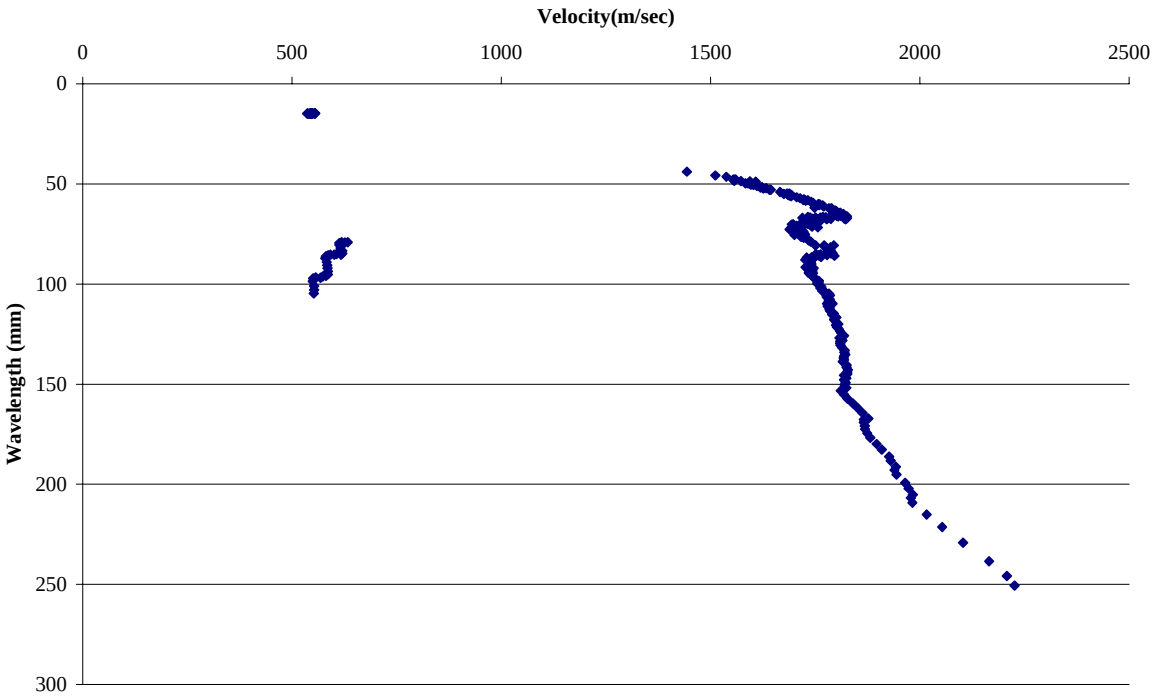

Figure 11. SASW Dispersion Curve.

Table 6. Surface Pavement Temperatures (°C / °F) During SASW Data Collection.

Section	Before Trafficking	PMS 1	PMS 5
01	24 / 75	25 / 77	14 / 57
35	31 / 88	24 / 75	13 / 55
37	23 / 73	23 / 73	12 / 54
38A	24 / 75	26 / 79	12 / 54
38B	22 / 72	27 / 81	12 / 54

After correcting to a standard temperature, estimated SASW moduli within trafficked sections, average control point moduli, and these average values plus and minus one standard deviation (across all monitoring sessions) were normalized by dividing by the average control point moduli for each corresponding section. Researchers then plotted these values against the number of load repetitions to determine if any fatigue or moisture damage was indicated during MMLS3 trafficking.

CHAPTER 6. FIELD RESULTS AND DISCUSSION

This chapter presents performance results of the selected sections based on MMLS3 and full-scale trafficking in the field.

RUTTING PERFORMANCE

The Reference and Single Profile RD analysis methods were used to analyze and compare data from MMLS3 and full-scale truck trafficking at WesTrack. Results for both methods including a statistical analysis are presented in this section. For both the MMLS3 and full-scale WesTrack trucks, Figure 5 provides the cumulative number of load repetitions for each PMS.

Reference Method Results

Figure 12 presents RD results based on the Reference method for both the MMLS3 and full-scale trucks. Logarithmic trend lines are shown for all data sets except Section 01 under full-scale trucks. Section 37 exhibited the largest potential for permanent deformation under the full-scale trucks, while trafficking under the MMLS3 showed that Section 35 experienced the largest amount of permanent deformation based on the Reference method. With the exception of Sections 35 and 37, the ranking provided by both MMLS3 and full-scale truck trafficking as shown by the trend lines was the same. In each case, Section 01 exhibited the lowest amount of rutting followed by Section 38. After approximately 100,000 load repetitions, the RD ratio for the replacement sections (MMLS3 to full-scale truck trafficking) varied from 0.4 to 0.6 at the critical temperature for permanent deformation (60 °C) (140 °F) during the selected hot summer period (Table 7). These ratios are within those suggested by scaling factors representing actual stress conditions and agree with the results of an analysis of pavement response at a different site in terms of maximum vertical compressive stress with application of a temperature and frequency correction factor (*11*). The RD ratio for Section 01 was greater than one due to substantial differences in temperature and aging between the two loading conditions and possible

differences introduced due to the fact that transverse profiles were measured with the Dipstick for Section 01 during truck loading. Results from the quantitative performance prediction analysis that accounts for the temperature and aging differences are presented subsequently (*11*).

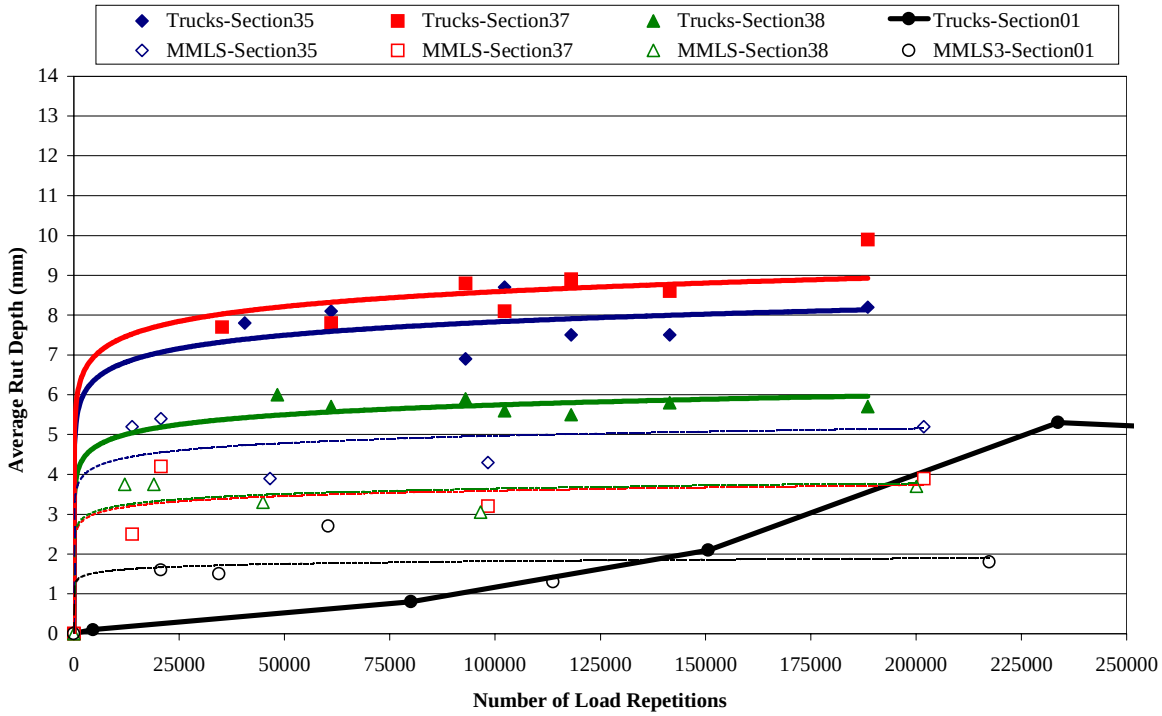

Figure 12. Reference Method Rut Depths.

Table 7. Ratio of Average Rut Depth (MMLS3/Trucks) at Approximately 100,000 Load Repetitions.

Section	RD Analysis Method	
	Single Profile	Reference
01	1.5	1.5
35	0.6	0.5
37	0.8	0.4
38	0.9	0.6

Researchers completed a statistical analysis of the RD data after 100,000 load repetitions to determine if there was any statistical difference among the results for each pair of sections. Assuming RD is normally distributed with equal variances across sections, *t*-tests at a 5 percent significance level (α=0.05) were conducted for each pair. For the MMLS3 data, three replicates

were used for all sections except Section 38 (six replicates). Replicate measurements were defined from RDs determined at three locations longitudinally along each section (0.4 m (1.3 ft), 0.6 m (2.0 ft), and 0.8 m (2.6 ft)) (Figure 4). The results for Sections 38A and 38B were combined (six replicates) based on the results of another *t*-test at a 5 percent significance level. For the full-scale truck data, two replicates were used for all sections. Replicate measurements were defined from RDs determined at two locations longitudinally along each section (at the beginning and end of the 40 m (131 ft) performance monitoring section). Table 8 provides results of this analysis.

Table 8. Statistical Analysis of Rut Depth by Reference Method at Approximately 100,000 Load Repetitions.

(Reject or Cannot Reject Null Hypothesis)
[α=0.05, Null Hypotheses: $\mu_X=\mu_Y$]

		Loading	
Section X	**Section Y**	**MMLS3**	**Trucks**
01	35	Reject	Not valid
01	37	Reject	Not valid
01	38	Cannot Reject	Not valid
35	37	Cannot Reject	Cannot Reject
35	38	Reject	Cannot Reject
37	38	Cannot Reject	Cannot Reject

Based on Table 8 (after 100,000 load repetitions), MMLS3 testing leads to the conclusion that the performance of Section 01 is statistically different than both Sections 35 and 37 but the same as Section 38. Section 35 is statistically only the same as Section 37, with Sections 37 and 38 also statistically the same. Average RDs for these sections after approximately 100,000 load repetitions were 1.8 mm (.008 in), 4.3 mm (0.17 in), 3.2 mm (0.13 in), and 3.1 mm (0.12 in) for Sections 01, 35, 37, and 38, respectively. Statistically significant differences in RD between sections ranged from 1.2 mm (0.05 in) to 2.5 mm (0.1 in). Differences in RD from 0.1 mm (0.004 in) to 1.3 mm (0.05 in) resulted in acceptance of the null hypothesis of equal means.

Based on full-scale truck trafficking, all the coarse-graded replacement sections with equivalent AV levels (Sections 35, 37, and 38) exhibited statistically equivalent performance after approximately 100,000 load repetitions (Table 8). Performance comparisons with Section 01 were not valid for reasons previously described. At this trafficking level, average RDs for

Sections 01, 35, 37, and 38 were 1.2 mm (0.05 in), 8.7 mm (0.34 in), 8.1 mm (0.32 in), and 5.6 mm (0.22 in), respectively. Among the replacement sections, the minimum and maximum RD differences between sections were 0.6 mm (0.02 in) and 3.1 mm (0.12 in) with both statistically equivalent. As expected, the ranges in performance required to statistically discern differences under full-scale loading are larger than for scaled loading.

Table 9 shows equivalent performance ranking results based on RDs by the Reference method under both the MMLS3 and full-scale trucks at approximately 100,000 load repetitions. These rankings are discussed at length in a subsequent chapter.

Table 9. Performance Ranking.

(A= Best Performance=Highest Stiffness=Most Aging)				
Laboratory / Field Test (RD Analysis Method)	**Section**			
	01	**35**	**37**	**38**
RSST-CH to 5% γ_p	A	D	C	B
Aging by RSST-CH (G*@100reps)	A	D	C	B
Static Creep Stiffness	A	C	D	B
Static Creep γ_p	A	B	D	C
HWTD	A	D	C	B
APA	C	A	D	B
MMLS3 (Single Profile) @ 100,000	A	C	D	B
MMLS3 (Reference) @ 100,000	A	D	C	B
WesTrack Trucks (Single Profile) @100,000	A	C	D	B
WesTrack Trucks (Reference) @100,00	A	D	C	B

Single Profile Method Results

Figure 13 presents RD results based on the Single Profile Method for both the MMLS3 and full-scale trucks. Logarithmic trend lines are shown for all data sets except Section 01 under full-scale trucks. Again, for both the MMLS3 and the full-scale trucks, Section 01 showed the best performance followed by Section 38. Section 37 exhibited the highest RD under the MMLS3, but a significant difference in RD under the full-scale trucks between Sections 35 and 37 could not be established using this method. Performance ranking by the trendlines or based on RDs at 100,000 load repetitions under the MMLS3 and the full-scale trucks was equivalent

(Table 9). Final analysis indicated that after 100,000 load repetitions, the RD ratio (MMLS3 to full-scale trafficking) varied from 0.6 to 1.5 (Table 7). These ratios are slightly larger than those based on the Reference method results but still reasonable.

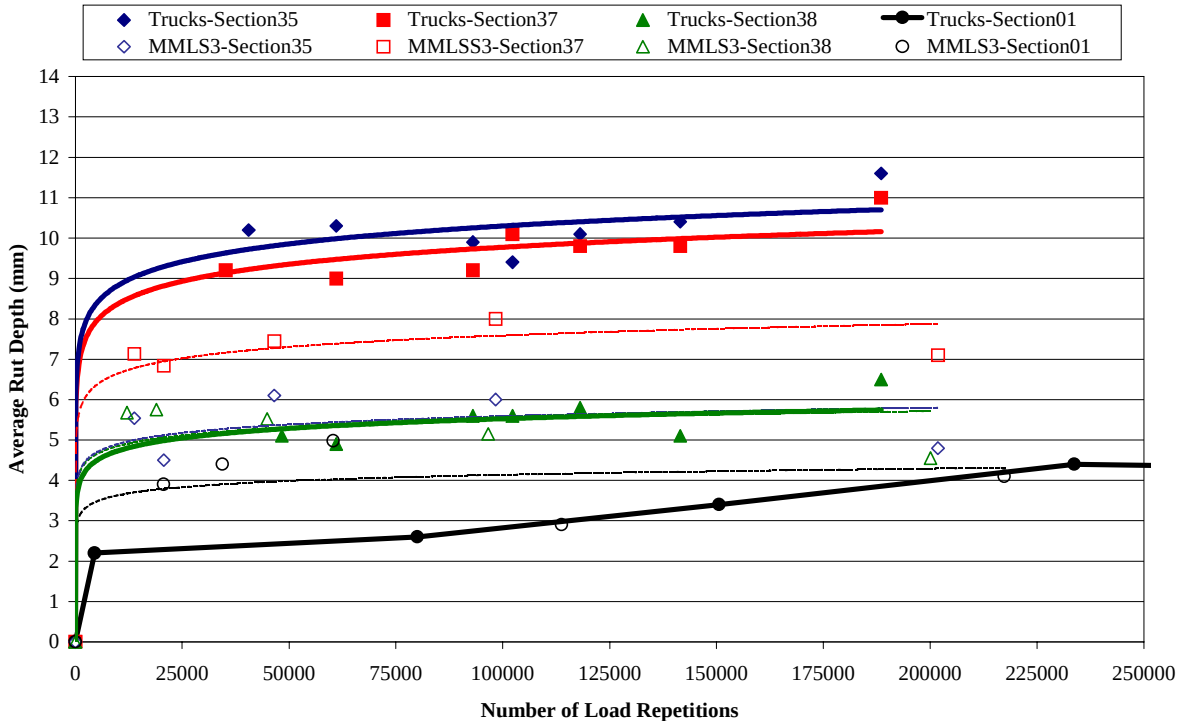

Figure 13. Single Profile Method Rut Depths.

Researchers completed a statistical analysis of the RD data after 100,000 load repetitions to determine if there was any statistical difference among the results for each pair of sections. Assuming RD is normally distributed with equal variances across sections, *t*-tests at a 5 percent significance level (α=0.05) were conducted for each pair. Replicates were defined in the same manner previously described. Table 10 gives results of this analysis.

Based on Table 10, MMLS3 testing leads to the conclusion that all sections are statistically different from each other. After approximately 100,000 load repetitions, average RDs for Sections 01, 35, 37, and 38 were 4.1 mm (0.16 in), 6.0 mm (0.24 in), 8.0 mm (0.32 in), and 5.1 mm (0.20 in), respectively. Differences in RD that ranged from 0.9 mm (0.04 in) to 3.9 mm (0.15 in) were shown to be statistically significant.

Table 10. Statistical Analysis of Rut Depth by Single Profile Method at Approximately 100,000 Load Repetitions.

(Reject or Cannot Reject Null Hypothesis)

[α=0.05, Null Hypotheses: $\mu_X=\mu_Y$]

		Loading	
Section X	**Section Y**	**MMLS3**	**Trucks**
01	35	Reject	Reject
01	37	Reject	Reject
01	38	Reject	Reject
35	37	Reject	Cannot Reject
35	38	Reject	Reject
37	38	Reject	Reject

Based on full-scale truck trafficking, Sections 35 and 37 performed equivalently but differently than Section 38. At approximately 100,000 load repetitions, average RDs for Sections 01, 35, 37, and 38 were 2.8 mm (0.11 in), 9.4 mm (0.37 in), 10.1 mm (0.40 in), and 5.6 mm (0.22 in), respectively. The smallest difference in RD was 0.7 mm (0.03 in) with acceptance of the null hypothesis of equal means. The range of statistically significant differences in RD between sections was 2.8 mm (0.11 in) to 7.3 mm (0.29 in). Again, the ranges in performance required to statistically discern differences under full-scale loading are larger than for scaled loading.

Table 9 shows equivalent performance ranking results based on RDs by the Single Profile method under both the MMLS3 and full-scale trucks at approximately 100,000 load repetitions. These rankings show RD increasing with AC for the replacement sections (Sections 35, 37, and 38). Section 01 with a different aggregate gradation (fine) showed the smallest RD or best performance.

Comparison of MMLS3 and Full-Scale Trucks

Table 11 shows the comparative results of a statistical analysis of RDs by section trafficked with the MMLS3 and full-scale trucks. This analysis for the replacement sections (Sections 35, 37, and 38) generally showed that the RDs are significantly different under the two different loads. Again, the comparison of RDs by the Reference method for Section 01 was not valid. RDs by the Single Profile method for this section were statistically equivalent. This result probably stems from the larger stiffness of the HMA layer at constant temperature as compared

to the other sections and the age of and representative temperature (and their effect on increasing stiffness) for Section 01 under the two different loading conditions (*22*). In other words, RDs under full-scale loading of a stiff section such as Section 01 may be equivalent to RDs under the MMLS3 tested at a high temperature. The MMLS3 trafficking temperature (approximately 60 °C (140 °F) at 12.5 mm (0.5 in) depth) was derived based on temperatures during the early life (up to 60,000 load repetitions) of the replacement sections. This temperature was substantially greater than a representative temperature (37 °C (99 °F) at 25 mm (1 in) depth) for the early life (up to 100,000 load repetitions) of Section 01 (*11*). Again, this effect complicates comparative analyses but can be accounted for in the quantitative performance prediction analysis presented subsequently.

Table 11. Statistical Comparison of Rut Depth for MMLS3 and Full-Scale Truck Loading at Approximately 100,000 Load Repetitions.

(Reject or Cannot Reject Null Hypothesis)
[α=0.05, Null Hypotheses: $\mu_X=\mu_Y$]

Section X (MMLS3)	Section Y (Trucks)	RD Analysis Method	
		Single Profile	Reference
01	01	Cannot Reject	Not valid
35	35	Reject	Reject
37	37	Reject	Reject
38	38	Cannot Reject	Reject

Comparison of RD Analysis Methods

In comparison, resulting RDs from the Single Profile method were generally larger than those obtained using the Reference method. Table 12 shows the comparative results of a statistical analysis of RDs by section determined by both methods (Figures 14 and 15).

Table 12. Statistical Comparison of Rut Depth for Reference and Single Profile Methods at Approximately 100,000 Load Repetitions.

(Reject or Cannot Reject Null Hypothesis)

[α=0.05, Null Hypotheses: $\mu_X=\mu_Y$]

Section X (Reference)	Section Y (Single Profile)	Loading	
		MMLS3	Trucks
1	1	Reject	Reject
35	35	Reject	Cannot Reject
37	37	Reject	Reject
38	38	Reject	Cannot Reject

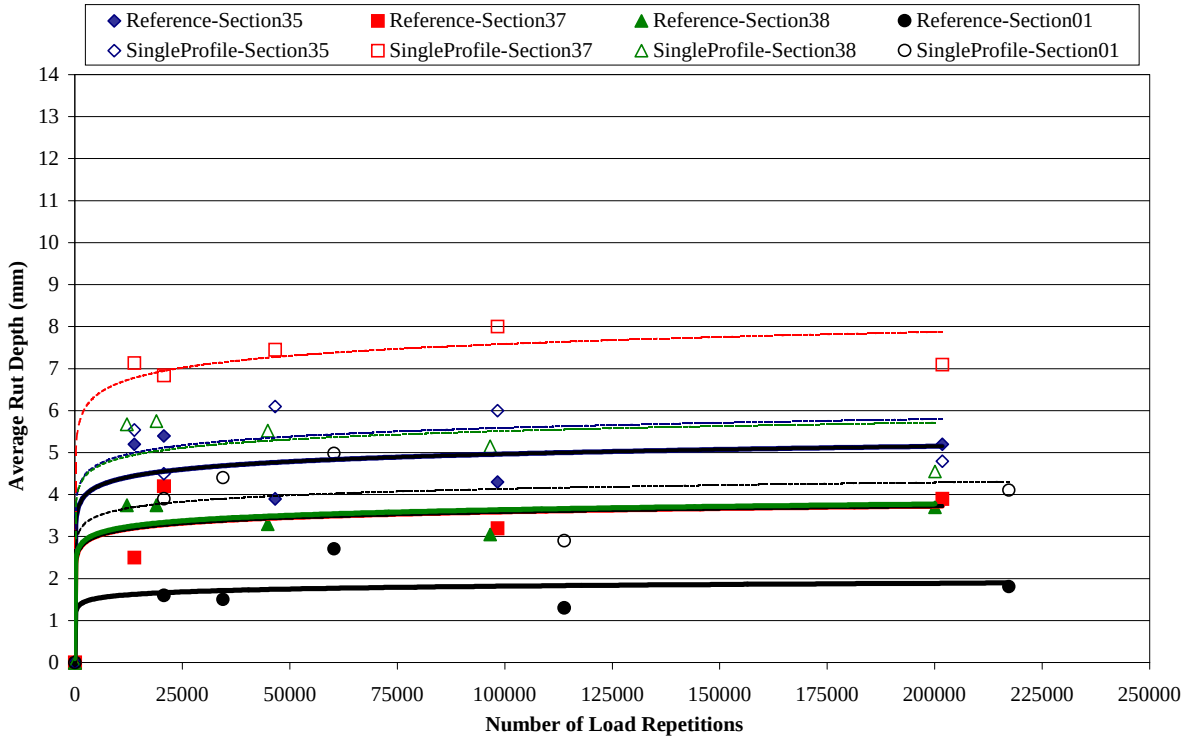

Figure 14. MMLS3 Rut Depths.

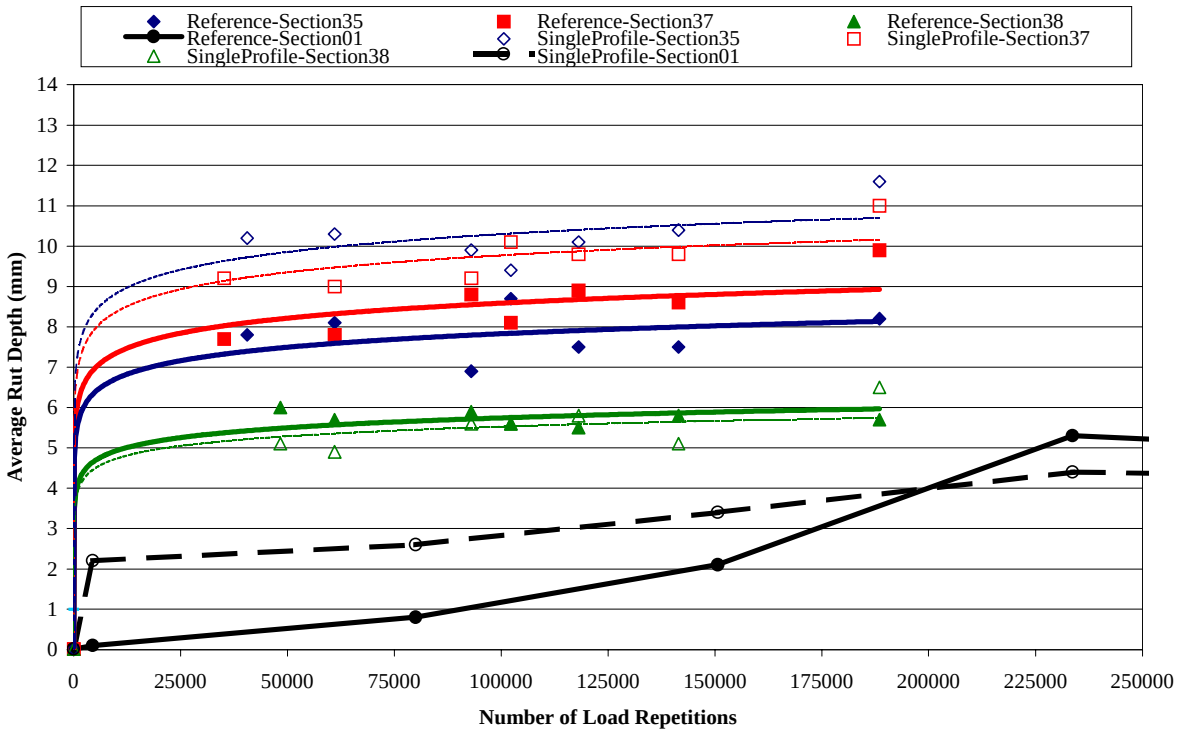

Figure 15. Full-Scale WesTrack Trucks Rut Depths.

Comparison of MMLS3 results indicated that RDs determined by the Reference and Single Profile methods were statistically different for all sections. For the full-scale truck results, RDs from both methods were statistically equivalent for Sections 35 and 38, but a significant statistical difference between the two methods was shown for Sections 01 and 37. In this case, a comparison for Section 01 RDs under full-scale trafficking was valid because Dipstick data was used in both analysis methods. These results emphasize the need to select a standard RD analysis method. Researchers recommend the Reference method because it is less subjective, and the probability of introducing error is minimized by consistently and systematically matching the untrafficked regions to an initial profile before trafficking.

OTHER EFFECTS OF MMLS3 TRAFFICKING

To analyze the effects of MMLS3 trafficking, researchers collected core samples before and after trafficking and took SASW measurements before, during, and after trafficking. Changes in AV and IDT strength were determined by laboratory tests. Table 13 presents results for the specimens cut from the top 75 mm (3 in) of each core. Property changes for the specimens cut from the bottom 75 mm (3 in) of each core were less than for the top specimens. The change in AV varied from 13 percent to 35 percent. These results indicated that the MMLS3 did cause densification in the HMA layer. Section 01 exhibited the smallest change in AV, again probably due to its age and relative stiffness.

Table 13. Effects of MMLS3 Trafficking.

Property	Section				
	01	**35**	**37**	**38A**	**38B**
AV Avg (Before)%	5.4	7.8	8.2	7.1	7.1
AV Avg (After)%	4.7	6.5	6.5	4.6	5.6
IDT Avg (Before) MPa (psi)	1.96 (284)	0.96 (139)	0.97 (141)	1.16 (168)	1.16 (168)
IDT Avg (After) MPa (psi)	1.93 (280)	1.00 (145)	0.99 (144)	1.31 (190)	1.16 (168)
AV Ratio	0.87	0.83	0.79	0.65	0.78
IDT Ratio	0.99	1.05	1.03	1.13	1

The results of IDT strength testing before and after trafficking showed that there was no significant change. These results were similar to what was found at another field site in Texas, emphasizing that this parameter cannot be used to clearly detect distress (*31*).

Figures 16 through 19 present the results of the SASW analysis conducted as previously described. Normalized ratios of trafficked to control point moduli are plotted against MMLS3 load repetitions, with the normalized average and average plus and minus one standard deviation of the control point moduli shown as horizontal lines. For all sections, the normalized ratios were approximately within one standard deviation of the normalized average control point moduli. Therefore, in agreement with visual inspection of the MMLS3 test sections and cores taken after trafficking, these results did not indicate any damage due to fatigue or moisture during MMLS3 trafficking. Some damage may have occurred but was offset by the

densification effect shown with both the AV results and the slight increasing trend in SASW moduli (*10*). These plots also show that there was more variability in the SASW moduli for the replacement sections (Sections 35, 37, and 38) than there was for the stiff Section 01.

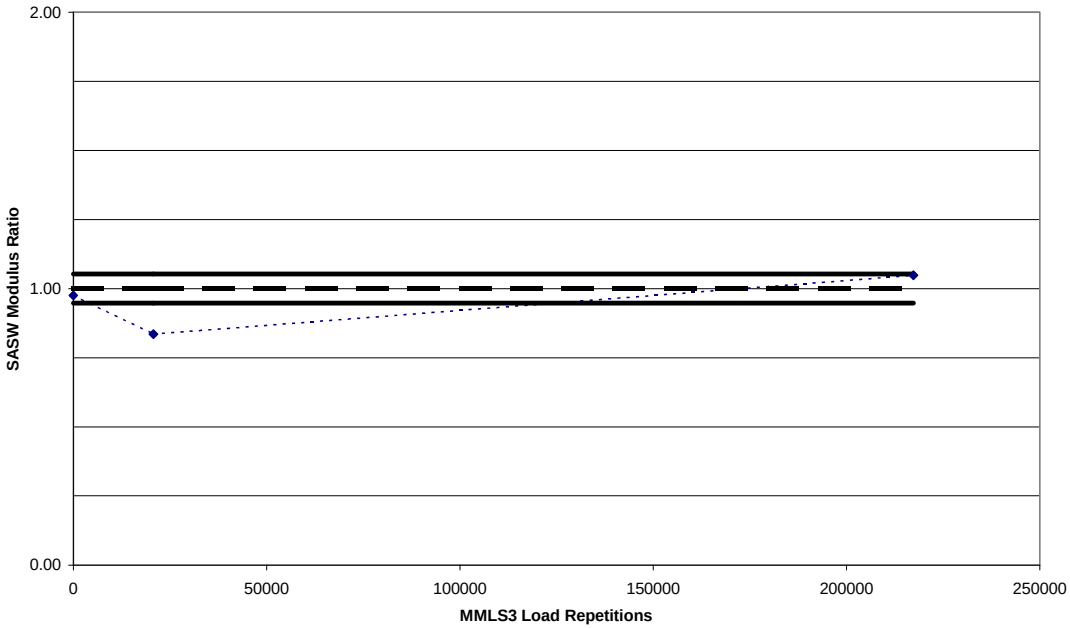

Figure 16. Section 01 SASW Analysis.

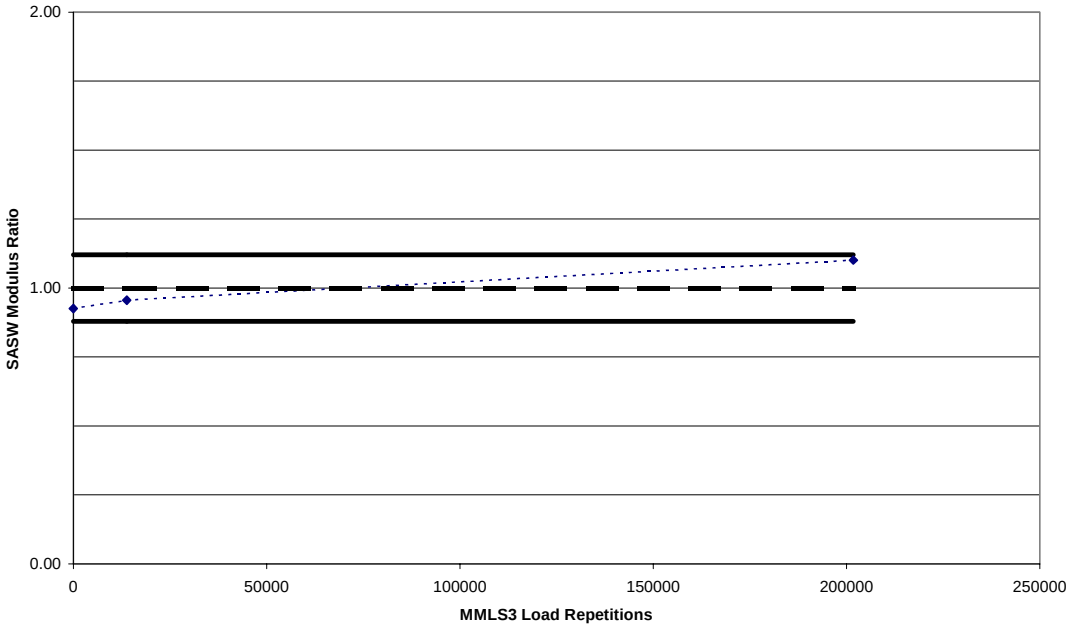

Figure 17. Section 35 SASW Analysis.

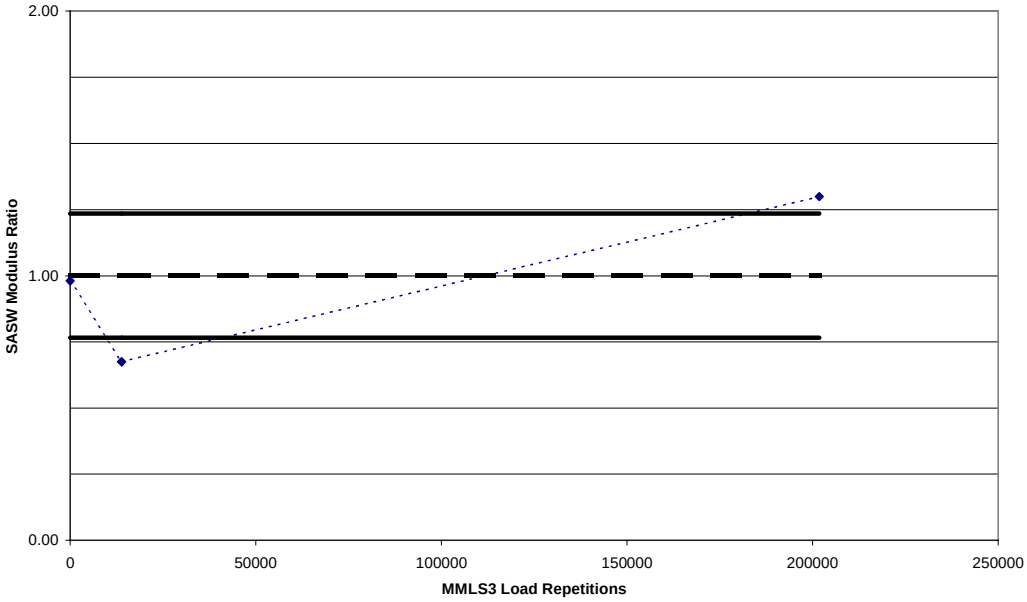

Figure 18. Section 37 SASW Analysis.

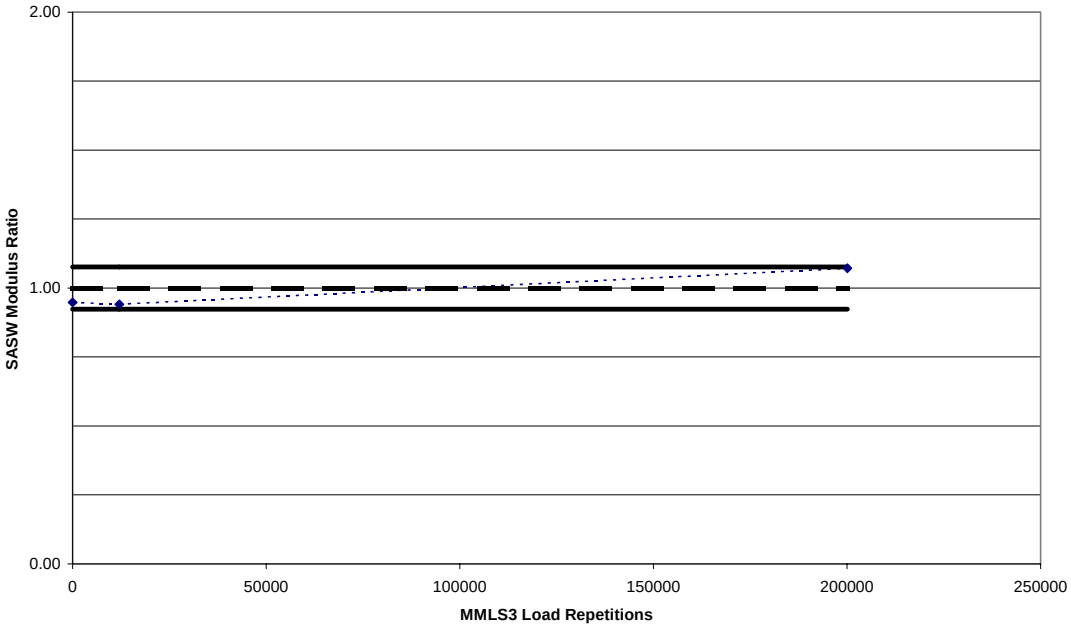

Figure 19. Section 38 SASW Analysis.

CHAPTER 7. LABORATORY RESULTS AND DISCUSSION

This chapter presents laboratory test results and a discussion of performance rankings based on these results.

WHEEL-TRACKING DEVICES

In the HWTD, one replicate specimen was submerged in water in a rigid mold and trafficked at 50 °C (122 °F). As the test proceeded, RD was measured automatically and continuously until either a 20 mm (0.8 in) rut was obtained or 20,000 wheel passes were applied. Table 14 shows the HWTD results for specimens from the top 50 mm (2 in) lift of the HMA layer. With a 10 mm (0.4 in) failure criterion, only Section 35 was predicted to fail. Table 9 shows performance rankings based on the measured RD at 20,000 wheel passes or when the test was stopped. These rankings show that Section 01 was predicted to perform the best in terms of rutting, followed by Section 38 and then Sections 37 and 35.

Table 14. HWTD Results at 50 °C (122 °F).

Section	Permanent Deformation mm (in)	Cycles to Failure	Stripping Inflection Point (cycles)	Creep Slope mm/cycle (in/cycle)	Stripping Slope mm/cycle (in/cycle)
01	4.6 (0.18)	> 20,000	N/A	-10.81 (-0.43)	N/A
35	19.7 (0.78)	19,600	10,240	-3.00 (-0.12)	-0.78 (-0.03)
37	9.5 (0.37)	> 20,000	13,580	-3.65 (-0.14)	-2.32 (-0.09)
38	7.4 (0.29)	> 20,000	N/A	-4.85 (-0.19)	N/A

In the APA, one replicate specimen from the top 75 mm (3 in) lift of the HMA layer was trafficked for 8000 cycles at 60 °C (140 °F) using a reciprocating steel wheel with an average load of 700 N (157 lbs) on top of a stiff rubber hose pressurized with air at 0.69 MPa (10 psi). As the test proceeded, average RD along the specimen was determined automatically based on four measurements taken along the length of the specimen. Table 15 provides the APA test results. With a 5 mm (0.2 in) failure criterion, all sections were expected to fail. Table 9 shows performance rankings based on the average RD at 8000 cycles. Contrary to most of the rankings

based on field and laboratory results, these rankings show that Section 35 was predicted to perform the best in terms of rutting, followed by Section 38 and then Sections 01 and 37.

Table 15. APA Results at 60 °C (140 °F).

Section	Permanent Deformation mm (in)	Cycles to Failure
01	5.7 (0.22)	< 8,000
35	5.0 (0.20)	8,000
37	6.0 (0.24)	< 8,000
38	5.3 (0.21)	< 8,000

OTHER PERFORMANCE PREDICTION TESTS

In the Static Creep test, three replicate cylindrical specimens from the top 50 mm (2 in) lift of the HMA layer were tested at 40 °C (104 °F). Table 16 provides the results from this test. All sections exhibited satisfactory creep stiffnesses based on a limiting value of 41 MPa (5945 psi). Table 9 shows performance rankings based on static creep stiffness and permanent strain. Based on the static creep stiffness values, Section 01 was predicted to perform the best in terms of rutting, followed by Section 38 and then Sections 35 and 37.

Table 16. Static Creep Test Results at 40 °C (104 °F).

Section	Creep Stiffness MPa (psi)	Permanent Strain	Creep Slope (/sec)
01	79 (11455)	0.17	2.2
35	52 (7540)	0.41	3.4
37	45 (6525)	0.61	5.6
38	54 (7830)	0.6	8.6

CHAPTER 8. PERFORMANCE PREDICTION

This chapter compares performance rankings based on field and laboratory results, followed by the results of the development of RD criteria. The chapter concludes with results demonstrating a methodology to quantitatively predict performance based on MMLS3 testing and theoretical analysis using measured laboratory data and maximum vertical compressive stress distributions under both loading conditions.

PERFORMANCE RANKING AND COMPARISON

All the laboratory tests and field tests were completed to enable a comparison of performance. Table 9 presents performance rankings for all field tests and all laboratory tests conducted in this project and laboratory test results obtained from the WesTrack database (*22*). This database was queried to find RSST-CH results that included the number of RSST-CH repetitions to 5 percent permanent shear strain (γ_p) and dynamic shear stiffness (G*) at 100 RSST-CH repetitions (*4*). Changes in shear stiffness (G*) from before WesTrack truck trafficking to after trafficking were used to assess aging. The number of RSST-CH repetitions to 5 percent γ_p was used to a predict performance to a failure criterion of 12.5 mm (0.5 in) of rutting.

Based on these results, Section 01 aged the most, as expected, and showed the highest shear and static creep stiffness values. Rankings by RSST-CH and HWTD performance prediction were equivalent. These ranking were also equivalent to the RD rankings by the Reference method. The RD rankings by the Single Profile method were also similar. In addition, all of the rankings based on the field results using either analysis method were in close agreement, especially when considering the results of the statistical analysis. The only two sets of rankings based on laboratory tests that were not consistent with the others were those from the Static Creep test (permanent strain) and the APA. This anomaly in the static creep γ_p ranking agrees with recent TxDOT experience. For the APA rankings, the discrepancy may partly be attributed to the fact that only one replicate specimen was used for each section. This coupled with a relatively high coefficient of variation (27 percent for Section 37 and 20 percent for

Section 38 for APA test results for WesTrack sections reported in a previous study) may have had an effect on the rankings (*22*).

RUT DEPTH CRITERIA

RD criteria were developed for using the MMLS3 as a performance prediction tool based on the methodology described previously. Results from the Reference RD analysis method were utilized in this methodology.

For the Reference method, the maximum average RD under the MMLS3 for a 10 mm (0.4 in) RD in the field under full-scale trucks was 4.5 mm (0.2 in) (Figure 20). For this value, the standard deviation (S) was 0.68 (Figure 21). Using these data, RD criteria for the MMLS3 after approximately 100,000 load repetitions with two to five replicate RD measurements were calculated and are shown in Table 17 for a 95 percent reliability level. These criteria were based on MMLS3 testing at the critical temperature for permanent deformation over an extremely hot period during the summer (*12*). For a sample size of three, an acceptable average RD by the Reference method under the MMLS3 is 3.5 mm (0.14 in). With this criterion, Section 35 (4.3 mm (0.17 in)) was assessed as failing to provide adequate resistance to rutting. This result concurs with the performance ranking results and the statistical analysis, with Section 35 exhibiting the worst rutting performance for the majority of field testing results (Tables 8, 9, and 10).

Table 17. Rut Depth Criteria for MMLS3 after Approximately 100,000 Load Repetitions.

Sample Size (n)	$t_{0.05}$	Acceptable Mean Rut Depth (mm / in)
2	2.92	3.0 / 0.12
3	2.35	3.5 / 0.14
4	2.13	3.7 / 0.15
5	2.02	3.9 / 0.15

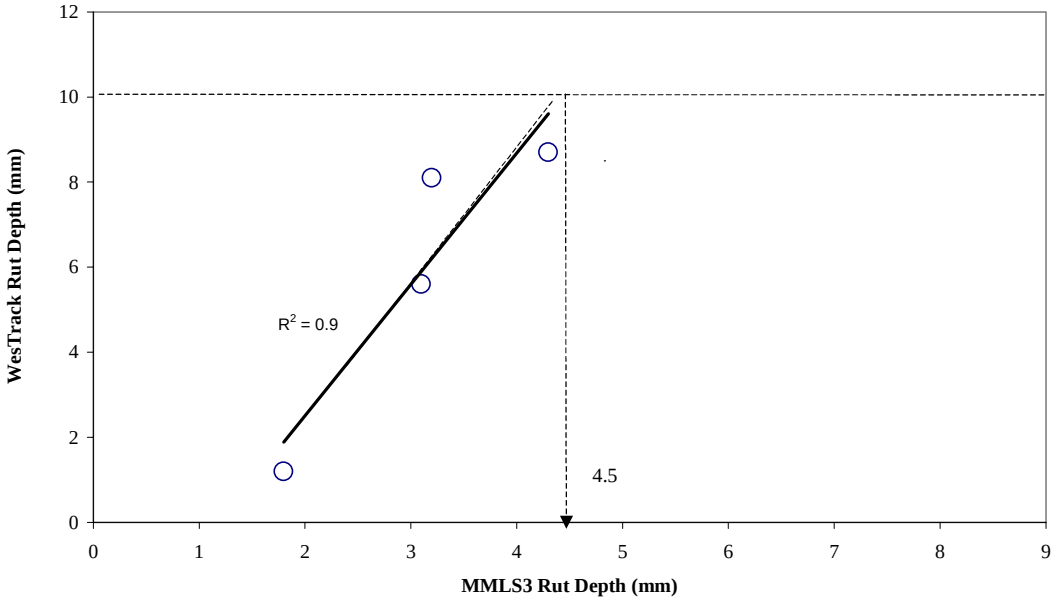

Figure 20. WesTrack Trucks versus MMLS3 Rut Depths after Approximately 100,000 Load Repetitions

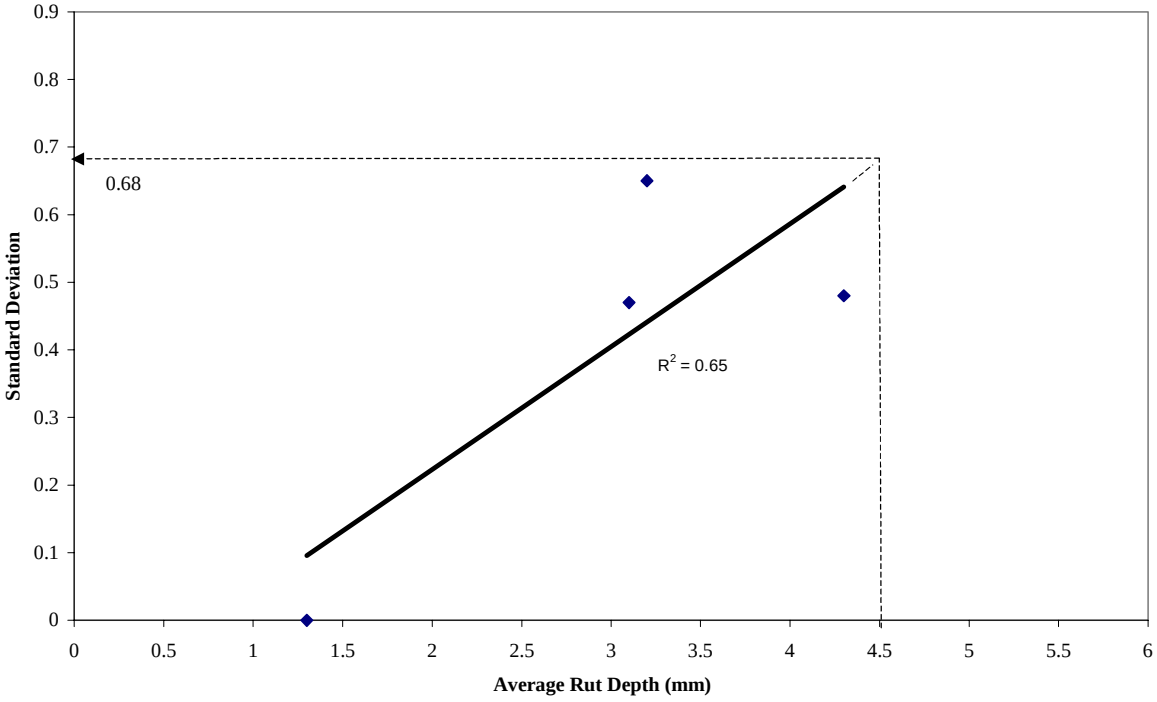

Figure 21. Average versus Standard Deviation of MMLS3 Rut Depth after Approximately 100,000 Load Repetitions

QUANTITATIVE PERFORMANCE COMPARISON AND PREDICTION

Figure 22 shows the distribution of maximum vertical compressive stress with depth output from the ELSYM5 analysis. This figure illustrates combined responses under the full-scale trucks with estimated tire contact stresses of 742 kPa (108 psi) and 777 kPa (113 psi) for Section 01 and the replacement sections (Sections 35, 37, and 38), respectively, and under the MMLS3 with a tire contact stress based on measured values of 766 kPa (111 psi). As expected, the full-scale trucks have a greater depth of influence in terms of pavement response for all sections, and corresponding performance between the stiff Section 01 and the replacement sections agrees with the stress distribution results.

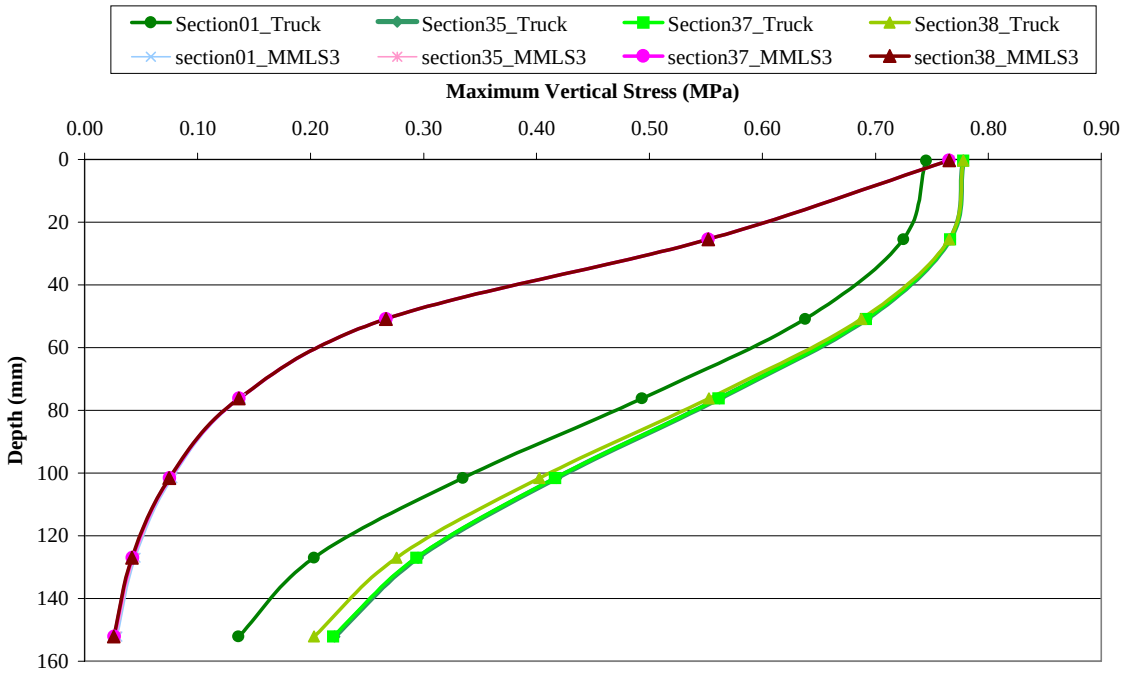

Figure 22. Maximum Vertical Compressive Stress Distributions with Depth.

Table 18 provides the results of the calculations for each section of FRR, SP, TFC, TRR, and $PR_{rutting}$ as previously defined. Only RDs determined using the Reference RD analysis method were utilized in calculating FRR values for reasons described previously. As expected,

the ratio of SP values for Section 01 was slightly larger than those for the replacement sections due to a higher HMA stiffness at the colder full-scale truck trafficking temperature. The TRR values shown indicate that RDs under full-scale loading for equivalent environmental conditions were predicted to be on average approximately 0.9 (the inverse of the TRR) times the RDs measured under scaled loading (MMLS3). This result differs considerably from a factor of three used to predict rutting in an entire single HMA layer on a stiff base because a significant portion of the stress distribution under the full-scale trucks was truncated in this initial analysis.

Table 18. Comparison of Theoretical and Field Rutting Performance.

Section	Loading	RD (mm / in)	FRR	SP (to 75mm) (MPa*mm / psi*in)	TFC	RPR = TRR	$PR_{rutting}$
01	MMLS3	1.8 / 0.07	1.5	67.8 / 387	2.9	2.0	1.3
	Trucks	1.2 / 0.05		100.3 / 573			
35	MMLS3	4.3 / 0.17	0.5	67.7 / 386	1.24	0.8	1.6
	Trucks	8.7 / 0.34		107.7 / 615			
37	MMLS3	3.2 / 0.13	0.4	67.7 / 386	1.24	0.8	2.0
	Trucks	8.1 / 0.32		107.7 / 615			
38	MMLS3	3.1 / 0.12	0.6	67.6 / 386	1.24	0.8	1.4
	Trucks	5.6 / 0.22		107.2 / 612			

The relatively high $PR_{rutting}$ values shown in Table 18 indicated that either (1) the hypothesis that the FRR can be assumed equivalent to the TRR was not valid or, more likely, (2) all factors affecting calculation of the TRR were not accounted for in this initial analysis.

FURTHER ANALYSIS

After completion of the project and prior to submission of the final report, one of the researchers, Dr. Hugo, performed further analysis of the project data in collaboration with Mr. Pieter Poolman at the University of Stellenbosch in South Africa. The purpose of this second analysis was to explore possible reasons for the apparent inconsistency of the $PR_{rutting}$ results when compared to previous findings in the Jacksboro study where the MMLS3 had been applied in a similar manner (*10*).

Results from this second, more detailed analysis highlighted important factors that must be considered for the quantitative performance prediction methodology described to produce accurate prediction of rutting performance under full-scale trafficking. These results are included in Appendices A and B and summarized in this section.

A Critical Analysis of WesTrack MMLS3 and Truck Rut Data

In a review of the project data described in Appendix A, inconsistencies caused by secondary deformation occurring as a result of lateral flow of the HMA were explored. Evidence of this phenomenon was found in the MMLS3 sections as well as in the truck sections. Corrections were made to account for a systematic measuring error that appeared to be caused by deflection of the profilometer beam. It was also necessary to shift the trafficked profile laterally to overlap with the untrafficked profile. The RDs were then determined using the Modified Reference method. In this method, the sum of squared differences between the untrafficked regions of the two required profiles was minimized. The revised RDs are shown in Table 19 as *basic* ruts determined without considering lateral wander effects (Table A1 in Appendix A). These ruts were averaged over all five MMLS3 transverse profiles (measured at 0.2 m (0.7 ft), 0.4 m (1.3 ft), 0.6 m (2.0 ft), 0.8 m (2.6 ft), and 1.0 m (3.3 ft)) and all four wheelpaths of the two truck transverse profiles (measured at the beginning and end of the 40 m (131 ft) performance monitoring section).

Another factor taken into account related to differences in lateral wander between the two loading conditions for the trafficking period analyzed (up to 100,000 load repetitions). This inequity was included in the analysis by defining the number of comparable load repetitions, accounting for trafficking at the centerline of rutted areas with widths equivalent to corresponding tire widths. When comparing the channelized truck trafficking and MMLS3 trafficking, the net effect was that two truck load repetitions were equivalent to three MMLS3 load repetitions. Thus, the RDs after 67,000 truck repetitions were compared to MMLS3 RDs after 100,000 load repetitions. These rut measurements were defined as comparable ruts. Since transverse profiles were not always specifically measured at the appropriate number of load repetitions, some values were estimated. When there was effectively no wander, as for Section 37, the comparable ruts were equivalent to the basic ruts determined by the Modified Reference

method. All rutting results determined from this modified RD analysis method (Table 19) were used in the revised analytical procedure to determine $PR_{rutting}$ described in Appendix B.

Table 19. Summary of Rut Depths (mm / in) at 100,000 MMLS3 Load Repetitions for Different Analysis Methods.

		Analysis Method			
				Modified Reference	
Section	Loading	Single Profile	Reference	Basic Rut	Comparable Rut
01	MMLS3	4.1 / 0.16	1.8 / 0.07	2.5 / 0.10	2.5 / 0.10
	Trucks	2.8 / 0.11	1.2 / 0.05	2.9 / 0.11	2.8* / 0.11
35	MMLS3	6.0 / 0.24	4.3 / 0.17	5.8 / 0.23	5.8 / 0.23
	Trucks	9.4 / 0.37	8.7 / 0.34	11.2 / 0.44	10.8* / 0.43
37	MMLS3	8.0 / 0.31	3.2 / 0.13	4.8 / 0.19	4.8 / 0.19
	Trucks	10.1 / 0.40	8.1 / 0.32	10.6 / 0.42	10.6# / 0.42
38	MMLS3	5.1 / 0.20	3.1 / 0.12	3.7 / 0.15	3.7 / 0.15
	Trucks	5.6 / 0.22	5.6 / 0.22	6.9 / 0.27	6.6* / 0.26

*66,700 truck load repetitions = 100,000 MMLS3 load repetitions
100,000 truck load repetitions = 100,000 MMLS3 load repetitions

On the basis of the comparable rut results for the MMLS3 and the trucks and a 10 mm (0.4 in) failure criterion under full-scale trafficking, Sections 35 and 37 fail to provide adequate resistance to rutting.

A Critical Review of the Quantitative Analysis of MMLS3 and Truck Rutting Performance at WesTrack

In reviewing the methodology to determine $PR_{rutting}$ and subsequent values obtained in the initial analysis, several additional factors that affect rutting performance were identified. These factors are listed in Table 20 (Table B1 in Appendix B). Some of these factors were more critical than others. Their effects on performance and the $PR_{rutting}$ results are briefly summarized in this section.

Table 20. Factors Affecting the Primary Elements of the Quantitative Analysis Hypothesis.

Nature of Vertical Contact Stress	Material Characteristics & Pavement Structural Composition	Prevailing Environmental Conditions Prior to and During Trafficking
Tire Pressure	Effective Stiffness	Fluctuations in Temperature
Static Load Amplitude	Multi-layer Characteristics	Fluctuations in Ultraviolet Radiation
Load Frequency	Response & Performance of Unbound Layers & Subgrade	Fluctuations in Moisture
Comparative Load Repetitions	Material History Prior to Trafficking	Fluctuations in Other Environmental Conditions
Vehicle/Pavement Dynamics		

There was evidence that permanent deformation had occurred throughout the HMA layer and not only in the upper 75 mm (3 in). To account for this, the HMA was divided into a number of discrete sublayers, each with its own characteristics in terms of G* and E, and the stress analysis was performed over the entire HMA layer depth. In addition, it was assumed that 0.9 mm of the surface rut in Section 01 was due to deformation in the underlying base course. This was taken into account in calculating the FRR.

Special attention was given to the stiffness of the HMA sublayers since this property affects the stress distribution as well as permanent deformation of the HMA layer. Differences in HMA aging were accounted for in terms of the effect on HMA stiffness. Measured G* values of the unaged HMA were multiplied by factors reported in the literature. The results were compared to measured G* values of HMA specimens extracted from the trafficked wheel paths after truck trafficking and aging and found to be reasonable. Since no values of G* were measured for the lower 75mm (3 in) HMA sublayer, corresponding stiffness values were estimated. This was done by proportionately decreasing the stiffness values of the upper HMA sublayer on the basis of respective indirect tensile (IDT) strength values measured for both sublayers. These values were deduced from a comprehensive set of IDT strength data. The procedures used for temperature and frequency correction were the same as those used in the initial analyses.

For the stress analyses, two procedures were used to determine values for the elastic stiffnesses. First they were determined by using the G* values as a reference for conversion to E values according to the method presented by Sousa and Monismith (*32*). At the 2001 AAPT meeting in Clearwater, Florida, Monismith pointed out that subsequent research indicated that this approach was invalid at high temperatures (*33*). Therefore, the four-point bending test (FPBT) results from U.C. Berkeley were used in a second procedure to determine elastic stiffness values. Because these values were measured for only the lower 75mm (3 in) HMA sublayer, values for the upper 75mm (3 in) HMA sublayer were estimated for each section by proportionately increasing the stiffness values of the lower HMA sublayer on the basis of respective IDT strength values measured for both sublayers. The stiffness values for the respective pavement sections and HMA sublayers were then calculated by making corrections for temperature and frequency in a manner similar to that described in a previous chapter. The stiffness values from both procedures were used in the revised theoretical stress analyses. All selected values are shown in Table 21 (Table B12 in Appendix B).

The stiffnesses of the base and the subgrade differed from those used in the initial analysis. The revised values were selected to reflect the response of the pavements and the effective stresses under the two loading conditions. While different values were used, the effect of these differences on the calculated stresses was very small.

Table 21. Comparison of HMA Stiffness Values at Mid-Depth Temperature Calculated from G* and FPBT Data.

Section	Layer	Basis for E (MPa / psi) Estimation / Loading			
		G*-Based / MMLS3	FPBT-Based / MMLS3	G*-Based / Trucks	FPBT-Based / Trucks
01	0-25mm	659 / 95,555	553 / 80,185	1156 / 167,620	1276 / 185,020
	25-50mm	449 / 65,105	377 / 54,665		
35	0-50mm	335 / 48,575	395 / 57,275	363 / 52,635	492 / 71,340
37		341 / 49,445	469 / 68,005	369 / 53,505	583 / 84,535
38		423 / 61,335	475 / 68,875	458 / 66,410	591 / 85,695
01	50-150mm	346 / 50,170	333 / 48,285	896 / 129,920	1327 / 192,415
35		356 / 51,620	479 / 69,455	488 / 70,760	729 / 105,705
37		344 / 49,880	541 / 78,445	472 / 68,440	825 / 119,625
38		427 / 61,915	563 / 81,635	585 / 84,825	857 / 124,265

The truck tires were probably operating at temperatures elevated to about the same level as that measured during MMLS3 trafficking. Therefore, the truck tire pressures had to be at least the same as those of the MMLS3. In addition, evidence suggested that it was feasible that differential contact stresses under the tires could have reached values as high as 1,200 kPa (174 psi). In the revised analysis, a range of contact stresses was investigated.

To account for the influence of the various factors considered, the calculation of the TRR was revised. The contribution towards rut formation by the different discrete HMA sublayers was accounted for in terms of individual Stress Potentials (SP) and related temperature-frequency correction (TFC) factors. This was different as compared to the procedure previously followed in the initial analysis where a single TFC value was used. Rutting Potential Ratios (RPR), Comparative Load Rut Ratios (CompLRR) that account for differences in lateral wander between the two loading conditions, and the TRR found by multiplying these two ratios were then calculated for each HMA sublayer as described in Appendix B.

It should be noted that the revised RD data in Appendix A was used in the revised analytical procedure to determine $PR_{rutting}$. Furthermore, owing to the limited extent of available data, the effect on $PR_{rutting}$ of the various factors was evaluated by varying the parameters in a sensitivity analysis.

Table 22 (Table B17 in Appendix B) gives the results of the revised analysis, where a vertical contact stress under the truck tires was 850 kPa (123 psi) and permanent deformation was assumed to occur throughout the HMA layer. Table 23 (Table B18 in Appendix B) shows a comparison of the $PR_{Rutting}$ values found when the E values from G* and the four-point bending tests (FPBT) were used. It is apparent that the effect of the differences in estimated stiffnesses is insignificant. In the same vein, the results remained virtually unchanged when the stress analysis was done with Poisson's value of 0.45 for the HMA layers. Furthermore, the ranges of the parameters used for evaluating the sensitivity of the analyses covered most feasible scenarios, including trafficking up to 200,000 load repetitions.

Considering the limited nature of the data, it is remarkable that the $PR_{Rutting}$ results are so close to unity. The major discrepancy is in Section 37, where there appears to be some unknown factor involved. This is also the section where there were problems with MMLS3 set up as a result of milling in the truck wheel paths. Thus, there is also a possibility that the RD is still underestimated.

Table 22. Comparison of $PR_{rutting}$ Results.

Section	Initial $PR_{rutting}$	Revised $PR_{rutting}$
01	1.3	1.0
35	1.6	1.1
37	2.0	1.2
38	1.4	1.0

Table 23. Comparison of $PR_{rutting}$ Results for Different E Values (Tire Contact Stress = 850 kPa (123 psi)).

Section	G*-Based	FPBT-Based
01	1.0	1.1
35	1.1	1.1
37	1.2	1.3
38	1.0	1.0

In summary, the following corrections were applied to the initial analyses described previously to enable more comprehensive and detailed results to be obtained:

1. Revised values of G* were used as well as E values that were correlated with IDT strength values.
2. Updated RDs were used.
3. The entire depth of the HMA layer was assumed to have undergone permanent deformation.
4. Different possible tire contact stresses were considered.
5. Settlement in the unbound layers underlying the HMA sublayers of Section 01 was included.
6. Comparable load repetitions were determined to allow for differences in lateral wander between the two loading conditions.

The revised $PR_{rutting}$ results indicate that the hypothesis required in the quantitative performance prediction methodology described previously (TRR=FRR) appears to hold for the four independent pavement sections, provided steps are taken to factor in differences in the respective loading and environmental conditions. The revised analytical procedure to determine $PR_{rutting}$ described in Appendix B includes a systematic sensitivity analysis of the effect of changes in the various parameters discussed.

CHAPTER 9. SUMMARY, CONCLUSIONS, AND RECOMMENDATIONS

Results of this study lend credence to and confidence in the use of the MMLS3 as a pavement performance prediction tool to screen for HMA mixtures or pavement structures with unacceptable rutting performance near the surface prior to expensive full-scale accelerated load tests or use in service.

Based on the data and analyses in this study after approximately 100,000 load repetitions with MMLS trafficking at a critical temperature for permanent deformation, researchers offer conclusions and recommendations presented in this chapter.

RUT DEPTH MEASUREMENT AND QUALITATIVE COMPARISON

- The MMLS3 successfully ranked the relative rutting performance of four independently trafficked WesTrack sections; however, RDs were dependent on the analysis method.
- The regression model correlating RDs under the MMLS3 and full-scale trafficking by the Reference method explained 90 percent of the variability in full-scale rutting performance.
- Section 01 RDs under full-scale trafficking by the Reference method were not used in most of the statistical comparisons due to the use of a different and less accurate measurement device (Dipstick) and lack of an initial profile.
- For Section 01, RDs by the Single Profile method were statistically equivalent under both loading conditions. For the replacement sections (Sections 35, 37, and 38), full-scale loading produced significantly different RDs when compared to RDs under MMLS3 loading for both RD analysis methods with the exception of Section 38 for the Single Profile method. These sections are less aged and less stiff than Section 01, and the effect of full-scale loading was more pronounced, especially considering the high characteristic temperature during full-scale loading of these sections.
- Statistical comparisons for each section between the two RD analysis methods for a single type of loading (MMLS3 or full-scale trucks) indicated that the two methods yielded equivalent results only for Sections 35 and 38 under full-scale loading. This emphasizes the need to select a standard RD analysis method for use with the MMLS3.

- The Reference method of RD analysis was recommended over the Single Profile method. The latter was dependent on judgement, and it did not include systematic matching of the profiles in the untrafficked regions. The Single Profile method also assumed the untrafficked profile to be a flat horizontal datum. Due to these differences, it was not surprising that the results from the two methods differed significantly except for Sections 35 and 38 under truck trafficking.
- Performance ranking of the sections according to the Single Profile method, from shallowest to deepest RD, was 01, 38, 35, and 37 under both trucks and the MMLS3. The initial analysis using the Reference method and results reported in Appendix A with the Modified Reference method found the ranking of Sections 35 and 37 reversed. This small difference in rankings was not surprising, especially when considering the results of the statistical analysis.
- The Modified Reference method included the following statistically based corrections to the transverse profile measurements:
  - vertical adjustment
  - rotational adjustment
  - horizontal, lateral displacement to match the untrafficked profile
  - correction for an error related to flexure of the profilometer beam
- Careful analysis of the transverse profiles clearly showed that the HMA was subject to shoving and upheaval due to lateral wander of the wheels during trafficking. This necessitated some estimation for the determination of comparable RDs of some sections. This finding is considered important for any analytical study to model rutting of HMA under trafficking. It was apparent that great care is required in determining RDs when conducting quantitative comparative rutting performance tests.

QUANTITATIVE COMPARATIVE ANALYSIS OF RUTTING PERFORMANCE

Demonstration of a methodology to quantitatively predict rutting performance using MMLS3 test results and a theoretical stress analysis was based on the hypothesis that the extent of rutting is dependent on the nature of the vertical contact stress under the tire, material characteristics and pavement structural composition, and the prevailing environmental conditions prior to and during trafficking. Initial results showed relatively high $PR_{rutting}$ values as compared to those found in a

previous study (*10*). This discrepancy pointed to the fact that there were probably additional factors not accounted for in the initial analysis.

A second, more detailed analysis was conducted to explore some of these additional factors necessary for successful implementation of this quantitative performance prediction methodology. These factors included an improved RD analysis method that accounted for lateral wander effects, transverse profile measurement errors, misalignment of the MMLS3, and tire contact stresses at elevated temperatures. This more comprehensive analysis involved improving material property estimates, revising RDs, considering deformation throughout the pavement structure including the base layer, and accounting for differences in lateral wander between the two loading conditions. Results from this second analysis indicated that the hypothesis required in the quantitative performance prediction methodology appears to hold for the four independent pavement sections at WesTrack, provided steps are taken to factor in differences in loading and environmental conditions between MMLS3 and full-scale truck trafficking.

With validation of the required hypothesis (TRR = FRR), the quantitative performance prediction methodology can be used to predict rutting performance under full-scale trafficking after conducting an MMLS3 test and a theoretical stress analysis that accounts for all factors affecting performance. This analysis requires inputs that include expected future traffic and prevailing environmental conditions and material properties throughout the prediction period.

OTHER CONCLUSIONS

As part of the experimental design, a number of other tests and analyses were conducted to assess rutting performance under full-scale trafficking or compare rutting performance with that determined using the MMLS3. Researchers offer the following conclusions based on these results:

- Predicted field rutting performance can be assessed as acceptable or not using RD criteria developed in this study. Different reliability levels, number of replicate RD measurements, and failure criterion under full-scale trafficking can all be adjusted using the methodology presented to produce a different set of criteria to compare to a calculated average RD from MMLS3 testing.
- For comparative quantitative analyses of HMA rutting performance, G* appears to be useful for taking into account differences in temperature, loading frequency, and HMA aging between full-scale and scaled (MMLS3) trafficking periods.

- Based on RSST-CH and Static Creep results, Section 01 aged the most, as expected, and showed the highest shear and static creep stiffness.
- Rankings by RSST-CH and HWTD performance prediction were equivalent. These rankings were also equivalent to the RD rankings by the Reference method.
- The two sets of performance rankings based on laboratory tests that were not consistent with the others were those from the Static Creep test (permanent strain) and the APA. This anomaly in the static creep γ_p ranking agrees with recent TxDOT experience. For the APA rankings, the discrepancy may partly be attributed to the fact that only one replicate specimen was used for each section and a relatively high coefficient of variation for APA tests was previously demonstrated through testing of WesTrack materials (*22*).
- AV results for cores sampled before and after trafficking indicated that the MMLS3 caused densification in the HMA layer. Section 01 exhibited the smallest change in AV, again probably due to its age and relative stiffness.
- As expected, the results of IDT strength testing before and after trafficking showed that there was no significant change.
- In agreement with visual inspection of the MMLS3 test sections and cores taken after trafficking, a comparison of HMA moduli (estimated from SASW data) for each section with and without MMLS3 traffic did not indicate any damage due to fatigue or moisture. Some damage may have occurred but it was offset by the effect of densification shown with the AV results and the slight increasing trend in SASW moduli.

RECOMMENDATIONS

Researchers offer the following recommendations for consideration when future MMLS3 tests are planned:

- It is important to select the MMLS3 testing temperature to reflect the conditions the pavement is expected to experience in the field. The selected temperature for this study (60 °C (140 °F)) was based on the critical temperature for permanent deformation over a four-day period in the summer when many of the replacement sections failed.
- To predict rutting performance using the MMLS3, researchers recommend that the testing temperature be selected as the critical temperature for permanent deformation over the hottest week

in the summer of a 30-year period. In addition, researchers suggest a minimum of 100,000 load repetitions and three RD measurements along the length of an MMLS3 test section.

- Comparative analyses of rutting performance under both the MMLS3 and full-scale trafficking are encouraged to further validate the required hypothesis (TRR = FRR) for quantitative performance prediction. These analyses must carefully take into account all factors that affect rutting performance.
- The need to accurately review transverse profiles during trafficking was demonstrated. Transverse profiles measured by laser profilometer before and after MMLS3 trafficking are recommended in conjunction with the Modified Reference method to determine average RD. Researchers recommend this method because it is less subjective, and the probability of introducing error is minimized by consistently and systematically matching the untrafficked regions to an initial profile before trafficking.

REFERENCES

(1) Epps, J., C. L Monismith, S. B. Seeds, S. C. Ashmore, R. Leahy, and T. M. Mitchell, "WesTrack Full-Scale Test Track: Interim Findings," *Journal of the Association of Asphalt Paving Technologists*, Vol. 67, pp. 738-782 (1998).

(2) Epps, J., C. L Monismith, S. B. Seeds, S. C. Ashmore, R.Leahy, and T. M. Mitchell, "WesTrack Performance-Interim Findings," *Proceedings of the 8th International Conference on Asphalt Pavements*, Vol. III, pp. 147-164 (1997).

(3) Asphalt Institute, *Performance Graded Asphalt Binder Specification and Testing*, Superpave Series (SP-1), 1997, Asphalt Institute, Lexington, Kentucky.

(4) McGennis, R., R. M. Anderson, T. W. Kennedy, and M. Solaimanian, *Superpave Asphalt Mixture Design and Analysis*, National Asphalt Training Center Demonstration Project 101, 1994, Asphalt Institute, Lexington, Kentucky, and FHWA.

(5) Hand, A., J. A. Epps, and P. E. Sebaaly, "Development of APT Based Permanent Deformation Prediction Models Translatable to Any Environment," *Proceedings of the International Conference on Accelerated Pavement Testing* (1999).

(6) Williams, R. C. and P. Romero, "Comparison of Superpave Shear Test Results to WesTrack Performance," *Proceedings of the International Conference on Accelerated Pavement Testing* (1999).

(7) Stuart, K. and W. S. Mogawer, "Validation of Asphalt Binder and Mixture Tests that Predict Rutting Susceptibility Using the FHWA ALF," *Journal of the Association of Asphalt Paving Technologists*, Vol. 66, pp.109-152 (1997).

(8) Williams, R. C. and B. D. Prowell, "Comparison of Laboratory Wheel Tracking Test Results to WesTrack Performance," *Transportation Research Record* 1681, pp. 121-128 (1999).

(9) de Fourtier Smit, A., F. Hugo, and A. Epps, *Report on the First Jacksboro MMLS Tests*, Research Report #1814-2, Center for Transportation Research, University of Texas at Austin, December 1999.

(10) Walubita, L., F. Hugo, and A. Epps, *Performance of Rehabilitated Lightweight Asphalt Concrete Pavements Under Wet and Heated Model MLS Trafficking: A Comparative Study with the TxMLS*, Research Report #1814-3, Center for Transportation Research, University of Texas at Austin, March 2000.

(11) Epps, A., L. Walubita, F. Hugo, and N. Bangera, "Comparing Pavement Response and Rutting Performance for Full-Scale and One-Third Scale Accelerated Pavement Testing," presented at the 80th Annual Meeting of the Transportation Research Board, Washington, D.C., January 2001.

(12) Deacon, J., J. Coplantz, A. Tayebali, and C. Monismith, "Temperature Consideration in Asphalt Aggregate Mixture Analysis and Design," *Transportation Research Record* 1454, pp. 97-112 (1994).

(13) *Manual of Testing Procedures,* Texas Department of Transportation, Materials Section, Construction Division.

(14) Prowell, B., "Development of Rutting Criteria for the Asphalt Pavement Analyzer," *Proceedings of the International Conference on Accelerated Pavement Testing* (1999).

(15) Brock, J. D., R. Collins, and C. Lynn. *Performance Related Testing with the Asphalt Pavement Analyzer*, Technical Paper T-137, 1998, Pavement Technology, Inc., Covington, Georgia.

(16) *Asphalt Pavement Analyzer*, Specifications Brochure, Pavement Technology, Inc., Covington, Georgia.

(17) Collins, R., H. Shami, and J. Lai, "Use of Georgia Loaded Wheel Tester to Evaluate Rutting of Asphalt Samples Prepared by Superpave Gyratory Compactor," *Transportation Research Record* 1545 (1996).

(18) Georgia Department of Transportation, *Method of Test for Determining Rutting Susceptibility Using the Loaded Wheel Tester*, GDT-115, August 1994, Georgia Department of Transportation, Atlanta, Georgia.

(19) Kandhal, P. and R. Mallick, *Evaluation of Asphalt Pavement Analyzer for HMA Mix Desig*n, National Center for Asphalt Technology, June 1999, Auburn University, Alabama.

(20) Sime, M. and S. C. Ashmore, *Tire Pavement Interface Pressure Patterns*, May 1999, Federal Highway Administration.

(21) Monismith, C. L., J. A. Deacon, and J. T. Harvey, *WesTrack: Performance Models for Permanent Deformation and Fatigue*, Draft to Nichols Consulting Engineers, Chtd., December 1999.

(22) WesTrack Database, Beta Version, 2000, Federal Highway Administration, Washington, D.C.

(23) Bell, C. A., M. J. Felling, and A. Wieder, "Field Validation of Laboratory Aging Procedures for Asphalt Aggregate Mixtures," *Journal of the Association of Asphalt Paving Technologists*, Vol. 63, pp. 45-80 (1994).

(24) Hugo, F., and T. W. Kennedy, "Surface Cracking of Asphalt Mixtures in Southern Africa," *Proceedings of the Association of Asphalt Paving Technologists*, pp. 454-491 (1985).

(25) Brown, S. F., K. E. Cooper, J. M. Gibb, J. M. Read, and T. V. Scholz, "Practical Tests for Mechanical Properties of Hot Mix Asphalt," *Proceedings of the 6th Conference on Asphalt Pavements for Southern Africa*, pp. IV-29 – IV-45 (1994).

(26) Nazarian, S., M. Baker, and R. C. Boyd, "Determination of Pavement Aging by High-Frequency Body and Surface Waves," *Proceedings of the 7th International Conference on Asphalt Pavement*, pp. 252-265 (1992).

(27) Aouad, M. F., letter to Dr. Fred Hugo, February 10, 2000.

(28) Healow, S. P., *Analysis and Development of Performance Models for WesTrack*, Masters Thesis, University of Nevada, Reno, May 1998.

(29) Lee, N.-K. J., F. Hugo, and K. H. Stokoe III, "Detection and Monitoring of Cracks in Asphalt Pavement Under Texas Mobile Load Simulator Testing," *Transportation Research Record* 1570, pp. 10-22 (1997).

(30) Roesset, J., D.-W. Chang, K. H. Stokoe III, and M. Aouad, "Modulus and Thickness of the Pavement Surface Layer from SASW Tests," *Transportation Research Record* 1260, pp. 53-63 (1990).

(31) Walubita, L. F., F. Hugo, and A. Epps, "Indirect Tensile Fatigue Performance of Asphalt After MMLS3 Trafficking Under Different Environmental Conditions," submitted for possible publication in *Journal of the South African Institute of Civil Engineering (SAICE)*, November 2000.

(32) Sousa, J. B., and C. L. Monismith, “Dynamic Response of Paving Materials,” *Transportation Research Record* 1136, pp. 57-68 (1988).

(33) Monismith, C. L., conversation with F. Hugo at Annual Meeting of Association of Asphalt Paving Technologists, March 2001.

APPENDIX A

A CRITICAL ANALYSIS OF WESTRACK MMLS3 AND TRUCK RUT DATA

A CRITICAL ANALYSIS OF WESTRACK MMLS3 AND TRUCK RUT DATA

by

Frederick Hugo* and Pieter Poolman**

*Director of the Institute for TransportationTechnology and **PhD candidate
University of Stellenbosch, South Africa

Summary

In 1999 the one-third scale Model Mobile Load Simulator (MMLS3) was used in TxDOT Project 0-2134 to evaluate its capability to simulate the rutting performance of WesTrack pavements under truck trafficking. This required a comparison of the rutting performance under the two systems of trafficking. MMLS3 tests were done on Sections 01, 35, 37, and 38. Some difficulty was experienced with the analysis of the measured rut data from Section 01 where the Dipstick had been used to measure the ruts under truck trafficking. All other measurements of transverse profiles were done with a specially developed laser profilometer.

After the initial comparative analysis of the rutting performance under the two systems of trafficking, it was decided to do a more comprehensive analysis of the ruts to explore whether there were any corrections needed to account for aspects that had not been considered. The initial analysis to determine rut depth (RD) was called the *Reference Method* and is described in TxDOT Report 0-2134-1 (*1*). In the more comprehensive analysis, corrections had to be made to account for a systematic measuring error due to beam deflection. It was also necessary to shift the trafficked profiles laterally where starting points of measurements did not overlap.

In addition, careful forensic analysis of the RD data showed that the ruts had to be scrutinized for the occurrence of inconsistencies due to secondary deformation occurring as a result of lateral flow of HMA as trafficking progressed. There was even evidence of upheaval. This had to be factored into the analysis. Due to lateral wander, the number of load applications were not equally distributed over the central areas of the respective ruts. This was accounted for by determining the *comparable load applications* and the related ruts. Since rut measurements

were not taken specifically at the appropriate number of load applications, the values had to be estimated from the curves of RD versus number of load repetitions in some cases.

The results of the more comprehensive *Modified Reference Method*, including the effect of *comparable load applications*, were used for the revised, comparative quantitative evaluation of the relative rutting performance of the two systems of trafficking in Appendix B (*2*).

Background

In 1999 the one-third scale Model Mobile Load Simulator (MMLS3) was used in TxDOT Project 0-2134 to evaluate its capability to simulate the rutting performance of WesTrack pavements under truck trafficking. This required a comparison of the rutting performance under the two systems of trafficking. MMLS3 tests were done on Sections 01, 35, 37, and 38. Some difficulty was experienced with the analysis of the measured rut data from Section 01 where the Dipstick had been used to measure the ruts under truck trafficking. All other measurements of transverse profiles were done with a specially developed laser profilometer.

After the initial comparative analysis of the rutting performance under the two systems of trafficking described in TxDOT Report 0-2134-1, a limited study was undertaken to:

- review the method of measurement of RDs and the accuracy of the laser profilometer
- review and amend or expand the procedures followed with the *Reference Method* in the initial analysis
- review the deformation profiles
- consider the comparable load applications under the two trafficking patterns to account for lateral wander

The results of this limited study that provide a more comprehensive analysis of the ruts are provided in this appendix.

Consideration of Possible Errors in Measurement

A *Modified Reference Method* was used in this analysis to determine RDs from transverse profiles under both full-scale trucks and the MMLS3. As a first step, this method called for

minimizing the sum of squared differences in the untrafficked regions between transverse profiles measured prior to and after a specific amount of trafficking based on the following sub steps:

- Shift the trafficked profile **horizontally** such that both profiles overlap horizontally (Figure A1).
- Shift the trafficked profile **vertically** and **rotate** it to compensate for any differences in setup of the profilometer between measurements.
- Compensate for changes in stiffness of the profilometer beam between transverse profile measurements since this affects the deflection of the beam (Figure A2). This is done by estimating parameters in a fourth power function for a profilometer beam of length L = 3.66m. An example of the correlation between beam flexure and the error term or residual in the untrafficked regions of a profile is shown in Figures A3.1 and A3.2 before and after removal of this nuisance factor.

The error term or residual between the two profiles in the untrafficked regions (prior to and after a specific amount of trafficking) is defined through the following regression model:

$$Y_{0k} + u_{0k} = Y_{nk} + \beta\,[X] + u_{nk} \qquad \text{(A1)}$$

where

Y_{0k} = untrafficked profile

Y_{nk} = trafficked profile in untrafficked region

$\beta\,[X]$ = deviation between untrafficked and trafficked profiles due to known causes (horizontal shift, vertical shift, rotation, and beam flexure) at each horizontal position X_i

u_{0k} , u_{nk} = disturbance or measurement noise assumed to be homoscedastic and independent with a mean value of zero and a variance of σ^2

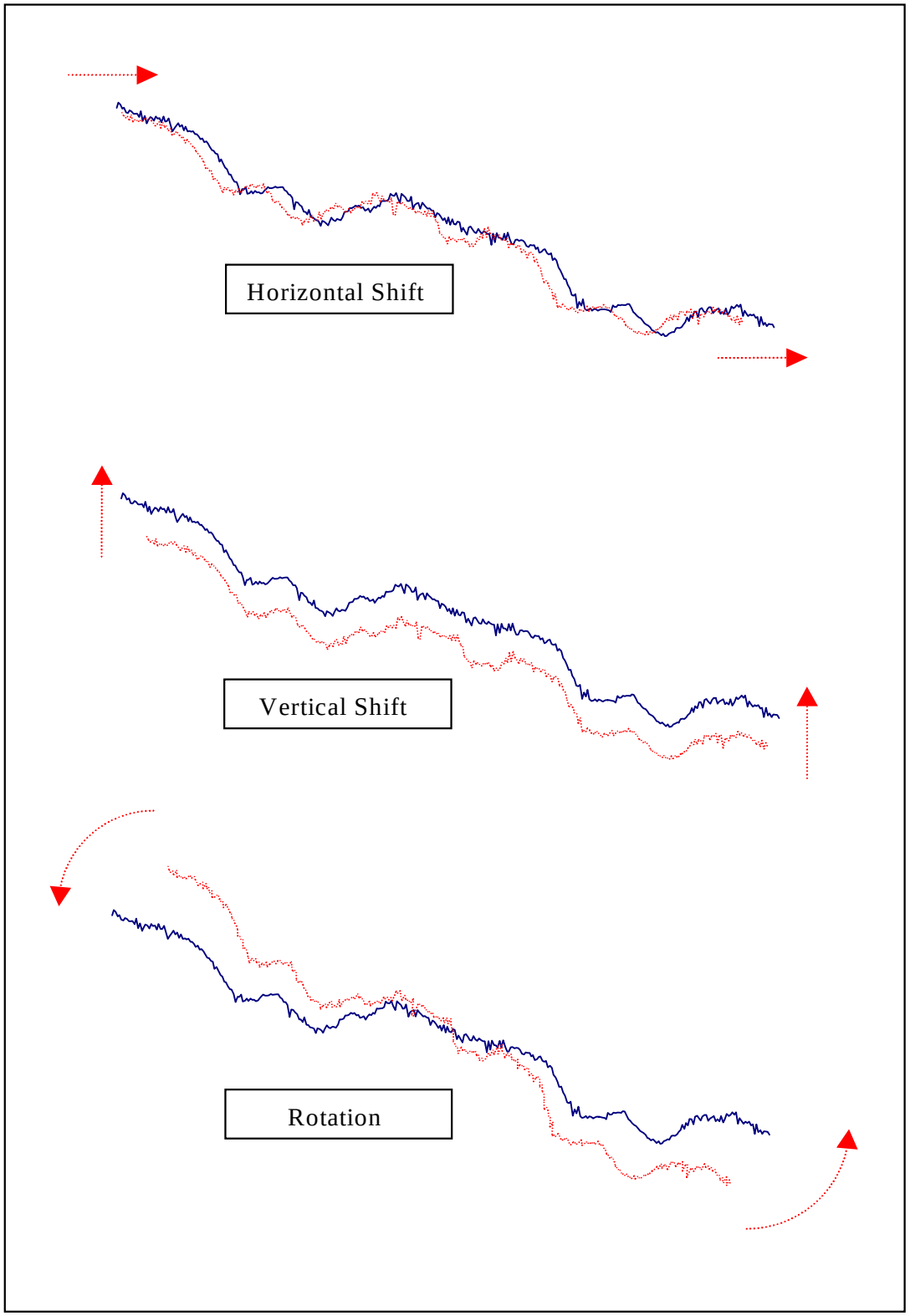

Figure A1. Shift and Rotation of Profiles.

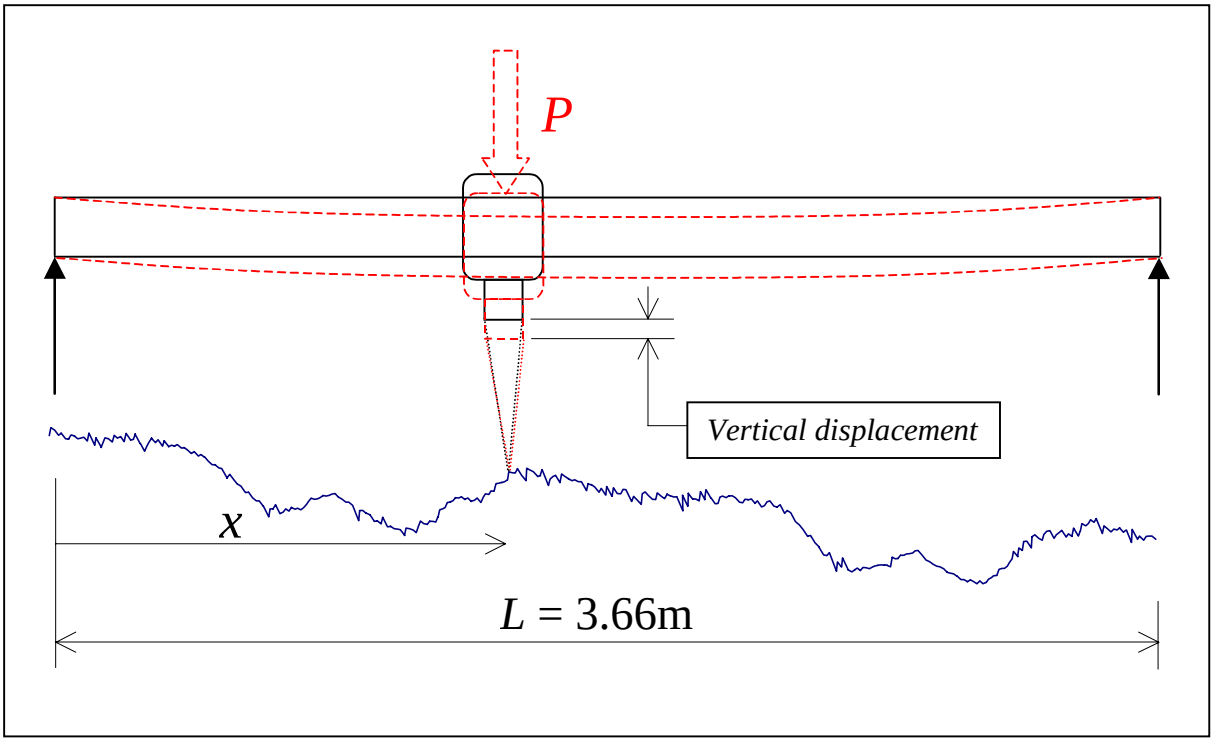

Figure A2. Flexure of Profilometer Beam.

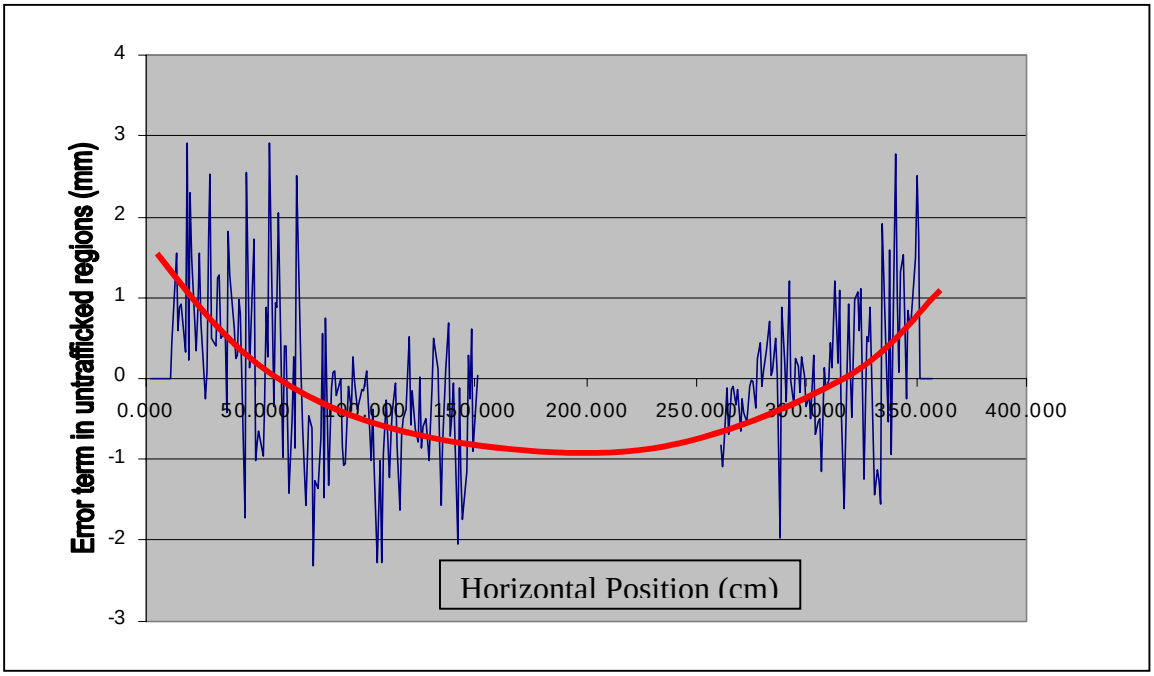

Figure A3.1. Effect of Beam Flexure on Error Term.

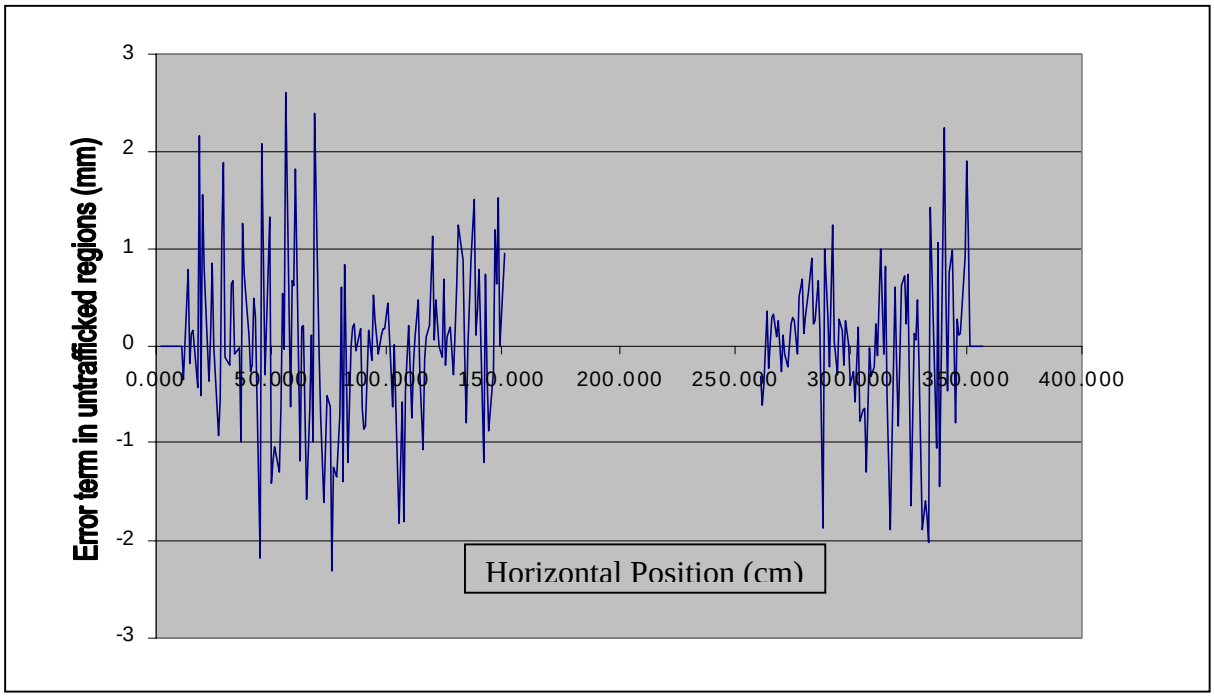

Figure A3.2. Error Term after Compensating for Beam Flexure.

The error term or residual after fitting the profiles is:

$$e = Y_{nk} + b[X] - Y_{0k} \qquad \text{(A2)}$$

In applying the least squares estimating principle, selection of b minimizes the residual sum of squares (Σe^2). The disturbance variance σ^2, related to the accuracy of the profilometer, can be estimated from the calculated residuals as:

$$s^2 = \Sigma e^2/2(n-m) \qquad \text{(A3)}$$

where

n = number of measurement pairs compared in untrafficked regions

m = number of parameters estimated in regression

In summary, k values were estimated for each regression, with different values for each of the two profiles at each performance monitoring session (PMS). Corrections were made to account for beam flexure as well as the other three possible causes of variation, lateral displacement, vertical displacement, and rotation. Some error between the two profiles in the untrafficked regions was still unaccounted for, and for the laser profilometer the s value was 0.52 mm for the data collected over the entire experiment.

The final step in the *Modified Reference Method* was to determine the RD as the maximum difference between the two adjusted profiles in the trafficked region. These ruts were averaged over all five MMLS3 transverse profiles (measured at 0.2 m, 0.4 m, 0.6 m, 0.8 m, and

1.0 m) and all four wheelpaths of the two truck transverse profiles (measured at the beginning and end of the 40 m performance monitoring section). For comparison, the initial analysis utilized only the middle three MMLS3 transverse profiles (0.4 m, 0.6 m, and 0.8 m) and only a single maximum value in the right truck wheelpath to determine RDs. In addition, the original *Reference Method* rotated the trafficked profile about one end, minimized the absolute sum of differences between the two profiles in the untrafficked regions, and did not consider the four phenomena under investigation in this subsequent analysis.

RDs under full-scale trucks using the modified analysis are shown in Figure A4. The profile data for Section 01 under full-scale trafficking was not measured with the same profilometer used for the other sections. Instead, the Dipstick was utilized. Dipstick data yielded fewer datapoints and a higher measurement error. The error for this device was not calculated. In addition to these difficulties, no initial untrafficked profile was available. The best alternative was a profile measured after 4500 load applications, clearly within the range of load applications known for rapid rut development. With these limitations in mind, RDs for Section 01 shown in Figure A4 are considered to be good estimates.

Results from the RD analysis of Section 01 under the MMLS3 are shown in Figure A5. Two tests were conducted with the MMLS3 at different positions on Section 38 and labeled MMLS3 sections 38A and 38B. The results of the modified rutting analysis are shown in Figure A6. Estimated rut values from the logarithmic fit are based on the average rut values from the two tests. The remaining MMLS3 RD results for Sections 35 and 37 are presented in the next section, as lateral wander had a significant effect.

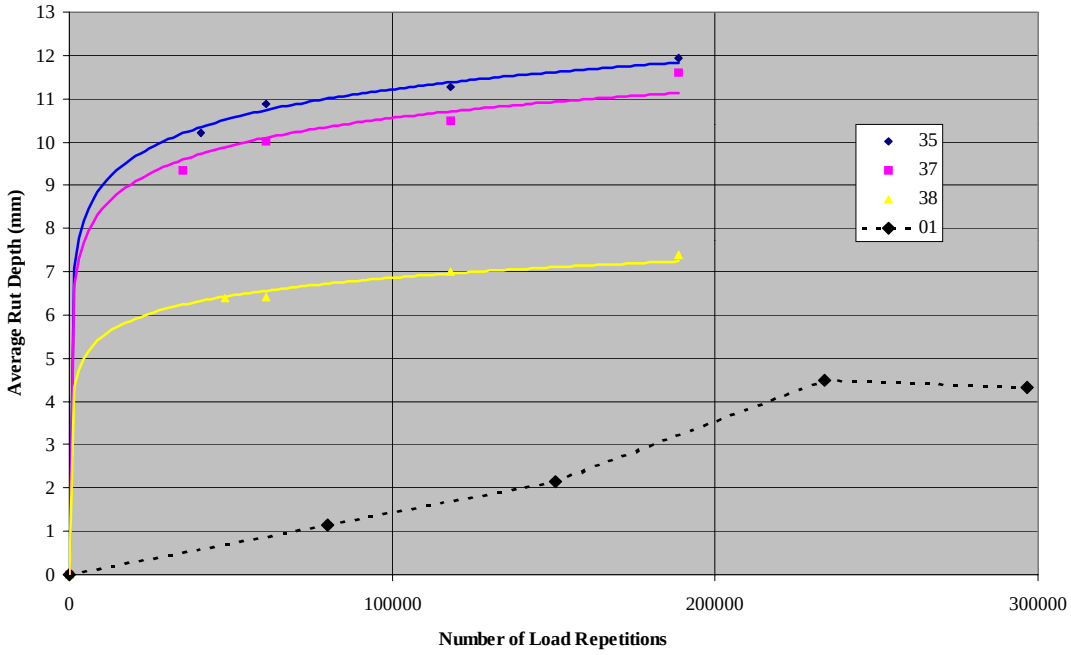

Figure A4. Modified Reference Method Rut Depths for Full-Scale Trucks.

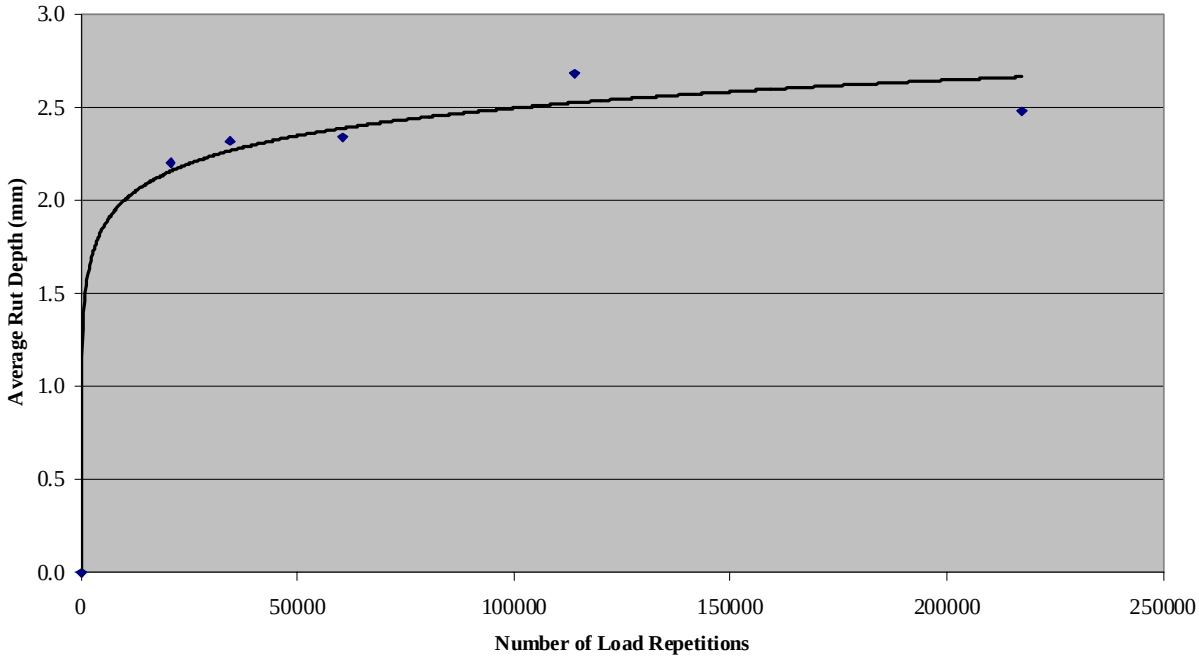

Figure A5. Modified Reference Method Rut Depths under the MMLS3 on Section 01.

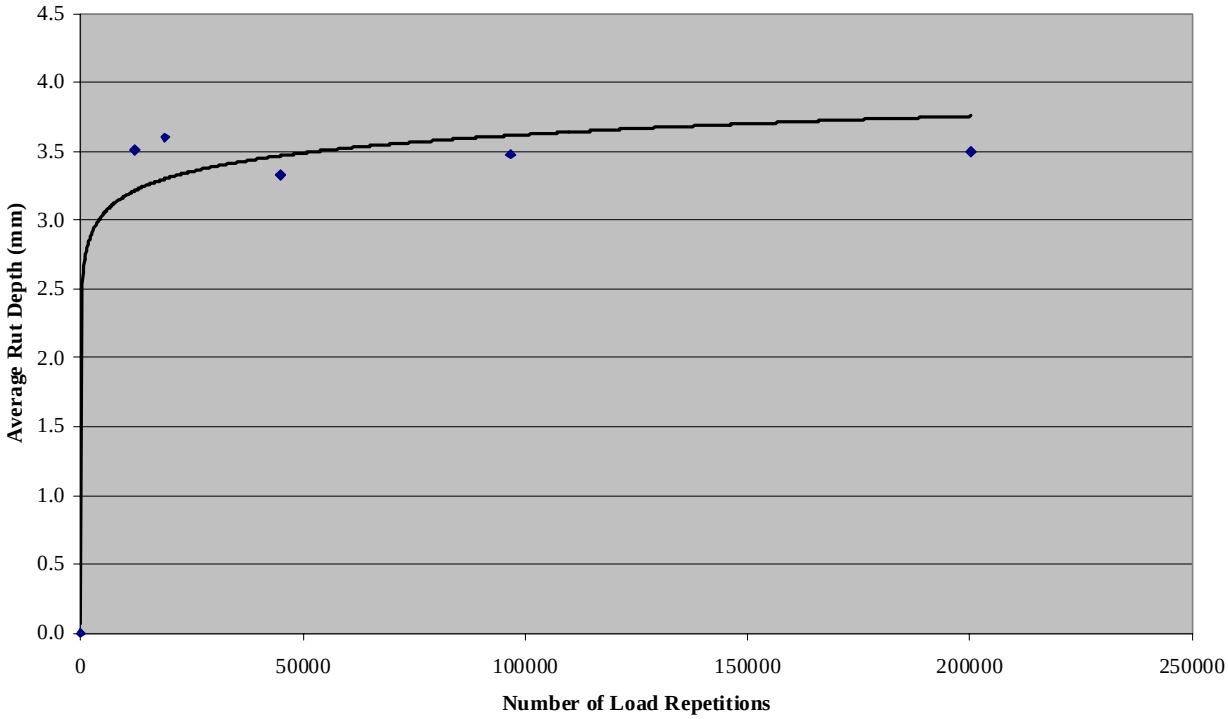

Figure A6. Modified Reference Method Rut Depths under the MMLS3 on Section 38.

Effect of Lateral Wander

Figures A7 and A8 show transverse profiles measured during truck trafficking at two measuring stations on Section 35. The cross-slope has been removed from these profiles. The pavement surface actually slopes downward from left to right, with corresponding larger RDs in the right wheelpath. On the cross-slope trucks also shoved material downhill. Some kind of undamped harmonic motion could be the cause of six tire ruts at Station 63 compared to the four tire ruts at Station 23 expected from dual tires on each axle. Apart from this resonance effect, the trucks did not wander substantially during application of the first 200,000 ESALS as compared to the amount of wander during most of the MMLS3 testing. The same pavement behavior is evident at measuring stations on Sections 37 and 38.

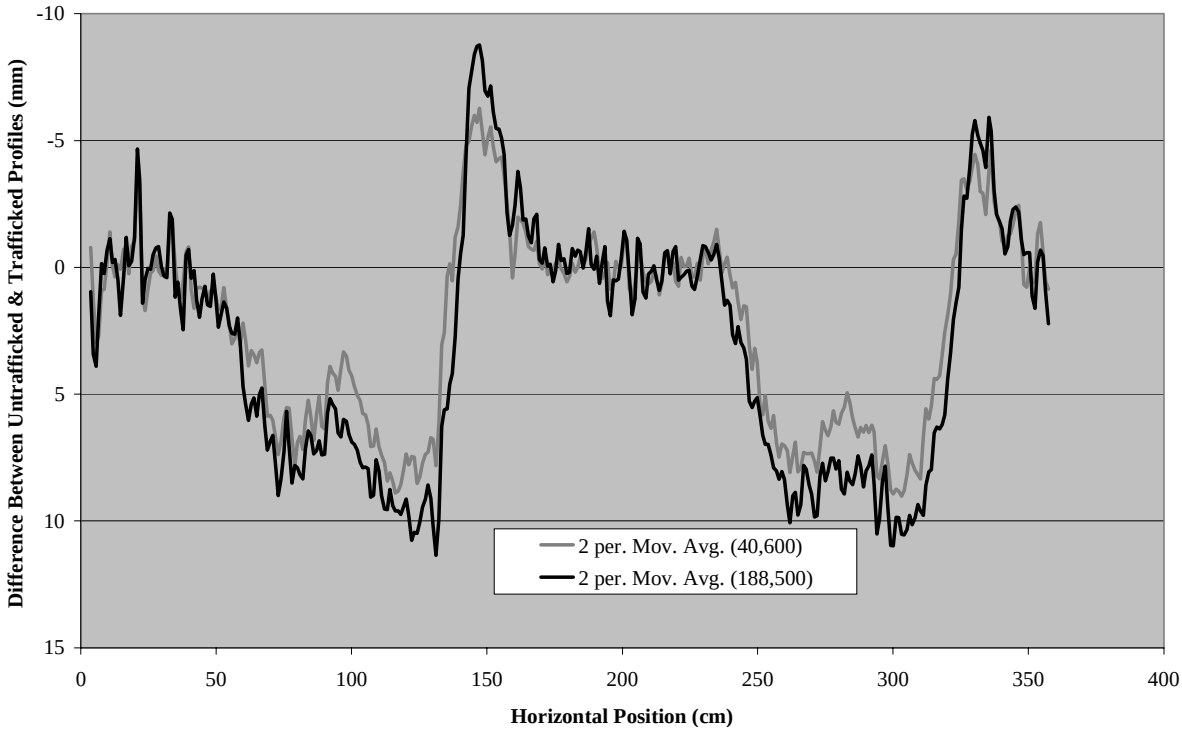

Figure A7. Profiles from Truck Test at Station 23 on Section 35.

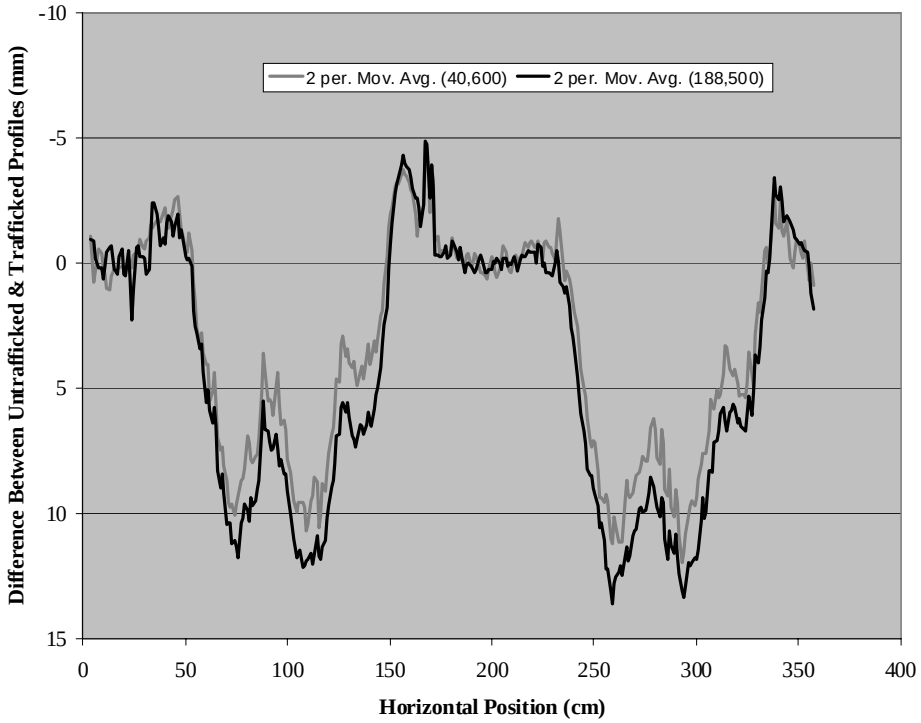

Figure A8. Profiles from Truck Test at Station 63 on Section 35

The tracking width under the full-scale trucks appears to have varied between 0.8 m and 1.0 m during application of the first 200,000 ESALS. The lateral location of this tracking width was varied over the entire WesTrack experiment (to 5 million ESALS) by moving the control equipment on the front of the trucks. In comparison, the wander was considerably less than the equivalent tracking width of the MMLS3. An allowance was necessary to account for this disparity when a quantitative comparison was made between rutting under the MMLS3 and full-scale trucks. In the analysis this was done by defining the number of *comparable load applications*, accounting for trafficking at the centerline of rutted areas with widths equivalent to corresponding tire widths. When comparing the channelized truck trafficking and MMLS3 trafficking, the net effect was that two load applications of truck trafficking were equivalent to three load applications of the MMLS3. Thus, RDs after 67,000 truck load applications were compared to MMLS3 RDs after 100,000 load applications. These rut measurements were defined as *comparable load ruts.* Since transverse profiles were not always specifically measured at the appropriate number of load applications, some values were estimated. If there was no wander, the *comparable ruts* would be equal to the *basic ruts* determined by the *Modified Reference Method*. The applicable results are shown in Table A1.

It should be noted that the MMLS3 stopped wandering during trafficking of Section 37, causing the load to be concentrated after 46,000 load applications. For this case, the *comparable ruts* were set equal to the *basic ruts.*

Unfortunately a secondary effect also surfaced through close inspection of the rut profiles. Trafficking outside the central comparison area based on wheel width was found to have caused upheaval in the center of some of the profiles, effectively reducing the RD at the centerline. Evidence of this phenomenon under the MMLS3 is discussed subsequently. It is difficult if not impossible to fully quantify this effect, but it would cause error in the quantitative analysis to predict rutting performance from MMLS3 tests. It is recommended that future comparison studies take this into account.

Lateral wander significantly affected the RD results under the MMLS3 for Sections 35 and 37. Due to an apparent but unplanned different setup of the MMLS3 on Section 35 after 46,600 load applications, the test was effectively split into two distinct sub-tests. The two setups differed with respect to the position of the longitudinal axis of the MMLS3 and the amount of lateral wander, which is less for the sub-test after 46,000 load applications. As shown in Figure

A9, the RD increased very slowly after 13,800 load applications. This is also evident from the profiles at 13,800, 20,700 and 46,600 load applications shown in Figure A10. With the reduced wander after 46,000 load applications, the rut is narrower and shoving of material into the existing rut (up to 46,600 load applications) can be seen along with a shift to a new horizontal location of maximum RD. At this new location, RDs after 46,600 load applications never reached the same levels as those prior to 46,600 load applications. It seems likely that, if the same setup were used for the duration of the whole test (up to 201,800 load applications), the ultimate RD at 100,000 load applications would be approximately 5.8 mm and about 6 mm at 200,000 load applications. These values are lower than values estimated by the logarithmic extrapolation (based on the RDs up to 46,600 load applications) shown in Figure A9 but considered to be good estimates.

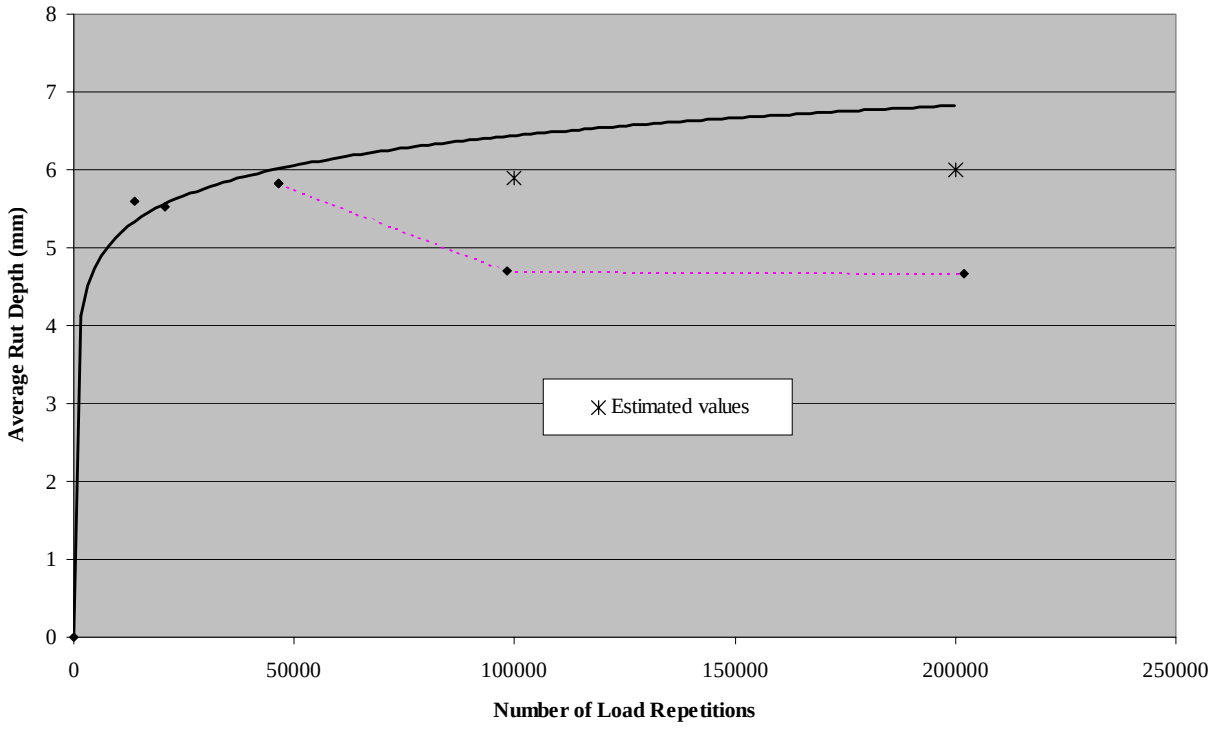

Figure A9. Modified Reference Method Rut Depths under the MMLS3 on Section 35.

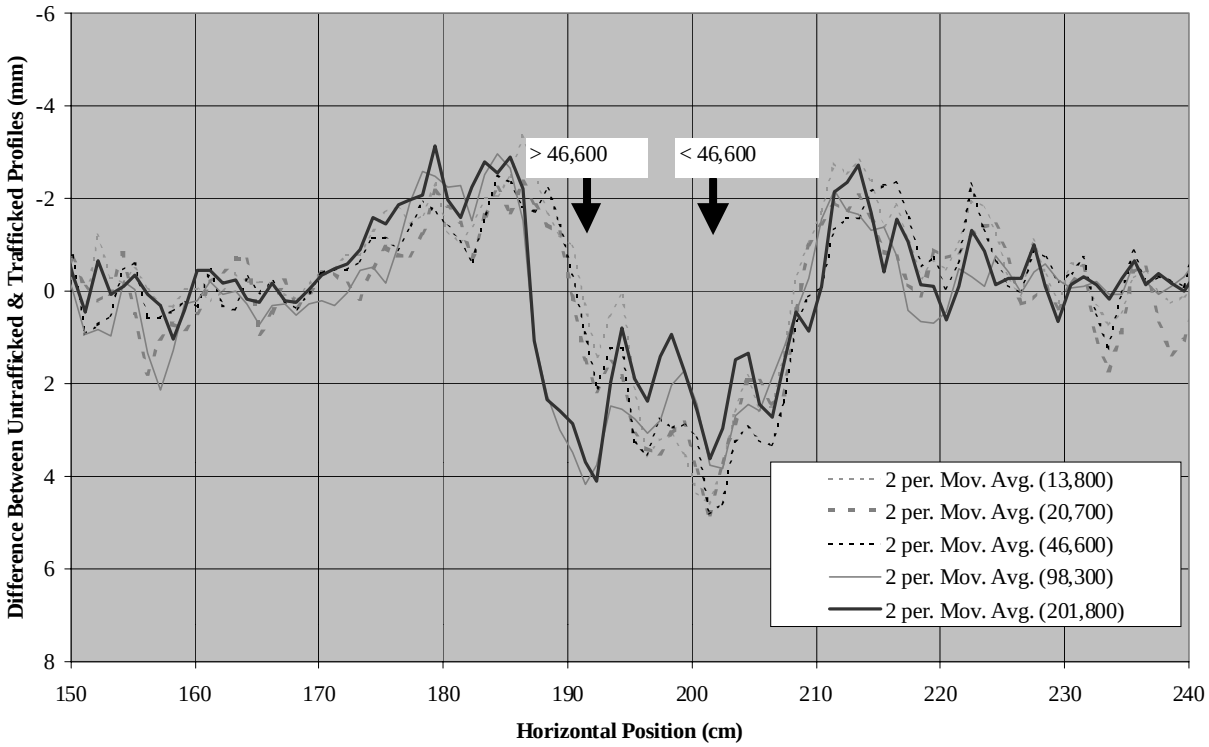

Figure A10. Transverse Profiles from the MMLS3 Test on Section 35.

The setup of the MMLS3 on Section 37 caused almost the same inconsistencies as those shown on Section 35. Due to differences in setup, the test on Section 37 was also split into two distinct sub-tests. The two setups differed with respect to the position of the longitudinal axis of the MMLS3 and the amount of lateral wander, which is less for the sub-test after 46,600 load applications. With the reduced wander after 46,600 load applications, the rut is narrower and shoving of material into the existing rut (up to 46,600 load applications) is again noticeable. This effect was accounted for by considering rutting after 46,600 load applications to be the result of a new test with a new horizontal location of maximum RD. The two circles in Figure A11 show RDs at load applications reduced by 46,600 load applications. As shown in Figure A12, the RD increased rapidly after 46,600 load applications. Thus, estimated RDs were based on a logarithmic fit of the adjusted RDs after 46,600 load applications, shown by the dotted line in Figure A11. The test conditions after 46,600 load applications resembled the conditions during full-scale trafficking better than prior to 46,600 load applications based on the limited

extent of wander. As a result, 100,000 truck load applications were assumed commensurable to 100,000 MMLS3 load applications.

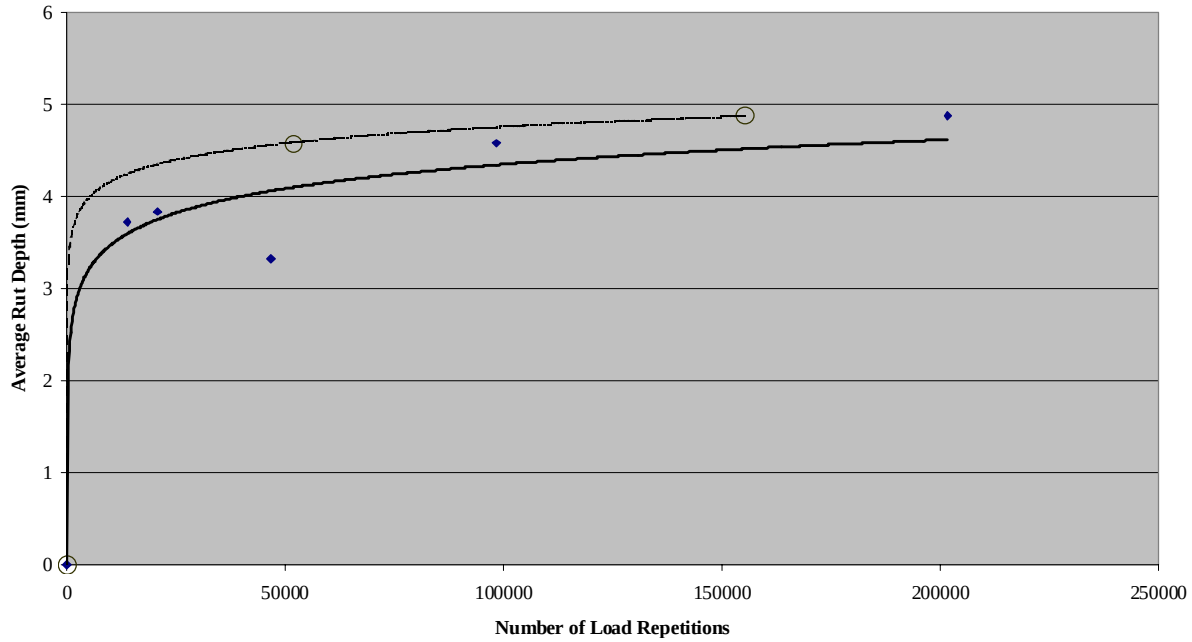

Figure A11. Modified Reference Method Rut Depths under the MMLS3 on Section 37.

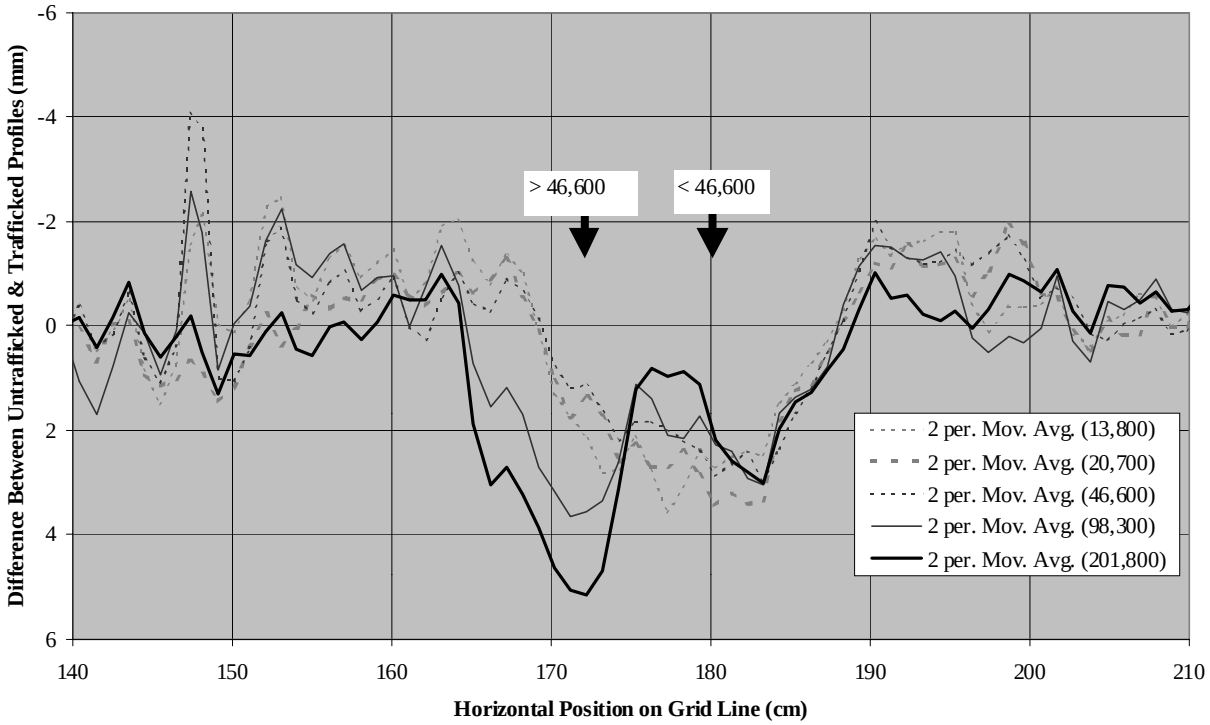

Figure A12. Transverse Profiles from the MMLS3 Test on Section 37.

Summary of Findings

A summary of the RDs at 100,000 MMLS3 load applications from different analysis methods is presented in Table A1. The ranking of the sections in order of increasing RDs are 01-38-35-37 according to the *Single Profile Method* (*1*). This differs from the ranking of 01-38-37-35 derived from both the *Reference Method* (*1*) and the *Modified Reference Method*. These differences emphasize that care should be taken when comparing sections based on RDs determined from analyses that ignore important supplemental information such as method of measurement, measurement errors, and secondary permanent deformation due to lateral wander.

The results of the more comprehensive *Modified Reference Method* of analysis, including the effect of *comparable load applications*, were used for the revised, comparative quantitative evaluation of the relative performance of the two systems of trafficking in Appendix B (*2*).

Table A1. Summary of Rut Depths (mm) at 100,000 MMLS3 Load Repetitions for Different Analysis Methods.

Section	Loading	Analysis Method			
				Modified Reference Method	
		Single Profile	***Reference***	**Basic Rut**	**Comparable Rut**
01	MMLS3	4.1	1.8	2.5	2.5
	Trucks	2.8	1.2	2.9	2.8*
35	MMLS3	6.0	4.3	5.8	5.8
	Trucks	9.4	8.7	11.2	10.8*
37	MMLS3	8.0	3.2	4.8	4.8
	Trucks	10.1	8.1	10.6	10.6#
38	MMLS3	5.1	3.1	3.7	3.7
	Trucks	5.6	5.6	6.9	6.6*

*66,700 truck load repetitions = 100,000 MMLS3 load repetitions
100,000 truck load repetitions = 100,000 MMLS3 load repetitions

References

1. Epps, Amy L., Tazeen Ahmed, Dallas C. Little and Frederick Hugo, *Performance Prediction with the MMLS3 at WesTrack,* Report 0-2134-1, for the TxDOT in co-operation with the FHWA, April 2001.

2. Hugo, Frederick and Pieter Poolman, *A Critical Review of the Quantitative Analysis of MMLS3 and Truck Rutting Performance at WesTrack,* Appendix B in Report 0-2134-1 by Epps et al., (2001) for the Texas Department of Transportation, April, 2001.

APPENDIX B

A CRITICAL REVIEW OF THE QUANTITATIVE ANALYSIS OF MMLS3 AND TRUCK RUTTING PERFORMANCE AT WESTRACK

A CRITICAL REVIEW OF THE QUANTITATIVE ANALYSIS OF MMLS3 AND TRUCK RUTTING PERFORMANCE AT WESTRACK

by

Frederick Hugo* and Pieter Poolman**

*Director of the Institute for Transport Technology and **PhD candidate
University of Stellenbosch, South Africa

Summary

In 1999 the one-third scale Model Mobile Load Simulator (MMLS3) was used in TxDOT Project 0-2134 to evaluate its capability to simulate the rutting performance of the pavements at WesTrack under regular truck trafficking. The quantitative analysis of rutting in the study was based on the hypothesis that the extent of the rutting is dependent on the nature of the vertical contact stress under the tire, the material characteristics and pavement structural composition, and the prevailing environmental conditions prior to and during trafficking. The initial analysis of the comparative performance of four sections appeared to indicate that the hypothesis did not hold. Consequently, a limited study was undertaken to explore whether all aspects had been accounted for in the initial analysis of the test results. This study also investigated whether additional factors needed to be considered in the analysis.

It was found that there were indeed several additional factors that had to be considered. Some of these factors were much more critical than others. The tire contact pressure and the depth of distress due to deformation were most prominent. Revised values of G* were also used, and the rut measurements were updated in accordance with the more comprehensive *Modified Reference Method* presented in Appendix A (*1*). This included consideration of *comparable load applications* to account for the effect of lateral wander during trafficking. Due to the limited extent of available data, the effect of the factors on performance was evaluated by varying the parameters in a sensitivity analysis. From the revised, comparative quantitative evaluation of the

relative rutting performance of the two systems of trafficking, it was concluded that the hypothesis appears to hold for the four independent test sections. The *Rutting Prediction Ratios* ($PR_{Rutting}$) were found to vary between 1.0 and 1.2, provided steps are taken to factor in differences in the respective trafficking and environmental conditions.

Background

The one-third scale Model Mobile Load Simulator (MMLS3) was used in 1999 in TxDOT Project 0-2134 to evaluate its capability to simulate the rutting performance of the pavements at WesTrack under full-scale truck trafficking (*2*). The quantitative analysis of rutting in the study was based on the hypothesis that the extent of the rutting is dependent on the nature of the vertical contact stress under the tire, the material characteristics and pavement structural composition, and the prevailing environmental conditions prior to and during trafficking.

The test program in Project 0-2134 consisted of an evaluation of the comparative performance of four sections at WesTrack under full-scale truck and MMLS3 trafficking. In the initial analysis it was found that the *Rutting Prediction Ratio* ($PR_{Rutting}$) varied between 1.3 and 2.0 for the *Reference Method* of rut depth analysis. In a similar study for TxDOT earlier in 1999 on US281 in Jacksboro, Texas, in the Fort Worth district (Project 0-1814), $PR_{Rutting}$ values of between 1.0 and 1.3 were found (*3*). Consequently a limited study was undertaken to explore whether all aspects had been accounted for in the initial analysis of the WesTrack MMLS3 test results and whether additional factors needed to be considered.

Three of the test sections (35, 37, and 38) consisted of hot mix asphalt (HMA) paved in June 1997 as replacement sections after the initial paved layers had failed. Section 01 was still the original HMA that was placed in October 1995. In all cases the MMLS3 tests were run between the truck wheelpaths. At the start of MMLS3 testing, Sections 35, 37, and 38 were on average 28 months old while Section 01 was 48 months old.

In the initial analysis of the test results, some steps were taken to address factors that could cause errors in the analytical procedure for determining the *Theoretical Rutting Ratio* (*TRR*). The factors were identified in terms of the hypothesis upon which the analysis is based. Accordingly temperature and frequency corrections were made to the stiffness of the HMA. In

addition aging of the HMA was accounted for and compared to the change in G* of the HMA in the wheelpaths before and after trafficking. The comparison was done on the assumption that deformation was limited to the top 75 mm of the pavement. From the results it was apparent that either all factors had not been accounted for or, that the hypothesis did not hold. A critical review of the entire process and possible mechanisms of distress was therefore undertaken. The results are presented in this appendix.

Influence factors were identified, their impact was considered, and the rut measurements were updated in accordance with the more comprehensive *Modified Reference Method* presented in Appendix A (*1*). This included consideration of *comparable load applications*, to account for the effect of lateral wander during trafficking. The analytical procedure was revised to incorporate the factors according to appropriate scientific principles. Due to the limited extent of available data, the effect of the factors on performance was evaluated by varying the parameters in a sensitivity analysis. From the results it was possible to draw conclusions regarding the validity of the hypothesis. Details are provided subsequently.

Influence Factors

Factors that could affect the three primary elements of the hypothesis on rutting performance were carefully considered to see whether all aspects of each had been taken into account. It was apparent that a number of items had to be considered. Table B1 gives an overview of the items that were identified for further investigation. More will be said about these later. A common thread in a study such as this is the availability of reliable data and sound measurement procedures. As could be expected by the exploratory nature of the project, gaps in the scope of the original test procedure and data collection were identified. To overcome these, the approach was to determine the possible range of the parameters involved and then explore how the performance was affected.

It should be noted that it was recognized that dynamics form an important aspect of the truck wheel loading and vehicle/pavement interaction. However, due to the limited scope of this study the effect of this was not further explored. In fact, it was found that there was considerable variability in the measured truck rut depths between the two measuring stations on each of the four sections. As an example Table B2 shows the data extracted from the WesTrack database for Section 37 (*4*). Possible causes for this phenomenon could be the variability in

amplitude of the wheel loads due to dynamics and construction quality. This was not investigated directly or statistically.

Table B1. Factors Affecting the Primary Elements of the Quantitative Analysis Hypothesis

Nature of Vertical Contact Stress	**Material Characteristics & Pavement Structural Composition**	**Prevailing Environmental Conditions Prior to and During Trafficking**
• Tire pressure • Static load amplitude • Load frequency • Comparative load applications • Vehicle/Pavement dynamics	• Effective stiffness • Multi-layer characteristics • Response & performance of unbound layers & subgrade • Material history prior to trafficking	• Fluctuation in temperature • Fluctuation in ultra-violet radiation • Fluctuation in moisture • Fluctuation in other environmental conditions

Table B2. WesTrack Rut Depths under Trucks for Section 37 [mm]

Station	Number of Load Applications	Left Wheel Path		Right Wheel Path		Average
		Left Tire	Right Tire	Left Tire	Right Tire	
23	35,200	8.7	10.5	10.3	11.2	10.2
	61,000	9.0	11.3	11.7	12.0	11.0
	118,100	9.1	11.4	10.8	13.2	11.1
	188,500	10.9	12.0	13.2	15.7	13.0
63	35,200	8.4	9.3	8.4	8.0	8.5
	61,000	8.5	9.1	10.3	8.3	9.1
	118,000	8.4	10.0	10.9	10.2	9.9
	188,500	8.7	10.9	11.7	9.8	10.3

A Revised and Restructured Analysis

The flow diagram in Figure B1 sets out the process followed with the analytical procedure. The acronyms relate to various elements of the analysis that are defined in the corresponding sections. Except for a few necessary changes, they are identical to those used in the initial analysis (*2*).

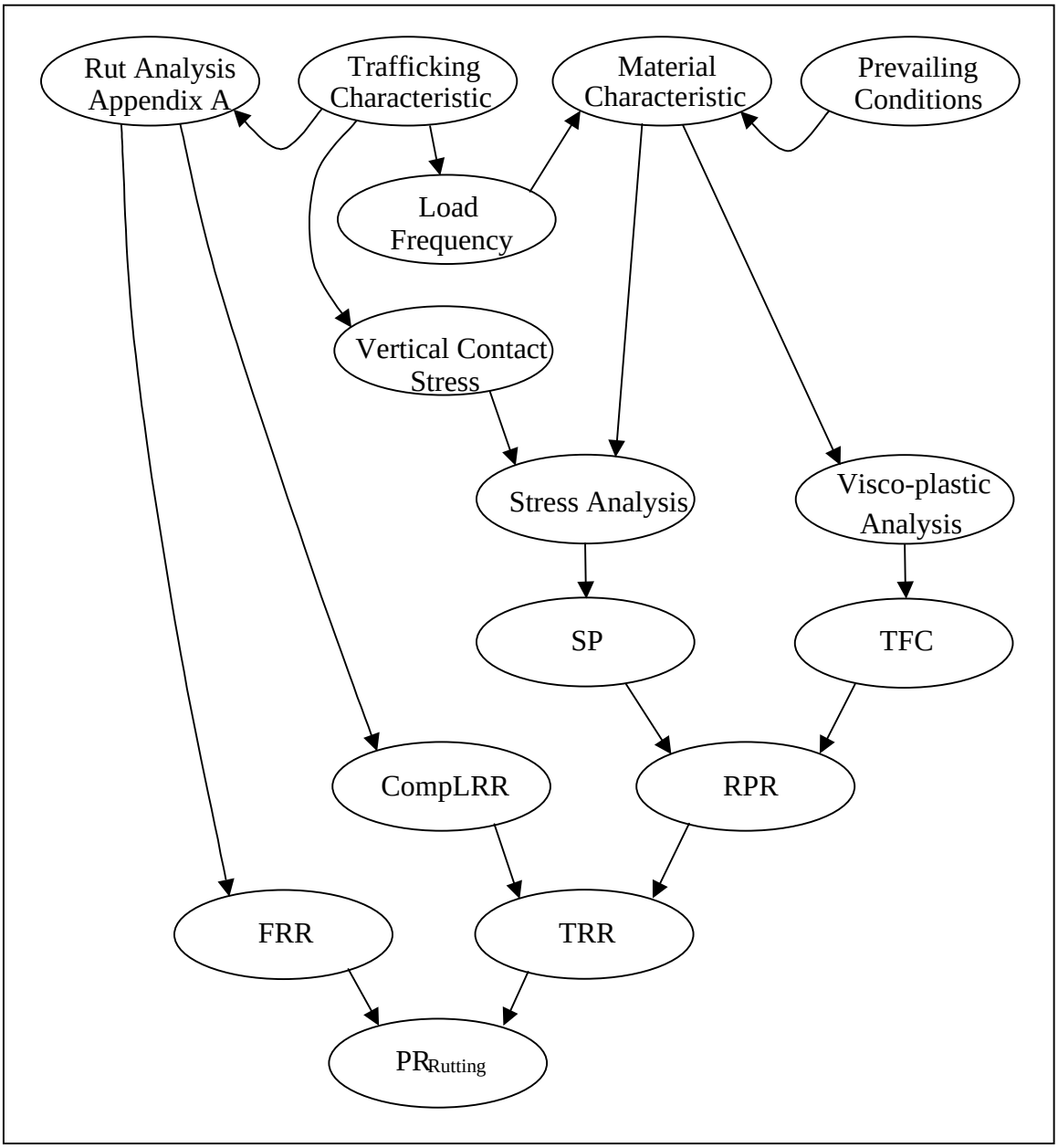

Figure B1. Schematic Layout of Revised Analytical Procedure

The *Field Rutting Ratio (FRR)* is one primary element of the analysis. The other part of the analysis consists of a series of interactive and iterative steps between the three elements of the hypothesis to produce the *Theoretical Rutting Ratio (TRR)*. The analysis follows a logical pattern that accounts for vehicle/pavement interaction as well as interaction between wheel load, material characteristics, and environmental conditions prevailing prior to and during trafficking. The following sections discuss the various aspects of the procedure.

Mathematical Aspects of the Analysis

In determining the *Theoretical Rutting Ratio (TRR)*, both elastic and visco-plastic analyses were conducted for the MMLS3 and trucks. For the elastic analysis with ELSYM5, the stiffness (E) value for each HMA sublayer incorporated temperature, load frequency, and aging effects. Table B3 sets out the stiffness values used for the analyses of the elastic response of the respective pavements. A discussion on the determination of these values is given later with a critical review of the chosen parameters as a part of the sensitivity analysis.

Table B3. Stiffness Values of WesTrack Sections [@ Mid-Depth Temperature]

Loading	Section	Stiffness (MPa) / Layer			
		Top 50 mm HMA	Bottom 100 mm HMA	300 mm Base	450 mm SG
Trucks	1	1156	896	200	100
MMLS3		659 (top 25 mm)/ 449 (bottom 25 mm)	346	100	100
Trucks	35	363	488	200	100
MMLS3		335	356	100	100
Trucks	37	369	472	200	100
MMLS3		341	344	100	100
Trucks	38	458	586	200	100
MMLS3		423	427	100	100

For the stress analysis, a Poisson's ratio equal to 0.35 was used and a *Stress Potential (SP_i)* value was calculated for each HMA sublayer as follows:

$$SP_i = \int_{z_i}^{z_{i+1}} \sigma_{v\,\max} dz \qquad \text{(B1)}$$

where

$\sigma_{vc\,max}$ = maximum vertical contact stress on the pavement beneath the tire

z = depth in the pavement structure

i = sublayer number

Figure B2 shows a schematic drawing of the analytical basis for the calculation of the *SP* with σ_{vc} as the tire contact stress.

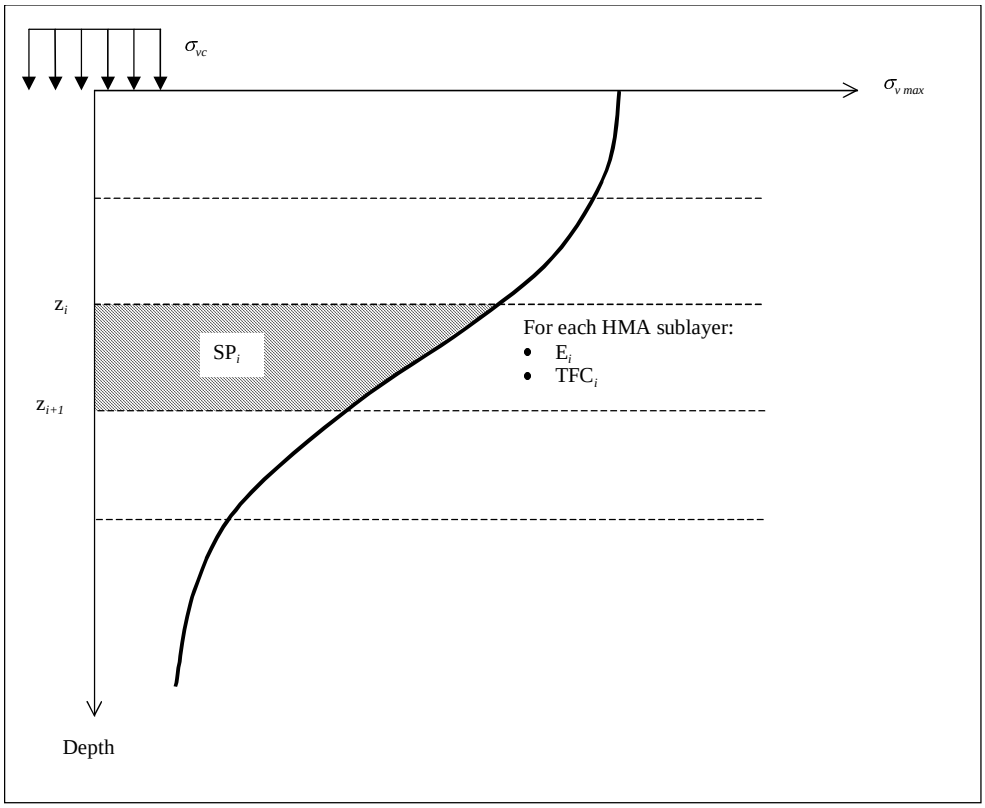

Figure B2. Layout of HMA Sublayers for Analysis

This differs from the approach used in TxDOT Report 0-2134-1, where SP was determined for the upper 75mm HMA sublayer treated as a single layer (*2*).

For the visco-plastic analysis a *Temperature-Frequency Correction (TFC)* value was calculated for each HMA sublayer for the respective sections to account for differences in temperature, load frequency, and age between the MMLS3 and truck tests. The procedure used was the same as that described in TxDOT Report 0-2134-1 based on work from Aouod (*2*, *5*).

The combination of the elastic and visco-plastic behavior yielded the *Rutting Potential Ratio (RPR)*. The *RPR* value of a combination of HMA sublayers gives an indication of the relative amount of rut formation (permanent deformation) after a single MMLS3 wheel load application compared to that of a single truck load application. The *RPR* value for *n* HMA sublayers is defined as follows (see Figure B2):

$$RPR = \frac{\sum_{i=0}^{n} TFC_i \times SP_i^{MMLS3}}{\sum_{i=0}^{n} SP_i^{Trucks}} \tag{B2}$$

where

n = number of HMA sublayers

To account for the differences in lateral wander between the two loading conditions, the concept of *Comparative Load Rut Ratios (CompLRR)*, as described in Appendix A, was used as follows (*1*):

$$CompLRR = \frac{\left(RD_{66.7k}^{Trucks}\right)_{HMA\ layer}}{\left(RD_{100k}^{Trucks}\right)_{HMA\ layer}} = \frac{\left(RD_{Top\ of\ HMA\ layer} - RD_{Bottom\ of\ HMA\ layer}\right)_{66.7k}^{Trucks}}{\left(RD_{Top\ of\ HMA\ layer} - RD_{Bottom\ of\ HMA\ layer}\right)_{100k}^{Trucks}} \tag{B3}$$

where

RD = measured rut depth at specified pavement depth

As described in Appendix A, the ruts after 66,700 truck load applications were commensurable to 100,000 MMLS3 load applications for Sections 01, 35, and 38 with related *Comp LRR* values of 0.97, 0.96, and 0.96, respectively (*1*). For Section 37, the *Comp LRR* was 1.00. It should be noted that $RD_{Bottom\ of\ HMA\ Layer}$ was zero for Sections 35, 37, and 38, so the

ratios of surface RDs were used to calculate *CompLRR*. For Section 01 with an assumed $RD_{Bottom\ of\ HMA\ Layer}$ value of 0.9mm at 100,000 truck load applications, it can be shown that the *CompLRR* value lies between 0.95 and 1.0. Because deformation in the underlying layers of this section was relatively small (30%) compared to the total RD, the ratio of surface RDs yielded a value within this range (0.97). Thus, this *CompLRR* value was considered a reasonable estimate for use in the revised analytical procedure. The *TRR* value for each section at 100,000 MMLS3 load applications was then calculated as the product of the *RPR* and the *CompLRR*.

The *Field Rutting Ratio (FRR)* was computed from the ratio of the measured RD values for the HMA layer at 100,000 MMLS3 load applications and 100,000 truck load applications as follows:

$$FRR = \frac{\left(RD_{100k}^{MMLS3}\right)_{HMA\ layer}}{\left(RD_{100k}^{Trucks}\right)_{HMA\ layer}} = \frac{\left(RD_{Top\ of\ HMA\ layer} - RD_{Bottom\ of\ HMA\ layer}\right)_{100k}^{MMLS3}}{\left(RD_{Top\ of\ HMA\ layer} - RD_{Bottom\ of\ HMA\ layer}\right)_{100k}^{Trucks}} \quad \text{(B4)}$$

As indicated, any RD at the bottom of the HMA due to permanent deformation in the underlying layers was subtracted when the *FRR* was calculated.

The ratio of the *TRR* and *FRR* values then yields the *Rutting Prediction Ratio* ($PR_{Rutting}$) value for each section.

Field Experimental Results

In Appendix A, different RD analysis methods were discussed (*1*). Table B4 presents a summarized version of the measured RDs (after Table A1 in Appendix A). These form the basis of the calculation of the *FRR*s in the revised analytical procedure.

Table B4. Summary of Rut Depths at 100,000 MMLS3 Load Applications from Different Analysis Methods [mm]

Section	Loading	Analysis Method				
		Single Profile	***Reference***	***Modified Reference***		
				Basic Rut	**Comparable Rut**	**Rut at Bottom of HMA layer** (Deformation in Base –Discussed Below)
1	Trucks	2.8	1.2	2.9	2.8*	0.9
	MMLS3	4.1	1.8	2.5		0
35	Trucks	9.4	8.7	11.2	10.8*	0
	MMLS3	6.0	4.3	5.8		0
37	Trucks	10.1	8.1	10.6	10.6#	0
	MMLS3	8.0	3.2	4.8		0
38	Trucks	5.6	5.6	6.9	6.6*	0
	MMLS3	5.1	3.1	3.7		0
*66,700 Truck load applications = 100,000 MMLS3 load applications #100,000 Truck load applications = 100,000 MMLS3 load applications						

Material Characteristics and Pavement Structural Composition

This section considers aspects of material characteristics and pavement structural composition that impact the analysis.

Deformation within the Respective Pavement Layers

In the initial analysis in TxDOT Report 0-2134-1 it was assumed that there was no permanent deformation below 75 mm depth based on a forensic investigation conducted by WesTrack researchers (*2*, *6*). However, from careful analysis of the pin data measured during MMLS3 trafficking, it was found that there was movement in the HMA layers up to a depth of at least 115 mm. In addition it was found that the HMA under the MMLS3 had deformed under traffic as expected at a depth of 50 mm. Therefore, the stress under the MMLS at this depth must have been on average the same as that which occurred at a depth of 120 mm under full-scale trucks. It was therefore apparent that permanent deformation was probably occurring at least to that depth but had not been measured accurately enough to be detected. Given the range of elastic compressive stresses from the stress analysis and temperature during trafficking it is

reasonable to assume that permanent deformation occurred throughout the entire depth of the HMA layer for both truck and MMLS3 trafficking.

From a review of a WesTrack report, it was concluded from the results of their modeling that permanent deformation did occur in the flexible base course of all sections (*7*). However, Sections 35, 37, and 38 were rebuilt, and therefore probably no deformation occurred in the unbound layers because of the stiffness due to post construction trafficking of the corresponding original Sections 05, 07, and 08. This would have limited or possibly even prevented permanent deformation in the underlying layers during trafficking of the replacement sections. However, Section 01 would have had some permanent deformation since it was an original section. For purposes of this analysis it was assumed to be 0.9 mm at 100,000 load applications based on the values reported by Epps et al in their modeling of the rutting at WesTrack (*7*). This is approximately 30% of the total rut. This RD at the bottom of the HMA layer was then factored into the recalculated comparative analysis of $PR_{Rutting}$ for Section 01 by reducing the measured rut under the trucks in the calculation of the *FRR*.

Stiffness of HMA Layers

The HMA stiffness affects the stress distribution in the pavement as well as the permanent deformation of HMA layers. For the stress analysis values of elastic stiffness had to be established. Some values of G* and E were available from the WesTrack database, but it was important to ensure that aging prior to MMLS3 trafficking was correctly taken into account.

Measurements of G* at the 100th load cycle of the RSST-CH test had been made when the HMA was originally placed, prior to truck trafficking and then again after truck trafficking had been completed (*4*). In the latter case G* was determined on cores extracted from the wheelpath. During the interim time period between measurements, the HMA aged and also densified under trafficking. Although distress develops due to load applications in the normal course of events, densification has been found to increase the stiffness and the fatigue life of the HMA (*3*). To some extent, this reduces the negative effects of aging that alone cause an increase in stiffening and brittleness of the HMA. The G* values are presented in Table B5.

The trafficking by MMLS3 was done on untrafficked, aged material. From the work of Bell et al and others such as Hugo and Kennedy, Brown et al, and Nazarian it was concluded that

the G* values after 28 months of aging (Sections 35, 37, and 38) had probably increased by 30 percent since construction (*8*, *9*, *10*, *11*). In contrast that of Section 01 probably increased by at least 75 percent in the top 75 mm. On the basis of these assumptions, G* values for the top 75 mm untrafficked, aged HMA were estimated. These are also shown in Table 5. As can be seen, the values are only slightly different from the actual measured values of G* after trafficking and aging.

Table B5. G* Values of Upper 75 mm HMA Layers Related to MMLS3 Test Sites

[MPa @ 50 °C, 1.4 Hz]

Section	Measured Before Truck Trafficking (Unaged)		Measured After Truck Trafficking (Aged)		Estimated Untrafficked (Aged)	
	G*	Date	G*	Date	G* Estimate	Date
01	53.75	Oct-95	89.95	Mar-99	94.0	ca Oct-99
35	34.25	Jul-97	41.35	Mar-99	44.5	ca Oct-99
37	34.85	Jul-97	44.9	Mar-99	45.3	ca Oct-99
38	43.25	Jul-97	54.25	Mar-99	56.2	ca Oct-99

Another factor that had to be considered was the acute increase in stiffness that occurs in the upper 15 to 25 mm of HMA layers after several years of aging due to UV effects and high temperature. Hugo and Kennedy reported that binder stiffness in the top 15 mm of HMA layers can increase by an order of magnitude (*9*). It was therefore decided to use a stiffness increase of 120 percent in the top 25 mm and a 50 percent increase for the layer between 25 and 50 mm for Section 01 that by the time of MMLS3 trafficking had been exposed to UV aging for approximately 4 years.

G* values were not measured in the second HMA layer. Therefore, modulus values for the lower HMA layer had to be estimated. This was done by proportionately decreasing the modulus values of the upper HMA on the basis of the respective indirect tensile strength (ITS) values that had been measured for both layers. In the case of Section 01, an average ratio of 1.46 was used, and a collective average value of 1.21 was used for Sections 35, 37, and 38. These values were deduced from the comprehensive set of ITS data contained in Table B10.

The values of G* at appropriate frequencies and temperatures for the respective pavement structures were subsequently calculated by using the corrections suggested by Aouod and Sousa and Monismith (*5*, *12*). The results are shown in Tables B6, B7, and B8. The same procedure is described in TxDOT Report 0-2134-1 and was used in the initial analysis (*2*).

Table B6. G* Values of WesTrack Sections Adjusted for Aging

[50 °C, 1.4 Hz]

Loading	Section	G* (MPa) / Layer	
		Top 50 mm HMA	Bottom 100 mm HMA
Trucks	1	53.8	36.8
MMLS3		118.3 (top 25 mm)/ 80.6 (bottom 25 mm)	36.8
Trucks	35	34.3	29.8
MMLS3		44.5	29.8
Trucks	37	34.9	28.8
MMLS3		45.3	28.8
Trucks	38	43.3	35.7
MMLS3		56.2	35.7

Table B7. Estimated G* Values of WesTrack Sections Adjusted for Aging and Corresponding Loading Frequencies [50 °C]

Loading	Section	G* (MPa) / Layer	
		Top 50 mm HMA	Bottom 100 mm HMA
Trucks	1	151	104
MMLS3		194 (top 25 mm)/ 132 (bottom 25 mm)	60
Trucks	35	96	84
MMLS3		73	49
Trucks	37	98	81
MMLS3		74	47
Trucks	38	122	101
MMLS3		92	59

Table B8. Estimated G* Values of WesTrack Sections Adjusted for Aging and Corresponding Loading Frequencies [@ Mid-Depth Temperature]

Loading	Section	G* (MPa) / Layer	
		Top 50 mm HMA	Bottom 100 mm HMA
Trucks	1	330	345
MMLS3		143 (top 25 mm)/ 98 (bottom 25 mm)	86
Trucks	35	91	136
MMLS3		73	89
Trucks	37	92	131
MMLS3		74	86
Trucks	38	115	163
MMLS3		92	107

Selection of E Values

E values of the lower HMA layers of the WesTrack materials were measured with four-point bending tests (FPBT) at 20 Hz by the University of California at Berkeley (UCB) (*13*). These values are shown in Table B9.

Table B9. Bottom HMA Sublayer E values (MPa) from Four Point Bending Tests (FPBT) [20 °C]

Layer	Section			
	01	35	37	38
Bottom	3,194	3,614	4,088	4,248

The modulus values of Section 01 appeared to be extraordinarily low relative to the other sections, especially when comparing these values with ITS values of the same material (Table B10). The ITS values were much more comparable to the relative G* values measured in the top layer. This correlation was also reported by Grobler in terms of ITS versus E values (*14*). The untrafficked ITS values of the upper and lower 75 mm HMA sublayers from the different sections (Table B10) were normalized with respect to the lowest strength in each layer. The results are shown in Table B11. It was interesting to find that the relative performance of the four sections, in terms of *comparable ruts* after 100,000 load applications (Table B4) appeared to be inversely proportional to the normalized ITS values.

In this study E values were initially deduced from values of G* to overcome the dilemma of not having readily available measured E values. For the conversion the following formula was used assuming elastic behavior:

$$E = 2G(1+\nu) \qquad \text{(B6)}$$

Poisson's ratio (ν) values were taken to be equal to those determined by Sousa and Monismith for the respective frequencies and temperatures (*12*).

Table B10. Indirect Tensile Strength (ITS) Comparisons between Top and Bottom HMA Sublayers [25 °C]

Section	Unaged & Untrafficked ITS (MPa) Top/Bottom	Unaged ITS Ratio (Top/Bottom)	Aged & Trafficked ITS (MPa) Top/Bottom	Aged ITS Ratio (Top/Bottom)
01	1.960	1.49	1.933	1.44
	1.313		1.347	
35	0.955	1.14	1.002	1.18
	0.841		0.852	
37	0.966	1.19	0.993	1.24
	0.814		0.799	
38	1.158	1.12	1.231	1.25
	1.034		0.983	

Table B11. Ratios of ITS for Top & Bottom HMA Sublayers of Different Sections

Layer	Section			
	01	35	37	38
Top	2.05	1	1.01	1.21
Bottom	1.61	1.03	1	1.27

Subsequent to doing the calculation and analyses, Monismith pointed out that later research had found this approach of relating G* and E to be invalid because the relationship yielded Poisson's values greater than one and their measurements never found such high values in hollow cylinder tests (*15*). Accordingly, the measured E values of the bottom HMA sublayer from the four-point bending test (FPBT) in Table B9 were taken as a point of departure for a second procedure for selecting E values.

Because these modulus values had been measured for only the lower HMA layer, values for the upper HMA layers had to be estimated. This was done by proportionately increasing the modulus values of the lower HMA on the basis of the respective ITS values that had been measured for both layers. The stiffness values for the respective pavement sections and sublayers were then calculated by making corrections for temperature and frequency in a manner similar to that used before (*2*). These values of E are shown in Table B12 together with the previously determined E values.

Table B12. Comparison of HMA E Values Calculated from G* and FPBT Data [MPa @ mid-depth temperature]

Section	Layer	E for MMLS3 trafficking		E for Truck trafficking	
		G*-based	FPBT-based	G*-based	FPBT-based
01	0-25mm	659	553	1156	1276
	25-50mm	449	377		
35	0-50mm	335	395	363	492
37		341	469	369	583
38		423	475	458	591
01	50-150mm	346	333	896	1327
35		356	479	488	729
37		344	541	472	825
38		427	563	585	857

The feasibility of the values was also checked through a comparison with the findings of Freeme and found to be realistic (*16*). They were then used for the stress calculations in the revised analytical procedure for determining $PR_{Rutting}$.

Stiffness of the Base and Subgrade

The stiffness values of the base (Table B3) differ from the values used by Epps et al. that were extracted from the UCB database (*2*, *13*). The revised values were selected to reflect the fact that very little settlement occurred in the base layers below the HMA under truck trafficking. Also the stress level in the base under MMLS3 trafficking was much lower than under the trucks. In the same vein, the value for the subgrade was rounded off to 100 MPa. It was found that the analyses were not sensitive to these small discrepancies in the stiffness values.

Stress Analysis

This section considers all aspects that could have an effect on the stress analyses.

Tire Pressure and Contact Stress

Epps et al reported on the determination of the MMLS3 tire pressure due to expansion of the air from 25 °C to 55 °C (*2*). It was found to increase to 738 kPa from 690 kPa. According to the ideal gas law it should have been 759 kPa for a fixed volume. The measured contact stress increased to 766 kPa. The same would hold for the trucks for an equivalent rise in temperature. In fact, the temperature of the tires could even have risen to 60 °C during the critical trafficking period.

An important side effect of this phenomenon is the likelihood of increased peak contact stress under full-scale tires. Based on the results of de Beer et al and Himeno et al, it is not unlikely that vertical contact stresses of 1,000 kPa or higher were developed during trafficking (*17*, *18*). It was therefore decided to do analyses for tire pressures at 690 kPa, 850 kPa, and 1,200 kPa to evaluate the impact on pavement performance.

Loading Characteristics

The truck trafficking was highly channelized (within +/- 125 mm) relative to a tire width of 525 mm. In contrast the MMLS3 was set to wander transversely +/- 80 mm in comparison to a tire width of 80 mm. As a result, the equivalent scaled middle width that was trafficked experienced fewer load applications than the equivalent width under trucks. As described in Appendix A, RDs at approximately 66,700 truck load applications were compared to RDs after approximately 100,00 MMLS3 load applications for Sections 01, 35, and 38. For Section 37, RDs after 100,000 load applications were compared for both loading conditions (*1*).

Stress Profile

The vertical compressive stress distribution with depth was analyzed to determine what the effect would be if deformation occurred throughout the HMA layer and not only in the top 75 mm. The results were used for the revised analytical procedure to determine $PR_{Rutting}$. As part of the sensitivity analysis, it was decided to use a contact stress of 850 kPa in order to incorporate the range of contact stresses that may have occurred under trafficking. In addition a high value of 1,200 kPa was also analyzed to see the effect of possible extreme contact stresses.

As pointed out previously, it was assumed that deformation occurred throughout the entire depth of the HMA layer. Therefore it was expected that the $PR_{Rutting}$ values would tend to unity at the bottom of the HMA layer. Moreover, if total deformation were measured in any HMA sublayer, the related $PR_{Rutting}$ value was also expected to be unity (*19*).

Results

The results of the revised analytical procedure for determining $PR_{Rutting}$ are shown in Tables B13, B14, B15, and B16. Several observations can be made:

- $PR_{Rutting}$ values of one were found for several possible combinations in the analyses
- None of the $PR_{Rutting}$ analyses for the 690 kPa tend towards unity, lending support for the viewpoint that the deformation took place throughout the HMA.
- In three of the four cases $PR_{Rutting}$ values were close to unity for a tire pressure of 850 kPa and deformation throughout the full depth of HMA. For the same conditions Section 37 had a $PR_{Rutting}$ value of 1.24 that only approached unity at a tire pressure of 1,200 kPa. The reason for this disparity is still unknown, but difficult site conditions due to milling in the truck wheelpaths may have contributed. It is also possible that the RD was underestimated.
- *TRR* values progressively reduced as the depth of analysis was increased. This served to indicate that rutting under the MMLS3 became proportionately less relative to rutting under the trucks as depth increased. This was expected.
- $PR_{Rutting}$ also tended towards unity where the tire pressure was 1,200 kPa and the depth of deformation was limited to 75 mm. This was however considered to be less likely to simulate

actual field conditions than the case with the tire pressure at 850 kPa and deformation throughout the HMA.

From an overall point of view it was apparent that the selection of the $PR_{Rutting}$ values from the analyses of total HMA depth at a contact stress of 850 kPa were reasonable representations of the actual field conditions.

Table B13. Revised Analysis for Section 01.

σ_{vc} (kPa)	Layer (mm)	*SP*		*TFC*	Layer (mm)	*RPR*	*Comp LRR*	*TRR*	*FRR*	$PR_{Rutting}$
		MMLS3	Trucks							
690										
	0-25	15963	16925	2.31	0-25	2.18		2.10		
	25-50	9350	15525	3.38	0-50	2.11		2.04		
	50-75	4500	12913	3.99	0-75	1.91		1.84		
	75-100	2400	9850	3.99	0-100	1.74	0.97	1.68		
	100-125	1350	7075	3.99	0-125	1.63		1.57		
	125-150	788	5088	3.99	0-150	1.55		1.50	1.25	1.20
850										
	0-25	15963	20838	2.31	0-25	1.77		1.71		
	25-50	9350	18788	3.38	0-50	1.73		1.67		
	50-75	4500	15213	3.99	0-75	1.58		1.52		
	75-100	2400	11238	3.99	0-100	1.45	0.97	1.40		
	100-125	1350	7788	3.99	0-125	1.37		1.33		
	125-150	788	5413	3.99	0-150	1.32		1.27	1.25	1.02
1200										
	0-25	15963	29075	2.31	0-25	1.27		1.22		
	25-50	9350	25513	3.38	0-50	1.25		1.21		
	50-75	4500	19575	3.99	0-75	1.17		1.13		
	75-100	2400	13663	3.99	0-100	1.09	0.97	1.06		
	100-125	1350	8975	3.99	0-125	1.05		1.01		
	125-150	788	5925	3.99	0-150	1.02		0.98	1.25	0.79

Table B14. Revised Analysis for Section 35.

σ_{vc} (kPa)	Layer (mm)	*SP*		*TFC*	Layer (mm)	*RPR*	*Comp LRR*	*TRR*	*FRR*	$PR_{Rutting}$
		MMLS3	Trucks							
690										
	0-25	16575	17100	1.24	0-25	1.20		1.16		
	25-50	10463	16175	1.24	0-50	1.01		0.97		
	50-75	5238	14088	1.52	0-75	0.88		0.84		
	75-100	2763	11338	1.52	0-100	0.78	0.96	0.75		
	100-125	1525	8675	1.52	0-125	0.71		0.69		
	125-150	863	6625	1.52	0-150	0.67		0.64	0.52	1.24
850										
	0-25	16575	21100	1.24	0-25	0.97		0.94		
	25-50	10463	19700	1.24	0-50	0.82		0.79		
	50-75	5238	16700	1.52	0-75	0.72		0.70		
	75-100	2763	12988	1.52	0-100	0.65	0.96	0.63		
	100-125	1525	9613	1.52	0-125	0.60		0.58		
	125-150	863	7113	1.52	0-150	0.57		0.55	0.52	1.05
1200										
	0-25	16575	29563	1.24	0-25	0.70		0.67		
	25-50	10463	27025	1.24	0-50	0.59		0.57		
	50-75	5238	21725	1.52	0-75	0.53		0.51		
	75-100	2763	15900	1.52	0-100	0.48	0.96	0.47		
	100-125	1525	11138	1.52	0-125	0.46		0.44		
	125-150	863	7863	1.52	0-150	0.44		0.42	0.52	0.81

Table B15. Revised Analysis for Section 37.

σ_{vc} (kPa)	Layer (mm)	*SP*		*TFC*	Layer (mm)	*RPR*	*Comp LRR*	*TRR*	*FRR*	$PR_{Rutting}$
		MMLS3	Trucks							
690										
	0-25	16563	17100	1.24	0-25	1.20		1.20		
	25-50	10400	16163	1.24	0-50	1.01		1.01		
	50-75	5175	14050	1.52	0-75	0.87		0.87		
	75-100	2725	11313	1.52	0-100	0.78	1.00	0.78		
	100-125	1500	8688	1.52	0-125	0.71		0.71		
	125-150	863	6650	1.52	0-150	0.66		0.66	0.45	1.46
850										
	0-25	16563	21088	1.24	0-25	0.97		0.97		
	25-50	10400	19663	1.24	0-50	0.82		0.82		
	50-75	5175	16650	1.52	0-75	0.72		0.72		
	75-100	2725	12950	1.52	0-100	0.65	1.00	0.65		
	100-125	1500	9613	1.52	0-125	0.60		0.60		
	125-150	863	7150	1.52	0-150	0.56		0.56	0.45	1.24
1200										
	0-25	16563	29525	1.24	0-25	0.70		0.70		
	25-50	10400	26938	1.24	0-50	0.59		0.59		
	50-75	5175	21638	1.52	0-75	0.53		0.53		
	75-100	2725	15838	1.52	0-100	0.48	1.00	0.48		
	100-125	1500	11125	1.52	0-125	0.45		0.45		
	125-150	863	7900	1.52	0-150	0.43		0.43	0.45	0.96

Table B16. Analysis for Section 38

σ_{vc} (kPa)	Layer (mm)	*SP*		*TFC*	Layer (mm)	*RPR*	*Comp LRR*	*TRR*	*FRR*	$PR_{Rutting}$
		MMLS3	Trucks							
690										
	0-25	16550	17075	1.24	0-25	1.20		1.15		
	25-50	10388	16075	1.24	0-50	1.01		0.96		
	50-75	5150	13888	1.52	0-75	0.88		0.84		
	75-100	2675	11050	1.52	0-100	0.78	0.96	0.75		
	100-125	1438	8313	1.52	0-125	0.72		0.68		
	125-150	800	6238	1.52	0-150	0.67		0.64	0.54	1.20
850										
	0-25	16550	21075	1.24	0-25	0.97		0.93		
	25-50	10388	19588	1.24	0-50	0.82		0.79		
	50-75	5150	16475	1.52	0-75	0.72		0.69		
	75-100	2675	12663	1.52	0-100	0.65	0.96	0.62		
	100-125	1438	9213	1.52	0-125	0.60		0.57		
	125-150	800	6700	1.52	0-150	0.57		0.54	0.54	1.01
1200										
	0-25	16550	29513	1.24	0-25	0.70		0.67		
	25-50	10388	26850	1.24	0-50	0.59		0.57		
	50-75	5150	21438	1.52	0-75	0.53		0.51		
	75-100	2675	15513	1.52	0-100	0.49	0.96	0.46		
	100-125	1438	10663	1.52	0-125	0.46		0.44		
	125-150	800	7388	1.52	0-150	0.44		0.42	0.54	0.78

The $PR_{Rutting}$ results from the revised analyses were compared to those from the initial analyses in TxDOT Report 0-2134-1 (*2*). Table B17 shows the findings for the four sections for a vertical contact stress of 850 kPa with deformation occurring throughout the HMA layer compared to those from the initial analyses. It is apparent that for this set of field conditions all four sections had $PR_{Rutting}$ values as close to unity as found in the Jacksboro case study after taking account of all the factors affecting the rutting performance (*3*). In fact, three of the four sections had $PR_{Rutting}$ values within 5 percent of unity. This is in contrast to the wide range of $PR_{Rutting}$ values that were found in the initial analyses by Epps et al (*2*).

Table B17. Comparison of *PR* $_{Rutting}$ Results.

Section	Initial $PR_{rutting}$	Revised $PR_{rutting}$
01	1.3	1.0
35	1.6	1.1
37	2.0	1.2
38	1.4	1.0

The analyses are of course dependent upon the correction factors that were used. However, the analytical parameters pass the test of reasonableness. The credibility of the findings is enhanced by the fact that despite the uncertainty about the values of the HMA sublayer stiffnesses, the results proved to be relatively insensitive to the range of E values that were considered plausible. This can be seen from the summary of the results of the analyses with different E values in Table B18.

Table B18. Comparison of $PR_{rutting}$ Results for Different E Values [Tire Contact Stress σ_{vc} = 850 kPa]

Section	G*-Based	FPBT-Based
01	1.0	1.1
35	1.1	1.1
37	1.2	1.3
38	1.0	1.0

In the same vein, the results remain virtually unchanged when the stress analysis is done with a Poisson's ratio value of 0.45 for the HMA layers. Furthermore, the ranges of the parameters that were used for evaluating the sensitivity of the analyses were such that they covered most of the feasible scenarios, including trafficking up to 200,000 load applications.

The key to the analysis was to understand how important it was to account for all factors that could impact the results. It was clear that some of the factors were much more critical than others. In this regard the tire contact pressure and the depth of distress due to deformation were

most prominent. A secondary effect of lateral wander was the phenomenon that depth of rutting was acutely dependent on the traffic pattern with mixes that were highly plastic. Similarly, the accurate determination of temperature was just as important, since it impacts on stiffness.

In summary, the following corrections were applied to the initial analyses in TxDOT Report 0-2134-1 to enable a more comprehensive analysis to be done:

1. Revised values of G* were used.
2. Updated measurements of rutting were used.
3. The entire depth of the HMA layer was assumed to have undergone permanent deformation.
4. Different possible tire contact stresses were considered.
5. Settlement in the unbound layers underlying the HMA layer of Section 01 was included.
6. Comparable load applications were determined to allow for the lateral wander.

Conclusions

The hypothesis appears to hold for the four independent test sections, provided steps are taken to factor in differences in the respective trafficking and environmental conditions. The procedure therefore provides a sound base for the MMLS3 to be used for performance prediction as described in TxDOT Report 0-2134-1 (*2*).

Recommendations

It is clear that sound controlled experiments can be used to further validate the findings of this limited study. Researchers should carefully draft protocols to ensure that they do not jeopardize accelerated pavement testing (APT) results with conditions that are insufficiently characterized to enable performance to be satisfactorily modeled.

References

1. Hugo, Frederick and Pieter Poolman, *A Critical Analysis of WesTrack MMLS3 and Truck Rut Data*, Appendix A in TxDOT Report 0-2134-1, by Epps et al., for the TxDOT in co-operation with the FHWA, April 2001.

2. Epps, Amy L., Tazeen Ahmed, Dallas C. Little and Frederick Hugo, *Performance Prediction with the MMLS3 at Westrack,* TxDOT Report 0-2134-1, for the TxDOT in co-operation with the FHWA, April, 2001.

3. Walubita, Lubinda, Fred Hugo and Amy Epps, Performance of Lightweight Aggregate Asphalt Concrete Pavements Under Wet and Heated Model Mobile Load Simulator Trafficking: A Comparative Study with the TxMLS, TxDOT Report 0-1814- for the TxDOT in co-operation with the FHWA, March, 2000.

4. WesTrack Database, Beta Version, 2000, Federal Highway Administration, Washington, D.C.

5. Aouod MF, *Evaluation of Flexible Pavements and Subgrade Spectral-Analysis-of-Surface-Waves Method*, PhD Dissertation, The University of Texas at Austin, Austin 1993.

6. Healow SP, *Analysis and Development of Performance Models for WesTrack*, Masters Thesis, University of Nevada, Reno, May 1998.

7. Epps J, CL Monismith, SB Seeds, SH Alavi, SC Ashmore, R Leahy, TM Mitchell, *WesTrack Performance-Interim Findings*, Journal of the Association of Asphalt Paving Technologists, Boston, Massachusetts, March 16 – 18, 1998, pp. 738 –782.

8. Bell CA, MJ Felling and A Wieder, *Field Validation of Laboratory Aging Procedures for Asphalt Aggregate Mixtures.* Journal of the Association of Asphalt Paving Technologists, Volume 63, St. Louis, Missouri, St. Paul MN, March 21 – 23, 1994, p.45 – 80.

9. Hugo F and TW Kennedy, *Surface Cracking of Asphalt Mixtures in Southern Africa*, Proceedings Association of Asphalt Paving Technologists, San Antonio, Texas, February 11 – 13, 1985, pp. 454 – 491.

10. Brown SF, KE Cooper, JM Gibb, JM Read and TV Scholz, *Practical Tests for Mechanical Properties of Hot Mix Asphalt*. Proceedings of the 6th Conference on Asphalt Pavements for Southern Africa, Cape Town, South Africa, October, 1994, pp. IV-29 – IV-45.

11. Nazarian S, M Baker and RC Boyd, *Determination of Pavement Aging by High-Frequency Body and Surface Waves*, Proceedings of the 7th International Conference on Asphalt Pavement, Nottingham, United Kingdom, 1992, pp. 252 – 265.

12. Sousa JB and CL Monismith, *Dynamic Response of Paving Materials*. Transportation Research Record No. 1136, Washington D.C., 1988, pp. 57 – 68.

13. Monismith CL, JA Deacon, and JT Harvey, *WesTrack: Performance Models for Permanent Deformation and Fatigue*. Unpublished draft to Nichols Consulting Engineers, Chtd., December 1999.

14. Grobler JE, *Development of Procedures for Large Stone Asphalt Mix Design*, Unpublished thesis, Master in Engineering (Civil), University of Stellenbosch, South Africa, December, 1990.

15. Monismith, Carl, Discussion during Technical Session IV at the 2001 Annual Meeting of the Association of Asphalt Paving Technologists, Clearwater, Tampa, Florida, March 19-21, 2001.

16. Freeme, CR, *The Behavior of Bituminous Surfacings in Asphalt Pavements*, D.Phil. Dissertation, University of Natal, South Africa, 1971.

17. De Beer M, C Fisher and F Jooste, *Determination of Pneumatic Tyre/Pavement Interface Contact Stresses under Moving Loads and Some Effects on Pavements with Thin Asphalt Surfacing Layers*, Proceedings of Eighth International Conference on Asphalt Pavement, Seattle, Washington, August 10-14, 1997, p.200 – 202.

18. Himeno K, T Kamijima, T Ikeda and T Abe, *Distribution of Tire Contact Pressure of Vehicles and its Influence on Pavement Distress*. Proceedings of Eighth International Conference on Asphalt Pavement, Seattle, Washington, August 10-14, 1997, p.129 – 139.

19. Epps A, L Walubita, F Hugo, and N Bangera, *Comparing Pavement Response and Rutting Performance for Full-Scale and One-Third Scale Accelerated Pavement Testing.* Presented at 80th Annual Meeting of the Transportation Research Board, Washington, D. C., January 2001.